Charles University in Prague
Faculty of Science

Program of Study: Biology
Field of Study: Immunology

Bc. Ladislav Sivák

Polymeric conjugates for delivery of cytostatic drugs and ABC transporters inhibitors in multidrug resistant tumors

Polymerní konjugáty sloužící k doručení cytostatických léčiv a inhibitorů ABC transportérů u nádorů s mnohočetnou lékovou rezistencí

Diploma thesis

Supervisor: RNDr. Marek Kovář, PhD.

Prague 2014

Prohlášení:

Prohlašuji, že jsem závěrečnou práci zpracoval samostatně a že jsem uvedl všechny použité informační zdroje a literaturu. Tato práce ani její podstatná část nebyla předložena k získání jiného nebo stejného akademického titulu.

Praha, 10. 4. 2014

Podpis

Acknowledgments

I would like to thank my supervisor RNDr. Marek Kovář, PhD. for excellent tutelage, great patience, motivation and invaluable advice. I would also like to thank all my colleagues in the Laboratory of Tumor Immunology for all the advice, practical help and for great working atmosphere.

Last but not least I express sincere gratitude to my family and my girlfriend Zuzana Radvanová for their support throughout all those years.

Abstract

Significant problem and important cause of failure of the cancer chemotherapy is that even originally very sensitive tumors become resistant to effects of cytostatic drugs. Loss of sensitivity to specific chemotherapeutics agent may not directly cause the loss of sensitivity to other chemotherapeutics. However, it have been described that tumors resistant to one type of chemotherapeutics were found to be resistant to several other anticancer drugs that are different in both structure and mode of action. This phenomenon has been described as multidrug resistance (MDR). MDR can develop in several ways, with the predominant mechanism being the overexpression of ATP-binding cassette (ABC) transporters, such as P-glycoprotein. These transporters acts as energy driven pumps and which, maintain intracellular drug concentration below toxic levels.

The aim of this study was to examine the potential of novel polymeric therapeutics based on *N*-(2-hydroxypropyl)methacrylamide (HPMA) copolymers bearing either anticancer drug, inhibitor of ABC transporters or both, for overcoming MDR mediated by P-glycoprotein in doxorubicin (Dox) resistant murine monocytic leukemia cell line P388/MDR. Series of low-molecular weight inhibitors reversin 121 (R121), reversin 205 (R205) and ritonavir (RIT) and their derivatives were tested for their ability to block the P-glycoprotein efflux pump. 5-methyl-4-oxohexanoyl R121 (MeOHe-R121) and 5-methyl-4-oxohexanoyl RIT (MeOHe-RIT) showed highest inhibitory activity out of all inhibitors derivatives tested. These derivatives were consequently conjugated to the HPMA copolymer carrier. Conjugate P-Ahx-NH-N=MeOHe-R121 showed superior ability to sensitize P388/MDR cells in dose-dependent manner and achieved almost 50-fold increase of cytostatic activity of Dox at 24 μM (highest concentration tested). Conjugate P-Ahx-NH-N=MeOHe-RIT at the highest tested concentration 12 μM was able to increase cytostatic activity of Dox more than 50 times. Finally, the cytostatic activity of three HPMA copolymer conjugates P-Ahx-NH-N=MeOHe-R121(Dox) bearing both Dox and P-gp inhibitor MeOHe-R121 both bound via pH-sensitive hydrazone bond with three different molar ratios of Dox: P-gp inhibitor (2:1, 1:1, 1:2) were tested and the best outcome was seen in conjugate with the higher content of P-gp inhibitor. The cytostatic activity was almost 45 times higher than that of the conjugate bearing only Dox in P388/MDR cells. Slightly less promising results were observed for P-Ahx-NH-N=MeOHe-RIT(Dox) conjugate with equimolar ratio of Dox and P-gp inhibitor, which exhibited about 10 times higher cytostatic activity than that of the conjugate with Dox only toward the P388/MDR cells.

Keywords: multidrug resistance, ATP-binding cassette transporters P-glycoprotein, ritonavir, reversin 121, reversin 205, inhibitors, *N*-(2-hydroxypropyl)methacrylamide

Abstrakt

Jednou z vážných komplikací chemoterapie nádorů a častou příčinou jejího selhání je schopnost nádorových buněk odolávat účinkům cytotoxických látek. Při ztrátě citlivosti k určitému cytostatiku může být zachována citlivost k jiným léčivům. Velmi časté jsou však případy zkřížené rezistence nádorových buněk, a to i mezi protinádorovými léčivy, které se liší jak strukturou, tak mechanizmem účinku. Tento fenomén byl popsán jako mnohočetná léková rezistence (multidrug resistance, MDR). Existuje mnoho mechanizmů vzniku MDR, ale hlavní příčinu představuje zvýšená exprese ABC transportérů (ATP-binding cassette) a to zejména P-glykoproteinu (P-gp). Tyto ABC transportéry fungují jako ATP dependentní membránové pumpy exportující protinádorové léčiva z buňky a způsobující tak jejich sníženou intracelulární koncentraci.

Cílem práce bylo prozkoumat potenciál polymerních léčiv na bázi *N*-(2-hydroxypropyl)metacrylamidových (HPMA) kopolymerů nesoucích buď cytostatikum, inhibitor ABC transportérů, nebo obojí vázané společně na jeden polymerní nosič pro překonání MDR mediované P-glykoproteinem na doxorubicin (Dox)-rezistentní buněčné linii myší leukemie P388/MDR. Bylo testováno několik nízkomolekulárních inhibitorů P-gp, a to reversin 121 (R121), reversin 205 (R205) a Ritonavir (RIT) a dále jejich derivátů, v inhibici P-glykoproteinu. 5-metyl-4-oxohexanoyl-R121 (MeOHe-R121) a 5-metyl-4-oxohexanoyl-RIT (MeOHe-RIT), vykazovali z testovaných derivátů těchto inhibitorů nejvyšší inhibiční aktivitu pro P-gp. Následně byly tyto vybrané deriváty navázány na HPMA kopolymerní nosič. Konjugát P-Ahx-NH-N=MeOHe-R121 byl schopen účinně sensitizovat P388/MDR buňky a téměř 50-krát zvýšit cytostatickou aktivitu Dox při použití nejvyšší testované koncentrace (24 μM) konjugátu. Konjugát P-Ahx-NH-N=MeOHe-RIT při koncentraci 12 μM, představující taktéž nejvyšší testovanou koncentraci, zvýšil cytostatickou aktivitu Dox více než 50-krát. Nakonec byla testována cytostatická aktivita tří konjugátů P-Ahx-NH-N=MeOHe-R121(Dox), nesoucích jak Dox, tak i P-gp inhibitor MeOHe-R121 společně navázaných na jeden polymerní nosič pH-sensitivní hydrazonovou vazbou, ve třech různých poměrech P-gp inhibitoru a Dox. Nejvyšší cytostatickou aktivitu vykazoval polymerní konjugát s vyšším obsahem P-gp inhibitoru, který měl 45-krát vyšší cytostatickou aktivitu než konjugát nesoucí pouze Dox. O něco horší výsledek byl získán u konjugátu P-Ahx-NH-N=MeOHe-RIT(Dox), obsahující Dox a P-gp inhibitor ve stejném molárním poměru, který měl 10-krát vyšší cytostatickou aktivitu než konjugát nesoucí pouze Dox.

Klíčová slova: mnohočetná léková rezistence, ABC transportéry, P-glykoprotein, ritonavir, reversin 121, reversin 205, inhibitory, *N*-(2-hydroxypropyl)methacrylamide

List of Abbreviations

ABC	ATP-binding cassette
AML	acute myeloid leukemia
BCRP	breast cancer resistance protein
CAR	constitutive androstane receptor
CD	cluster of differentiation
CFTR	cystic fibrosis transmembrane conductance protein
cMOAT	hepatocellular canalicular multiple organic anion receptor
CsA	cyclosporine A
CTR1	copper uptake protein 1
DCM	dichloromethane
DIPEA	*N*,*N*-diisopropylethylamine
DMAP	4-(dimethylamino)pyridine
DMF	*N*,*N*-dimethyl formamide
E217G	estradiol-17β
EDC	*N*-ethyl-N`-(3-dimethylaminopropyl)carbodiimide hydrochloride
EPR	Enhanced Permeability and Retention
FTC	fumitremorgin C
GS-DNP	S-glutathionyl 2,4-dinitrobenzene
GSH	glutathione
GST	glutathione S-transferase
HMW	high-molecular weight
HOBT	1-hydroxybenzotriazole hydrate
HPMA	*N*-(2-hydroxypropyl)methacrylamide
Hsp70	heat shock protein 70
ICL	intracytosolic loop
JNK	c-Jun terminal kinase
LMW	low-molecular weight
LRP	lung resistance related protein
LTC_4	leukotriene C_4
LTE_4	leukotriene E_4
MAP	mitogen activated protein kinase
MDR	multidrug resistance

MDR1	multidrug resistance protein 1
MRP	multidrug resistance protein
MTX	mitoxantrone
MVP	major vaults protein
NBD	nucleotide biding domain
NSCLC	non-small lung cancer
P-gp	P-glycoprotein
PKA	protein kinase A
PKC	protein kinase C
PXR	pregnane X receptor
RNP	ribonucleoprotein
SNP	single nucleotide polymorphism
SP	side population
SUR	sulfonylurea receptor
TEP1	telomerase associated protein 1
TMD	transmembrane domain
VPARP	vault poly-(ADP-ribose) polymerase
VRP	verapamil

Contents

1 Introduction

Chemotherapy represents one of the principal approaches for the treatment of cancer. The effectiveness of chemotherapy is limited by drug resistance, which represents significant and the most important cause of the failure in cancer chemotherapy. It is increasingly recognized that tumors consist of mixed populations of malignant cells, some of which are drug sensitive while others are drug resistant. Thus, resistance of tumors can arise through chemotherapy induced selection of resistant minor subpopulation of cells that was present at low frequency in the original tumor. The resistance to anticancer drugs can be divided into two broad categories: intrinsic (natural) and acquired (secondary). Intrinsic resistance indicates that before receiving chemotherapy, resistant-mediating factors pre-exist in tumor that make chemotherapy ineffective from the outset. Acquired drug resistance can develop during chemotherapy of tumors that were initially sensitive and after several cycles of treatment become insensitive to anticancer drugs [1]. Loss of sensitivity to specific chemotherapeutic agent may not directly cause the loss of sensitivity to other chemotherapeutic agents. Additionally, if resistance to particular cytostatic drug led to the resistance to another, structurally related drugs, this type of resistance is termed cross-resistance. However, there have been described cases where tumors resistant to one type of drugs were found to be resistant to several other anticancer drugs that are often quite different in both structure and mode of action. This phenomenon has been described as multidrug resistance (MDR) phenotype [2].

1.1 Multidrug resistance

Multidrug resistance is defined as a resistance of tumor cells to the cytostatic or cytotoxic actions of multiple, structurally dissimilar and functionally unrelated chemotherapeutic agents commonly used in cancer chemotherapy [3]. MDR phenomenon was first described in lung cell line isolated from chinese hamster and P388 murine leukemia cell line in 1970. The authors observed a cross-resistance of actinomycin D resistant cells on vinblastine and daunomycin. Other working groups have shown that this cross-resistance extends to the vinca alkaloids, anthracyclines and

even to mitomycin C [4]. The cytotoxic drugs that are most frequently associated with MDR are hydrophobic, amphipathic natural products, which are often used in clinical practice, such as the taxanes (paclitaxel and docetaxel), vinca alkaloids (vinorelbine, vincristine and vinblastine), anthracyclines (doxorubicin, daunorubicin and epirubicin), epipodophyllotoxins (etoposide and teniposide), antimetabolites (methotrexate, 5-fluorouracil, cytarabine, 5-azacytosine, 6-merkaptopurine and gemcitabine) topotecan, irinotecan, dactinomycin and mitomycin C [5-8].

A number of mechanisms have been described to explain the phenomenon of MDR. They have been broadly classified into cellular and non-cellular mechanisms of multidrug resistance [7].

1.1.1 Non-cellular mechanisms of resistance to chemotherapy

Non-cellular drug resistance is typically associated with solid tumors which exhibit unique physiological properties. Solid possess vasculature that is characterized by higher geometric flow resistance, where blood vessels are fenestrated, tortuous and the branching pattern is different from normal vessels. Consequently, poor vascularization and heterogeneity in tumor vessels can result in reduced drug access to tumor and thus protect it from cytotoxicity. The extracellular microenvironment associated with solid tumor consists of extracellular matrix, cancer-associated fibroblasts, immune cells and it is characterized by increased interstitial fluid pressure due higher vasculature permeability and near absence of functional lymphatic vessels. These unique features of tumor microenvironment provide protection for cancer cells from cytotoxic agents [9]. Moreover, physiological properties of solid tumors also result in tumor regions that are deficient in nutrients and oxygen or acidic regions due to lactic acid generation by hypoxic tumor cells. Such properties may also participate in tumor resistance for example in the case of weak basic anticancer drugs, where cellular uptake is dependent on the pH gradient across membrane [7].

1.1.2 Cellular mechanisms of resistance to chemotherapy

Cellular mechanisms of drug resistance are mediated by different mechanisms operating at different level of cytotoxic action of the drug from decrease of drug accumulation in the cell to the abrogation of apoptosis (Figure 1.1). Such mechanisms can be classified into two major categories: non-classical MDR phenotypes and transport-based classical MDR phenotype [10].

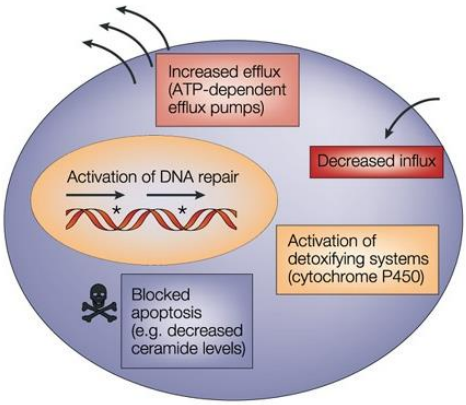

Figure 1.1: Mechanisms of cellular multidrug resistance. Cancer cells may become resistant to anticancer drugs via several distinct mechanisms. One possible way how cancer cells become resistant results from overexpression of ATP-dependent efflux pumps with broad drug specificity. This mechanism generally known as a classical multidrug resistance mediates drug efflux resulting in reduced intracellular accumulation of anticancer agents. Multidrug resistance can also be provided by activation of detoxifying systems, DNA repair mechanism or as a result of reduced drug influx for the agents that enter the cell by the means of endocytosis. Finally, resistance may occur as a result of defective apoptotic pathway or expression of anti-apoptotic proteins. Adopted from Gottesman et al. [10].

1.1.2.1 Non-classical MDR phenotypes

The term non-classical MDR is used to described non-transport resistant mechanisms. This type of resistance can be caused by altered activity of specific enzymes such as glutathione S-transferase (GST) or topoisomerase which can decrease the cytotoxic activity of some anticancer drugs in a manner independent of intracellular drug concentration. In addition, changes in the balance of proteins that control apoptosis can also reduce chemosensitivity, since most anticancer drugs exert their cytotoxic effects via apoptosis [11].

1.1.2.1.1 Glutathione S-transferases

Glutathione S-transferases (GSTs) are phase II detoxification enzymes involved in protection against drugs and xenobiotics. Specifically, GSTs catalyze the conjugation of glutathione (GSH) with endogenous and exogenous compounds resulting in excretable polar molecules. GSTs are divided into two distinct groups the membrane-bound microsomal GSTs and cytosolic GSTs. Cytosolic GSTs are divided into six classes (*α, μ, ω, π, θ* and *ζ*) which share about 30% sequence homology [12].

Cancer cells can acquire resistance to chemotherapy by overexpressing GSTs enzymes that may increase detoxification and circumvent the cytotoxic action of anticancer drugs. Overexpression of several GSTs has been associated with resistance to variety of anticancer drugs currently used in cancer therapy such as chlorambucil, cyclophosphamide, cisplatin and mitoxantrone [13]. For example, the overexpression of α class GST has been correlated with resistance to alkylating agents and doxorubicin [14]. Moreover, overexpression of μ class GST has been associated with chlorambucil resistance in human ovarian carcinoma and with poor prognosis in childhood acute lymphoblastic leukemia [15].

Beside active role of GSTs in the detoxification of anticancer drugs, several studies have demonstrated a regulatory role of the π and μ GSTs classes of in mitogen-activated protein (MAP) kinase pathway and therefore in cellular survival and death signaling, particularly through inhibition of c-Jun-terminal kinase (JNK) signaling pathway [12]. Adler et al. demonstrated that elevated level of GSTs inhibits the activation of JNK and thus protect tumor cells from apoptosis [16]. This link between GSTs and MAP kinase pathway may provide an explanation for numerous examples of drug resistance to anticancer agents that are neither subject to conjugation with GSH, nor substrate for GSTs but induce apoptosis dependent on MAP kinase pathway, specifically via JNK [12].

1.1.2.1.2 Deregulation of apoptosis

Anticancer drugs typically induce apoptosis. This type of cell death is characterized by nuclear condensation and DNA fragmentation. However, anticancer drugs can also trigger responses that promote cancer cell survival [17].

Tumor cells can acquire resistance to apoptosis by various mechanisms. The most important mechanism is overexpression of anti-apoptotic proteins from Bcl-2 family. It has been demonstrated that overexpression of Bcl-2 can confer resistance to the cytotoxic effects of a number of anticancer drugs including doxorubicin, taxol, etoposide, camptothecin, mitoxantrone and cisplatin [18]. When the high level of Bcl-2 is mechanism of resistance in tumor cells, it has been shown that the effects of anticancer drugs are cytostatic rather than cytotoxic [19]. Moreover, other proteins from Bcl-2 family have been demonstrated to play a role in regulation of chemotherapy-induced apoptosis. These include the anti-apoptotic proteins such as Bcl-xL and MCL1. Furthermore, down regulated expression of pro-apoptotic proteins such as Bax, Bad, and Bak as well as various BH-3 only proteins could be also a mechanism how cancer cells became resistant to chemotherapy-induced apoptosis [20].

1.1.2.2 Transport-based classical MDR mechanisms

The classical MDR is generally mediated via overexpression of ATP-binding cassette (ABC) transporters. 48 human ABC genes have been identified so far, and they are divided into seven subfamilies on the basis of their sequence homology. Resistance mediated by ABC transporters is a result of decreased intracellular drug concentrations due to intensive ATP-dependent drug efflux. Resistance of cancer cells can also be mediated by others transporters which does not belong to ABC superfamily [21].

1.1.2.2.1 Vaults in the drug resistance

Vaults were first described in the middle 1980s as a large ribonucleoprotein (RNP). After twenty years later, characterization of 110 kDa protein, called lung resistance related protein (LRP), isolated from resistant but P-gp negative lung cancer cell line lead to discovery that this protein is identical to human major vaults protein (MVP). These finding represented firs observation of the link between MDR and the vaults [22]. The vaults are multimeric structures made by multiple copies of four proteins, the MVP, two minor vaults proteins termed as vault poly-(ADP-ribose) polymerase (VPARP), telomerase associated protein 1 (TEP-1) and untranslated vault RNA (VRNA) [23].

The mechanism which links the MDR to expression of vaults has not been yet fully described. Several studies suggested that vault protein acts as transporter of molecules from nucleus to the cytoplasm and it is believed that vault has ability to arrest molecules in vesicles and transporting them out of the cell (Figure 1.2) [24]. The evidence of correlation between high expression of vault and development of resistance was first observed in patients with acute myeloid leukemia (AML) [25]. Confirmation of this observation has been observed in various solid tumors such as ovary and kidney [26]. However, several studies did not confirm the correlation between overexpression of vault and resistance to anticancer drugs such as etoposide, daunorubicine and vincristine. These uncertain results indicate the multifactorial nature of MDR phenomenon [27].

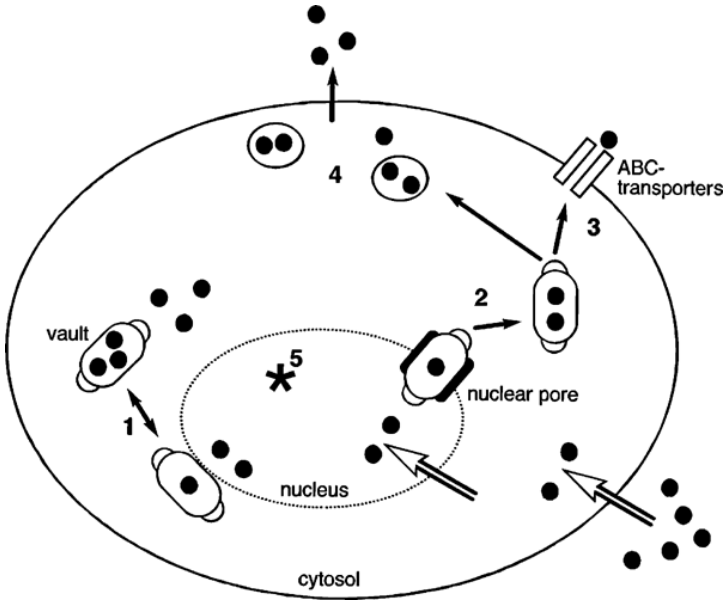

Figure 1.2: Scheme of the hypothetical role of vaults. Based on vaults transport function and cellular distribution of anticancer drugs in vault-overexpressing cell line was proposed that vaults may be involved in development of multidrug resistance. Vaults may mediate resistance by transporting anticancer drug away from their intracellular targets (2) or by transporting them to efflux pumps (3) or even entrapped anticancer drug into the exocytotic vesicles (4). Moreover, it has been proposed that vaults may also play important role in the intracellular compartmentalization and transport of various biomolecules, particularly as it concerns nucleocytoplasmic transport (1). Adopted from Mossink et al. [28].

1.1.2.2.2 Copper transporter in MDR

The correlation between expression of copper transporters and degree of resistance to platinum-based chemotherapeutics has been observed. Based on these findings, it has been proposed that copper homeostasis mediated by the copper transporters such as high affinity copper uptake protein 1 (CTR1) and copper-transporting ATPases known as ATP7A and ATP7B is involved in regulation of platinum-based drugs efflux [29-30].

The role of CTR1 in platinum-based drug resistance was demonstrated via transfection of human *CTR1* cDNA in human cancer cells which resulted in development of cisplatin resistance [31]. Moreover, the role of ATP7A and ATP7B in transport of platinum-based chemotherapeutics was demonstrated by transfection into human epidermoid carcinoma and human ovarian carcinoma, which in both cell line lead to resistance to cisplatin and its two derivatives, carboplatin and oxaliplatin. This were further confirmed by finding the correlation between overexpression of ATP7A and ATP7B and the resistance to platinum-based chemotherapeutics also in other types of cancers [32-34].

1.2 ABC transporters superfamily

The ATP-binding Cassette (ABC) transporter superfamily is one of the largest and most broadly expressed protein superfamilies known. Members of this family are found in all living organisms from microbes to humans. The wild-spread presence of these proteins with a relative conserved structure and function suggests their fundamental role [10]. The vast majority of ABC transporters is responsible for the active transport of a wide variety of compounds across biological membrane including phospholipids, ions, bile acids, drugs and other xenobiotics. This is critical for many aspects of cell physiology, including the uptake of nutrients, energy generation and cell signaling [35].

The ABC superfamily divide into two subfamilies. The larger one contains primary active transporters that utilize the energy of ATP hydrolysis to translocate substrates across cellular membranes. These ABC transporters (P-glycoprotein or breast cancer resistant protein) are highly expressed in the gut, liver, kidney and epithelia of

various tissues where they perform barrier functions [36]. The second subfamily comprises ABC proteins localized in the cytosol or nucleus and they employed in chromatin organization, DNA repair, telomere maintenance and mRNA trafficking through the nuclear pore [35]. 48 ABC transporters have been identified in humans so far, and they are divided into seven subfamilies (ranging from ABCA to ABCG) based on gene organization and location, configuration of domains and sequence homology [37]. Mutations in genes coding human ABC transporters have been linked to various disorders such as Tangier disease (mutation in ABCA1), progressive familial intrahepatic cholestasis type 2 (mutation in ABCB11) or Dubin-Johnson syndrome (mutation in ABCC2). Furthermore, ABC transporters have been implicated not only in the development of resistance of tumors to anticancer drugs but also in antibiotic resistance of pathogenic microorganisms [10].

1.2.1 Structure of ABC transporters

In first publications, the ABC structures were studied for monomers, and the authors suggested formation of dimers, in which two ABC unit were positioned "back-to-back" orientation. However, this assembly represents an energetically unfavorable interaction of the two monomers and suggests two highly exposed nucleotide binding sites [38]. The later studies documented that the two functionally interacting ABC subunits dimerize in a "head-to-tail" orientation. This orientation was first suggested in studies describing Rad50cd structure (bacterial ABC-ATPase) [39]. Later, similar structures were found in the ABC domains of various bacterial and human ABC transporters. The high-resolution structures are only available for bacterial ABC transporters so the structure and mechanisms of action of ABC transporters are based on these data and models [40-42].

The canonical architecture of ABC transporters comprises two transmembrane domain (TMD) and two cytosolic nucleotide-binding domains (NBDs), also known as ATP-binding cassettes [43]. The structural organization of ABC transporter is shown in Figure 1.3 [44].

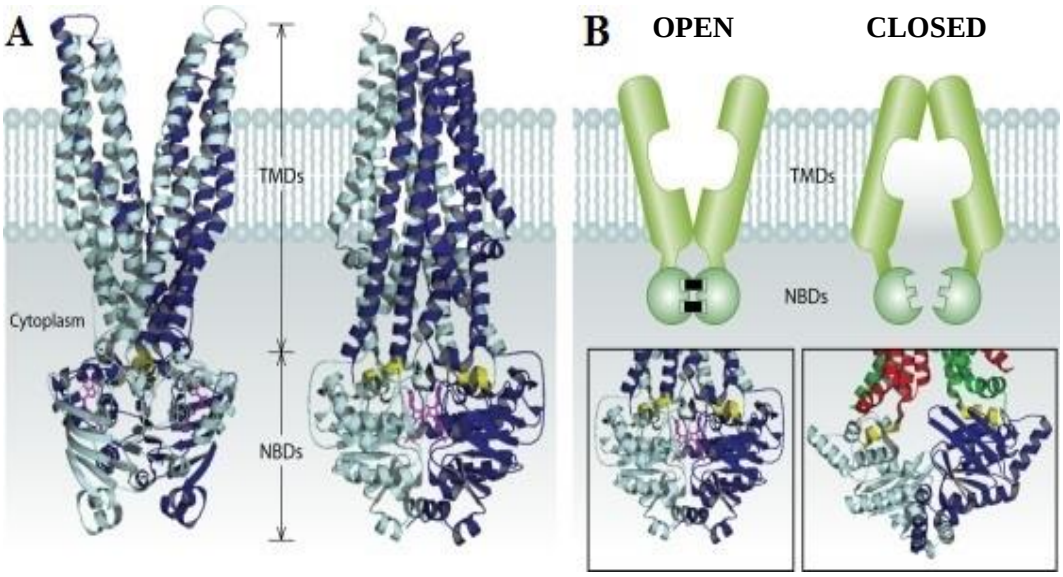

Figure 1.3: Structure model of ABC transporter. (A) Structure of the complete Sav1866 ABC exporter illustrated from two angels rotated by 90° around the vertical axis. Each subunit (identified by different shades of blue) contains one transmembrane domain connected to one nucleotide-binding domain. The coupling helices are highlighted in yellow. (B) Representative models of open and closed conformation of ABC transporter. The model illustrates link between ATP hydrolysis with conformation changes in ABC transporter molecule. Conformational changes are transmitted from the NBD with ATP hydrolysis to the TMDs through the coupling helices (highlighted in yellow). Adopted from Cuthbertson et al. [45] and Dawson et al. [46] with minor changes made.

1.2.1.1 Transmembrane domains

The transmembrane domains contain poorly defined substrate-binding sites and transmembrane channel-forming part for unidirectional import or export [47]. The TMDs extend beyond the phospholipid bilayer as intracytosolic loops (ICLs) that form the interface between the NBDs and TMDs (Figure 1.3). The ICLs are helical bundles, with each containing α-helix at right angles of the bundle and which fits into a groove between the core and helical subdomains of the NBDs (Figure 1.4). The coupling helices (CH1 and CH2) are proposed to transmit the energy of ATP hydrolysis to substrate transport [46-47].

1.2.1.2 Nucleotide-binding domains

Each NBD has a roughly L-shaped configuration and contains a number of conserved sequence motifs. These comprise the Walker A and Walker B consensus motifs for nucleotide binding, of which Walker A (or phosphate-binding "P-loop") is a

glycine-rich motif (consensus G-X-X-G-X-G-K-S/T), while the Walker B motif has consensus sequence H-H-H-D, where ”H” is any hydrophobic residue [48]. Additionally, there is the LSGGQ signature sequence or C-motif that is unique and defines the ABC superfamily. Moreover, the Q-loops, D-loops and H-loops help to complete the ATP-binding site and are also involved in the catalytic activity. The NBD is constituted from RecA-like subdomain (containing Walker A and Walker B motifs), ABCβ subdomain that is integrated into a core subdomain and a helical subdomain which contains the LSGGQ signature motif. The helical subdomain is flexibly attached via Q-loop at its N-terminus and via P-loop at its C-terminus (Figure 1.4) [49-51].

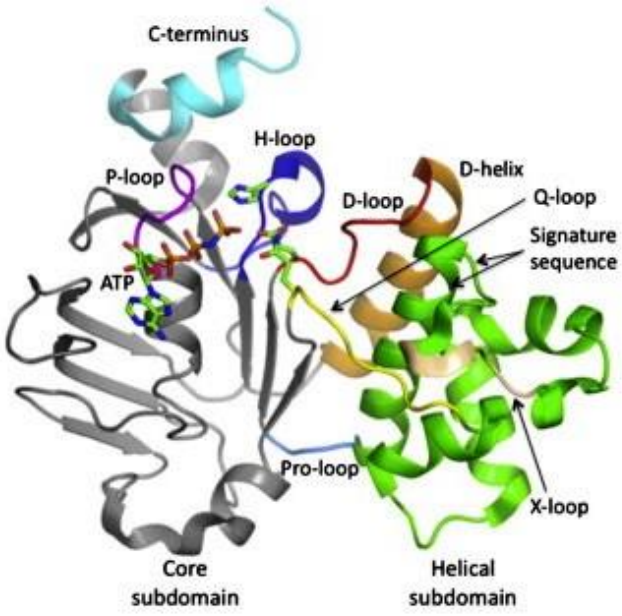

Figure 1.4: Nucleotide binding domain monomer with the major conserved motifs and residues shown. NBD monomer is in ribbon representation with ATP. The core subdomain is colored grey and the helical subdomain is green. The Walker A (P-loop) motif is colored magenta. The catalytic glutamate is depicted at the star of the D-loop (red) followed by the D-helix (orange). The Q-loop is in yellow and the H-loop is in dark blue. The C-terminus is colored cyan and the short orange helix and loop in the center of the helical subdomain is the X-loop. The Pro-loop is in light blue connecting core and helical subdomain. Adopted from Gregor et al. [41] with minor changes made.

The NBDs form a head-to-tail sandwich dimer in which each LSGGQ motif is opposed to the Walker A and Walker B of the opposite monomer, forming ATP-binding site. The D-loops run in antiparallel fashion between the active sites at the dimer interface and communicate with the active sites from opposite monomers [51-52]. The conserved

Q-loop glutamine is involved in the organization of the hydrolysis-capable active site. The strategic location of Q-loop and its flexibility suggests additional roles in the separating rotation of the subdomains after hydrolysis [53-54].

1.2.2 ATPase catalytic cycle

Transport of substrate across the membrane by ABC transporter is powered by hydrolysis of ATP within two cytoplasmic NBDs. First evidences that transport of substrates is coupled to hydrolysis of ATP were performed with bacterial ABC transporters [55-56]. Subsequently, Senior and colleagues defined the biochemistry of the ATPase cycle of the mammalian P-glycoprotein [57]. The recent studies proposed two potential models in order to explain the sequence of events in the efflux cycle [40].

1.2.2.1 The ATP-switch model

The ATP-switch model was devised to explain the function of ABC transporters, especially how cycling between high and low-affinity states for ligand on different sides of membrane are coupled to the ATP catalytic activity. This model is also known as "tweezers-like" or "processive clamp" model. For simplicity, this model is basically a switch between two principal conformations of the NBDs, formation of a closed dimer upon binding two ATP molecules at the dimer interface, and dissociation to an open dimer facilitated by ATP hydrolysis and release of P_i and ADP [58].

The characteristic facet of this model is that transport is divided into four steps and involving transmission from one step to next one via conformational changes. The first step in the ATP- switch model is binding of substrate to the TMDs high-affinity binding site in the nucleotide-free form of NBD dimer conformation. Binding of substrate to the TMDs induces conformational changes in NBDs which lower the activation energy for ATP-dependent dimerization. The second step is represented by formation of the close NBD dimer around the bound ATP molecules which induces a large conformational change in the TMDs to initiate substrate translocation. These conformational changes allow conversion and relocation of high affinity binding site from the cytoplasmic face of the membrane to a low-affinity binding site at the extracellular face of the membrane. This model assumes that ATP binding and closed

dimer formation rather than ATP hydrolysis generate energy to utilized in key conformational changes involved in substrate transport [51]. In the third step the hydrolysis of the ATP initiates transition of the NBD closed dimer to the open dimer configuration and return the transporter to its basal state. For some ABC transporters such as P-glycoprotein hydrolysis of both ATPs is necessary for completion of transport cycle. In the other ABC transporters, for example MRP1 and CFTR, hydrolysis of only one ATP is sufficient [59-60]. However the trigger which initiates ATP hydrolysis is still unknown. After hydrolysis, released Pi remains within the NBD dimer, which is consistent with finding that one ATP and one ADP are present in some kind of transition state. Urbatsch et al. assumed that this transition state has distinct conformation of the TMDs and it retains a low-affinity for substrate [61]. The sequential release of Pi and ADP restores the transporter to its basal state in the final fourth step. The remaining ADP in transition state is unable to stabilize the NBD dimer and the dissociation occurs after which the energy stored in the torsion of NBD helix is released to displace ADP (Figure 1.5) [51].

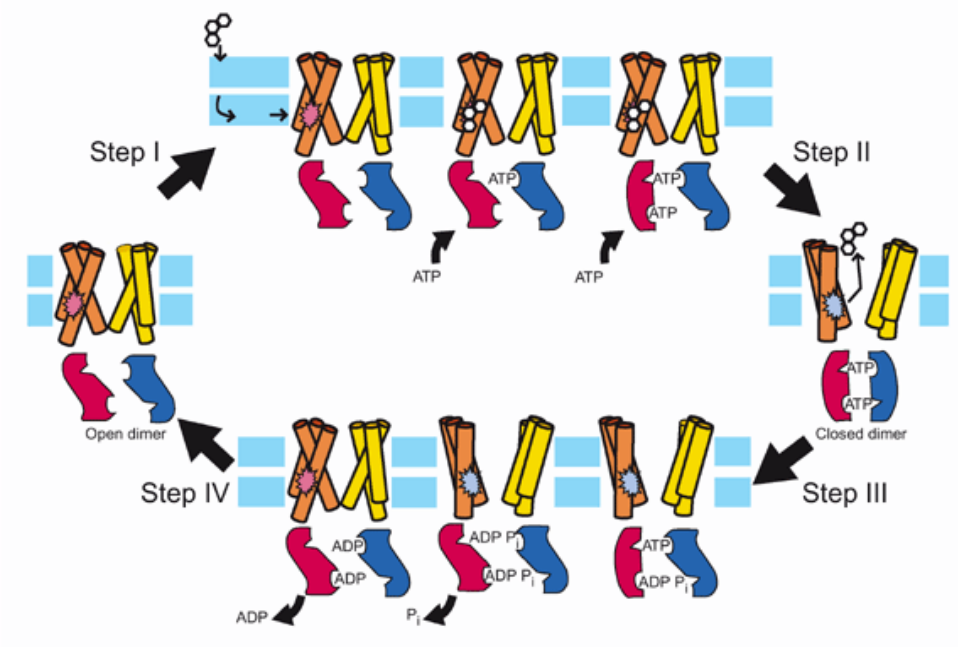

Figure 1.5: Schematic chart of the ATP-switch model of the ABC transporter. The TMDs are shown as cylinder spanning membrane and the NBDs as blue/red shapes at the cytoplasmic site of the membrane. The substrate binding site is shown as star exposed to the inner leaflet of the membrane in the open dimer configuration or extracellularly in the closed dimer configuration. Adopted from Higgins et al. [62].

1.2.2.2 The constant contact model

The major difference from switch model is that active sites hydrolyze ATP and open alternately with the two NBDs remaining in contact throughout catalytic cycle [57, 63]. Basically, for each catalytic site there are two distinct substrates ATP-open and ATP-occluded or ADP(Pi)-open and ADP(Pi)-occluded, allowing nucleotide exchange. Thus, when ATP-bound active site is occluded the opposite site is empty and ATP hydrolysis occurs. Then the occluded active site with hydrolysis products bound, induce in empty low-affinity site switch to the high-affinity state, enabling ATP binding. After ATP binding to the empty site, the Pi is released from the occluded post-hydrolysis site promote opening of the ADP-bound site and release ADP and occlusion of the ATP-binding site. Thus, when one site is open sufficiently for nucleotide release without fully separated NBD monomers, then as this site closes with a new ATP molecule, the opposite catalytic site becomes primed for hydrolysis. This process is repeated in alternating cycle [64].

1.3 ABC transporters in MDR

It is well know that many human cancers, such as breast, ovarial, and colon carcinomas or leukemias develope cross-resistance to a broad spectrum of structurally unrelated cytotoxic drugs such vinca alkaloids, anthracyclines or taxanes [65]. MDR phenotype is mainly associated with overexpression of certain ABC transporters [10]. To date, 15 members of ABC transporters family have been implicated in potentially conferring resistance to chemotherapeutic agents. However, three ABC transporters appear to account for most observed MDRs in human malignancies, namely P-glycoprotein, multidrug resistance protein 1 (MRP1) and breast cancer resistant protein (BCRP). Together, these three transporters are able to mediate efflux of wide range of anticancer drugs that are commonly used in cancer treatment [66].

1.3.1 P-glycoprotein

Resistant phenotype in cancer was for the first time linked to plasma membrane glycoprotein in the 1976, which has been named P-glycoprotein (P-gp, ABCB1 or also

designated as MDR1) for its ability to reduce the apparent cellular permeability of drugs [67]. P-glycoprotein belongs to sub-family B of the ABC transporters superfamily, containing 11 transporter genes, and is the most intensively investigated protein related to the MDR. P-gp is expressed in different tissues and protect them from wide range of endogenous and exogenous substances. Additionally, P-gp appears to regulate hormone distribution and probably may regulate cell differentiation, proliferation, immune response and programmed cell death [68].

1.3.1.1 Structural characteristics of P-gp

P-gp exists in a number of different isoforms which have over 70% sequence homology and are encoded by a family of closely related genes. Mice have two closely related homologues of ABCB1 (*Abcb1*a and *Abcb1b*). In humans, P-gp is encoded by two multidrug resistance genes *MDR1* and *MDR3*. Both genes are located on the long arm of chromosome 7 (7q21). MDR phenotype is associated with *MDR1* gene only [69].

MDR1 gene have 28 exons encoding 1280 amino acids. The first evidence for genetic variability was found in 1994 by Stein and colleagues. Today, over 50 polymorphisms (single nucleotide polymorphisms, insertion and deletion) have been identified in *MDR1* gene (Figure 1.6). Among them, several single-nucleotide polymorphisms (SNPs) have been identified to be responsible for alternated expression and function of P-gp. The best known variants associated with the change of the P-gp function are 1236C>T and 2677G>T/A. “Silent” polymorphism caused by 3435C>T was associated for example with decrease of intestinal expression of P-gp and increasing digoxin plasma levels after oral administration [70-73].

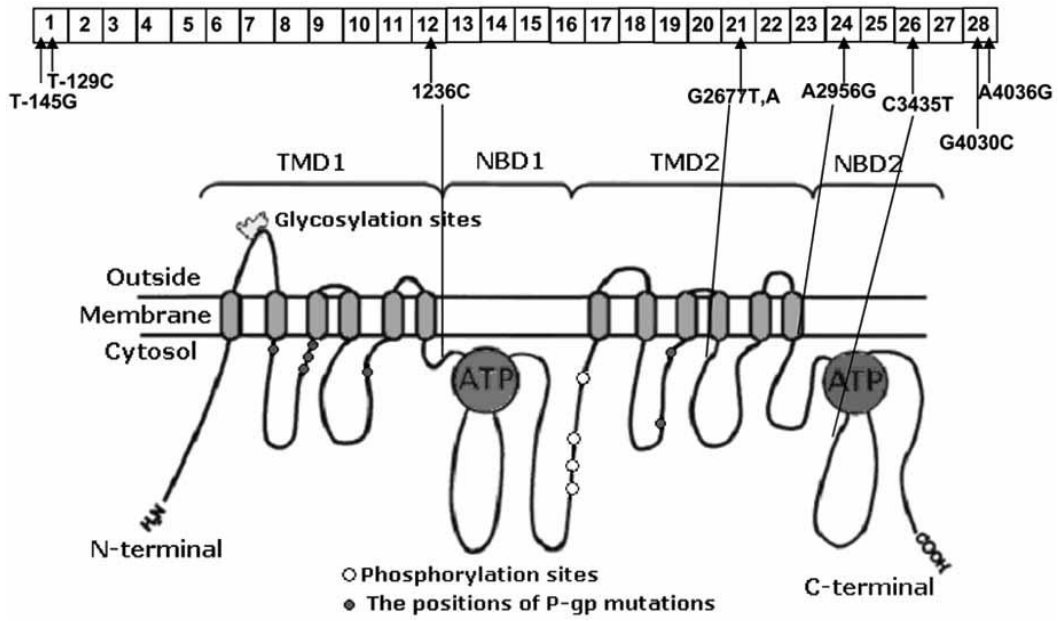

Figure 1.6: Structural model of P-glycoprotein. P-gp is a 170 kDa transporter with 12 transmembrane segments (form two halves composed of the six transmembrane α-helices each) and two cytosolic NBDs containing an ATP-binding sites. Both N-terminus and C-terminus are located intracellularly and the first extracellular loop contains three N-glycosylation sites. The two closely halves of the molecule are separated by highly charged linker region which is phosphorylated at several sites by protein kinase C (PKC) and protein kinase A (PKA). So far, more than 50 naturally occurring polymorphisms have been identified. The vast majority of them are silent, however; some of the *MDR1* gene mutations are associated with altered oral bioavailability of the P-gp substrates, variation in P-gp expression levels and susceptibility to human diseases. Adopted from Li et al. [74].

P-gp is a 170 kDa transmembrane protein which is organized in two tandem repeats of 610 amino acids joined by a linker region consisting of 60 amino acids. The protein have raised from gene duplication fusing two related half molecules. P-gp protein is synthesized in the endoplasmic reticulum as a glycosylated intermediate with molecular weight 150 kDa and is associated with chaperons such calnexin and Hsp70 (70 kDa heat shock protein) during folding [75-76]. P-gp is modified in Golgi apparatus after proper folding and prior to export to the cell surface. P-gp is glycosylated in the Golgi apparatus at three asparagine residues within the first extracellular loop. The role of glycosylation is not fully understood. The evidence suggests that the absence of glycosylation does not directly affect the P-gp ability to confer drug resistance, however, glycosylation may play a role in trafficking and stability of P-gp. Additionally, P-gp is also substrate for protein A and C kinases and can be phosphorylated at the four residues in linker region [77].

1.3.1.2 Mechanism of P-gp action

Two TMD enclose a very large (6000 $Å^3$) cavity which appears that has ability to accommodate more than one drug molecule simultaneously. The mechanism by which P-gp transport drugs across the plasma membrane is not completely understood. However, several models have been proposed including hydrophobic vacuum cleaner and flippase model (Figure 1.7) [78-80].

The hydrophobic vacuum cleaner model suggests that P-gp expels the lipophilic molecules embedded in the inner leaflet of the plasma membrane directly to the external aqueous medium. This model assumes that the substrates have access to the binding sites of P-gp through gates formed between TMDs in plasma membrane. Thus the transporter is able to bind and transport substrates before they enter the cytosol [79].

The flippase model assumes that P-gp work as a drug translocase or flippase, moving its substrates from in the inner to the outer leaflet of the membrane. After reaching the outer leaflet, substrate would then either passively diffuse into extracellular aqueous phase, which is very fast process, or move back to the inner leaflet by spontaneous flip-flop. In order to maintain the substrate concentration gradient across the membrane, this model suggests that the rate of passive transmembrane flip-flop is much slower than P-gp mediated flipping so that the substrate concentration remains higher in the outer leaflet.

Both models make the assumption that the substrate first solubilize in the lipid phase of cytoplasmic membrane prior to interacting with P-gp [81].

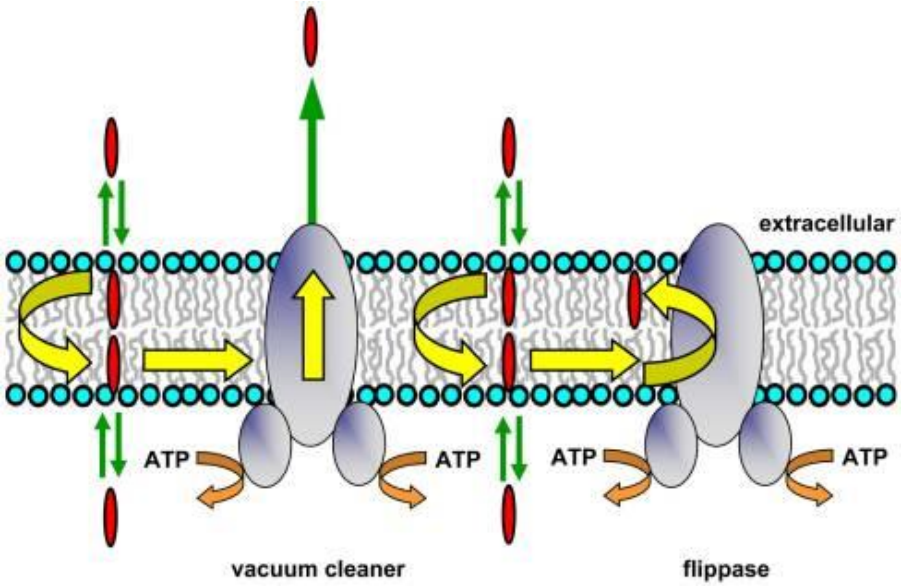

Figure 1.7: Hydrophobic vacuum cleaner and flippase model of P-glycoprotein activity. Adopted from Sharom et al. [82].

1.3.1.3 Biological role of P-gp

P-gp is expressed in many human tissues and organs, particularly with excretory role such as kidney (on the brush border of proximal tubule cells), gastrointestinal tract (on the apical membrane of mucosal cells in the small intestine), liver (on the canalicular apical membrane of hepatocytes) and on the luminal surface of capillary endothelial cells of the blood brain barrier [83]. Although P-gp is primarily expressed on plasma membrane, it has been shown that it is also localized intracellularly such as endoplasmic reticulum (ER), Golgi apparatus (GA), endosomes and lysosome [84-87]. The physiological significance of P-gp in healthy tissue is probably in the transport of endogenous molecules and metabolites. Possible endogenous substrates include phospholipids, glycolipids and amyloid-β peptides [88]. Recent studies indicate that there are few common features among P-gp substrates. They are usually organic molecules containing aromatic groups but linear or circular non-aromatic molecules may also be transported. Most of the substrates are uncharged or weakly charged and basic in nature however acidic molecules such as methotrexate (MTX) can also be transported, albeit at a low rate. The only common feature for all P-gp substrates is their amphipathic nature [89].

P-gp interacts with many drugs, including a large number of anticancer drugs, anti-histaminiss, immunosuppressive agents, cardiac glycosides, HIV protease inhibitors, calcium channel blockers and antibiotics [74].

It is well known that cytotoxic effects of chemotherapeutics like vincristine, vinblastine, doxorubicin, docetaxel or paclitaxel promotes transcription of P-gp. The mechanism of their capacity to induce MDR is of great importance and it has been not fully understand so far. The P-gp expression in MDR tumors might be also enhanced upon application of compounds that are not substrates of P-gp but are a ligands of several others receptors such as pregnane X receptors (PXR) or constitutive androstane receptors (CAR), in which have been shown transcriptional control of P-gp expression [90-92].

1.3.2 Multidrug resistance proteins

The multidrug resistance protein (MRP) subfamily, the C subset of the ABC transporter superfamily, is composed of twelve members and nine of them are involved in MDR. The other three members of the MRP subfamily, namely cystic fibrosis transmembrane conductance regulator (CFTR or ABCC7), sulfonylurea receptor 1 (SUR1 or ABCC8) and ABCC9 (SUR2) are not involved in conferring MDR. ABCC7 is regulated chloride channel whereas ABCC8 and ABCC9 are intracellular ATP sensors and regulate the specific K^+ channel permeability. On the basis of their structure, the nine main MRPs can be divided into two groups. One has a typical ABC transporter structure with four domains comprising two TMDS and two NBDs. These can be referred as a short MRPs and include MRP4, MRP5, MRP8 and MRP9 (ABCC4, ABCC5, ABC11 and ABCC13, respectively). The second group, which includes MRP1, MRP2, MRP3, MRP6 and MRP7 (ABCC1, ABCC2, ABCC3, ABCC6 and ABCC7), have an additional TMD (TMD_0) and are designated as long MRPs (Figure 1.8) [93].

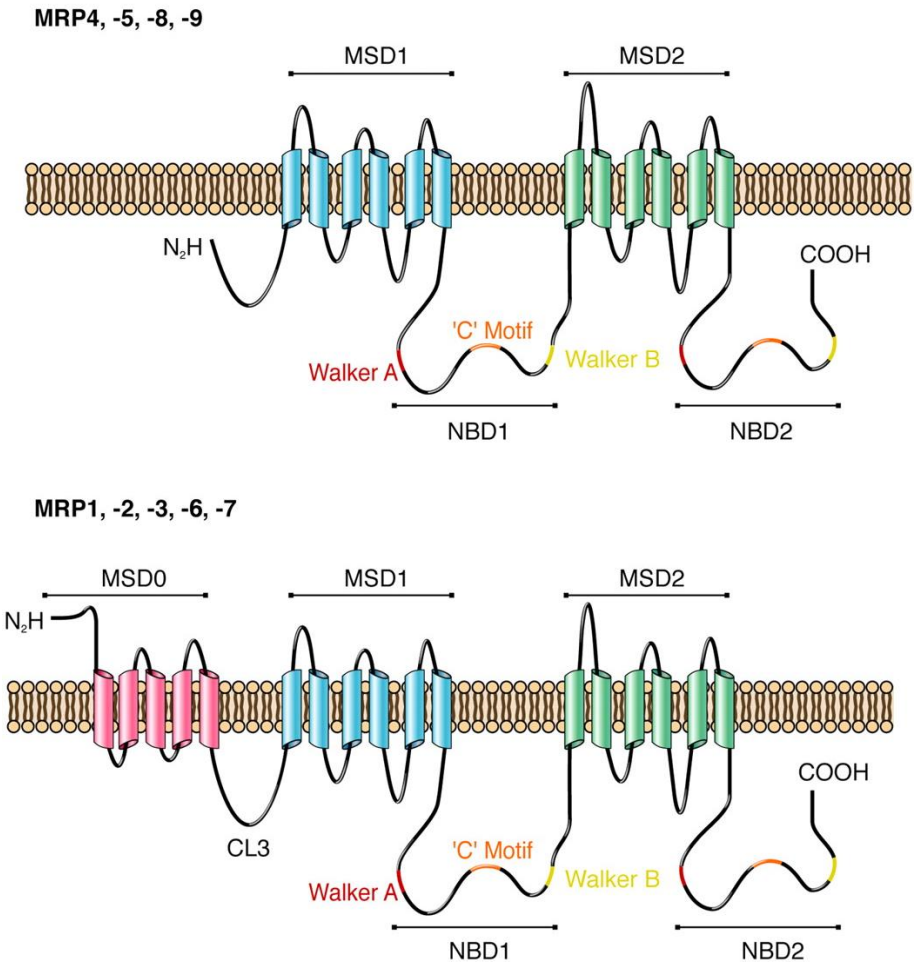

Figure 1.8: Topology of short and long MRPs. The MRPs can be divided into two subfamilies, long (MRP1, -2, -3, -6, and -7) and short (MRP4, -5, -8, -9, and 10). The short MRPs have typical ABC transporter structure with two membrane spanning domains (MSDs) and two NBDs, while long MRPs have additional NH_2-terminal MSD. Adopted from Deeley et al. [93] with minor changes made.

1.3.2.1 MRP1 structure and function

Multidrug resistance protein 1 (ABCC1/MRP1) was the first drug transporting ABCC protein cloned. It was identified in 1992 to be responsible for multidrug resistance phenotype in an anthracycline selected human small cell lung carcinoma cell line H69/AR. The *MRP1* gene is located at chromosome 16 and spans approximately 200 kb. It contains 31 exons and encodes the protein of 1,531 amino acid residues with molecular weight 190 kDa [94]. The murine ortholog of human MRP1 (Mrp1 / Abcc1) was cloned in 1996 and these two proteins share 88% amino acid identity [95]. Nucleotide and protein sequences from several other animal species including rat, canine or bovine, share 88%, 92% and 91% amino acids identity with human MRP1,

respectively. Despite the high level of sequence homology between human MRP1 and MRP1 of other species, some differences in substrates specificity exists [96-98].

A large number of MRP1 gene polymorphisms have been identified. Most identified polymorphisms of MRP1 are single nucleotide polymorphisms, although repeats, insertion or deletion are also found. Most polymorphisms have frequency less than 5% and only few of them showed altered function. The interesting polymorphism is G1299T (exon 10) which was described to increase resistance to Dox and simultaneously to decrease transport of several negatively charged organic compounds [99]. The correlation between polymorphism of MRP1 and sensitivity to anthracyclines was also observed in non-Hodgkin lymphoma where patients with MRP1 polymorphism have more severe anthracyclines-induced cardiotoxicity than those with wild-type MRP1 [100].

MRP1 is expressed in various tissues with the relatively high levels found in the lung, testis, kidney, skeletal and cardiac muscle and peripheral blood mononuclear cells. It has also been found to be predominantly expressed in blood-tissue barrier, such as choroid plexus cells of the blood-cerebrospinal fluid barrier, the bronchial epithelium and apical syncytiotrophoblast membrane of the placenta [101-103]. In the most tissues, MRP1 is localized at the basolateral cellular surface. MRP1 transports a variety of endogenous molecules with significant biological activity. It has been shown *in vitro* that MRP1 is a high-affinity transporter of glutathione conjugated arachidonic acid derivate leukotriene C_4 (LTC_4) [104]. Additionally, most direct evidence demonstrating the physiological importance of MRP1 has come from studies of $Mrp1^{-/-}$ knockout mice. For example, study conducted by Robbiani et al. revealed that the expression of MRP1 is crucial for the migration of dendritic cells (DC) from peripheral tissues to the lymph nodes. Migration of DC was restored to the levels found in wild-type mice when exogenous LTC_4 were administered to the $Mrp1^{-/-}$ mice, demonstrating that LTC_4 efflux from these cells by MRP1 was critical for migration [105]. MRP1 also transports variety of conjugates of endogenous substrates including glutathione-conjugated prostaglandins and glucoronide or sulfate modified compounds.

Increased expression level of MRP1 have been also reported in numerous cancers such as non-small lung cancer (NSCLC), breast cancer, prostate cancer and several hematological malignancies. Overexpression of MRP1 provides resistance to various anticancer drugs such as anthracyclines, vinca alkaloids, epipodophylltoxins,

camptothecins and methotrexate. Interestingly, unlike P-gp MRP1 does not confer resistance to taxanes [106-109].

1.3.2.2 MRP2 structure and function

Multidrug resistance protein 2 (MRP2, ABCC2) is the second member of the MRP subfamily of ABC transporters. It was first cloned from rat hepatocyte and named as hepatocellular canalicular multiple organic anion transporter (cMOAT). MRP2 shares 49% amino acids sequence homology with MRP1 but it has different expression pattern [110]. Unlike MRP1 but similar to P-gp, MRP2 is localizes at the apical membrane of the polarized cells. While MRP1 is widely expressed in many tissues, MRP2 is mainly expressed in luminal membrane of the small intestinal epithelium and in the luminal membrane of the proximal tubules in kidney. Moreover, the mRNA of MRP2 has been reported in peripheral nerves, placenta, trophoblast and $CD4^+$ lymphocytes [110-113].

Spectrum of physiological compounds transported by MRP2 and MRP1 is similar, though with different affinities. MRP2, similar to MRP1, transports organic anions including sulfates, glucuronide, and GSH conjugates such as leukotriene D_4 (LTD_4), leukotriene E_4 (LTE_4), LTC_4, estradiol-17β ($E_2$17G), S-glutathionyl 2,4-dinitrobenzene (GS-DNP) and the some food-derived (pre-)carcinogens. Furthermore, MRP2 is involved in biliary elimination of endogenous conjugates such as conjugated bilirubin [114-115].

MRP2 showed similar substrate profile to MRP1 with respect to anthracyclines, vinca alkaloids, epipodophyllotoxins, and camptothecin derivatives CPT-11 and SN-38. However, MRP2 appears to have somewhat reduced potency. In addition, MRP2 is also able to confer resistance to cisplatin which distinguishes it from the MRP1 [116]. Further, MRP2 is involved in the hepatobiliary excretion of inorganic arsenic (As) and therefore may also be involved in protection against arsenic trioxide (As_2O_3) which is a compound recently used for the treatment of acute promyelocytic leukemia and is not a substrate of MRP1 [117].

1.3.2.3 MRP 3

Multidrug resistance protein 3 (MRP3, ABCC3) was first cloned shortly after MRP2 and within the MRP subfamily showed the highest degree of sequence homology (58%) to MRP1 [118]. MRP3 expression was found in adrenal glands, kidney, small intestine, colon, pancreas and gallbladder. Lower expression of MRP3 was found in the lungs, spleen, stomach and tonsils [119]. Substrate selectivity overlaps with that of MRP1 and MRP2 particularly in the transport of glutathione and glucuronate conjugates. However, the affinity of MRP3 for these substrates is considerably lower.

Overexpression of MRP3 has been found in hepatocellular carcinomas, primary ovarian cancer and adult acute lymphoblastic leukemia. MRP3 probably confer low levels of resistance to etoposide, teniposide, MTX and vincristine. In view of its ability to confer low resistance to several anticancer drugs, the overexpression of MRP3 might be clinically relevant to poor chemotherapeutic response, however, there is no solid evidence for such conclusion so far [113].

1.3.3 Breast cancer resistant protein

The first evidence of breast cancer resistant protein (BCRP) was discovered by analyzing cell lines selected for resistance to mitoxantrone (MTX), which is poor substrate for P-gp and MRP1. The name BCRP was derived as a result of its isolation from the drug resistant breast cancer cell line MCF-7/Adr. BCRP belongs to the ABC transporters superfamily and it is the second member of the G subfamily. Because orthologs of human BCRP has been identified in the other species, the gene symbol for human BCRP has been designated as a *BCRP/ABCG2* (upper case letter), while rodent (mouse or rat) BCRP has been determined as a *Bcrp1/Abcg2* (lower case letters). Regarding the CD nomenclature, BCRP was assigned to be CD338 [120].

1.3.3.1 Expression and function

The human ABCG2 gene is located on chromosome 4q22, contains 16 exons and 15 introns and spans over 66 kb. The BCRP is a 72 kDa glycoprotein (655 amino acids) containing a single NH_2-terminal cytosolic nucleotide-binding domain and six

transmembrane domain. Membrane insertion and function requires dimerization of BCRP and double glycosylation site at asparagine play significant role in maintaining protein stability.

Given the putative role of ABCG2 in pharmacology and cancer treatment, single nucleotide polymorphisms (SNP) and their impact on expression and function of BCRP may play a role in response to chemotherapy. BCRP gene harbors over 80 SNPs including missense, nonsense and frame-shift mutations with the potential of altering the interaction with the substrate. A mutational hot spot is located in position 482 in third transmembrane segment where single amino acid change (R482G or R482T) resulted in a gain-of-function mutant which had altered substrate specificity. These mutants showed increased resistance to mitoxantrone and anthracyclines and also increased transport capacity for rhodamine 123. In contrast, mutants were not able to transport methotrexate, which is a substrate of wild type ABCG2. Several other amino acid substitutions at R482 led to changes in substrate transport and specificity, indicating that this residue may play critical role in ABCG2 function as multidrug resistant ABC transporter (Figure 1.9) [121-122].

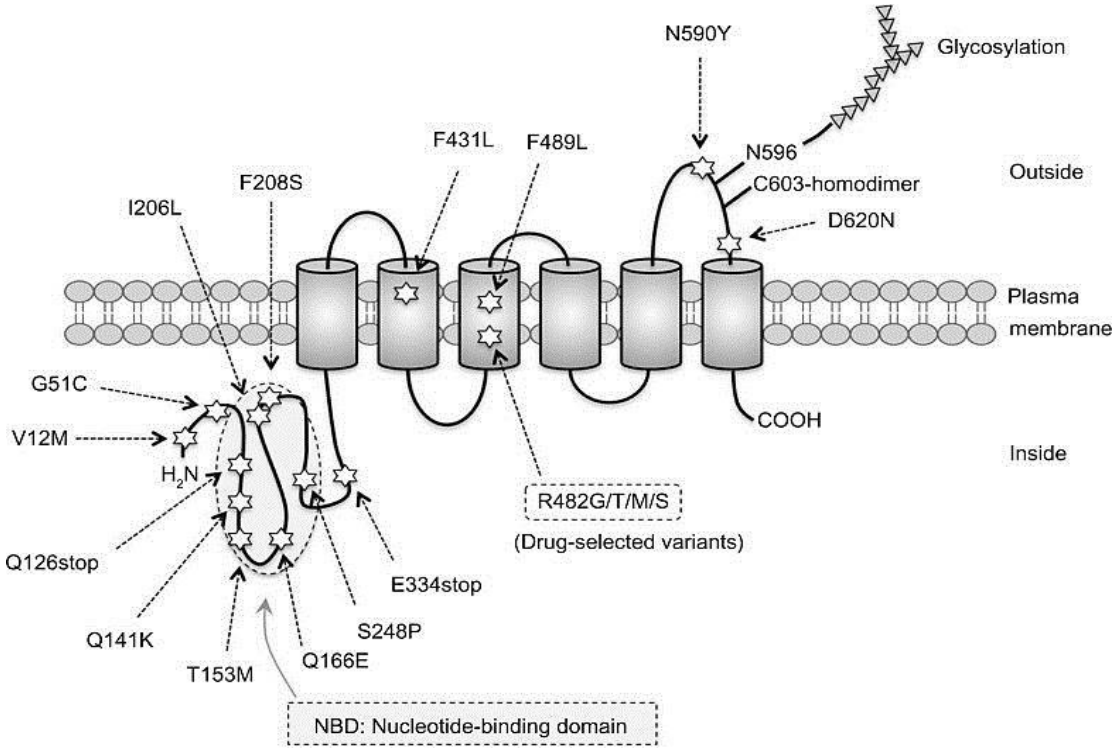

Figure 1.9: Structural model of ABCG2/BCRP protein with its amino acids variations. Single-nucleotide polymorphisms are marked with stars. Transmembrane domains are shown as cylinder. Adopted from Noguchi et al. [123].

1.3.3.2 BCRP in normal physiology

Studies on tissue distribution revealed that ABCG2 is preferentially located at the apical side of the membrane in tissues with excretory functions such as canalicular membrane of hepatocytes, apical membranes of capillary vessels in the blood-brain barrier and apical membrane of trophoblasts. Expression of ABCG2 was found in several other tissues including small and large intestine, kidney and endothelial cells. Interestingly, BCRP is expressed in a subset of progenitor cells where it acts as a marker of so called side population (SP), which is determined by efflux of Hoechst dye. SP cells generally possess stem cell features such as resistance to chemotherapeutic drugs, self-renewal, enhanced engraftment capacity and quiescence. ABCG2 appears to interact with heme and prevent accumulation of porphyrins, enhancing cell survival under hypoxic conditions.

1.3.3.3 BCRP role in multidrug resistance

ABCG2/BCRP is a broad specificity dug transporter and like P-gp confers cross-resistance to several unrelated classes of cancer chemotherapeutics such as mitoxantrone, anthracyclines or camptothecins. On the other hand BCRP does not transport taxols, cisplatin and verapamil (P-gp substrates), calcein (MRP1 substrate) or vinca alkaloids (substrate of both P-gp and MRP1). In contrast to P-gp, it appears that BCRP can transport both positively and negatively charged drugs, including sulfate conjugates [124]. The substrate spectrum of BCRP indicates, that its specificity partially overlaps with that of the P-gp and MRP1. Moreover, the list of BCRP substrates has currently expanded to include physiological compounds, dietary xenobiotics as well as novel anticancer drugs, Gleevec® (imatinib) and Iressa® (gefitinib) highlighting the importance of this protein [125-126].

1.4 Modulators of ABC transporters

MDR results mainly from overexpression of ABC transporters. Once MDR appears, chemotherapy is ineffective even when using high doses of drugs. Several strategies have been developed to overcome MDR such as using drugs that could bypass

the resistance mechanism including alkylating drugs, antimetabolites or anthracyclines modified in a way that they are not substrates for ABC transporters [127-128]. Other approaches include hammerhead ribozymes, antisense oligonucleotides or siRNAs directed against the expression of ABC transporter genes. However, the most straight forward method to overcome MDR is to use drugs that inhibit ABC transporters collectively also known as MDR modulators, reversers, inhibitors or chemosensitizers [129]. Inhibitors of ABC transporters show the same diversity of chemical structures as their substrates and act in several different ways. Most modulators interact with TMD and thus compete with the substrates for the drug-binding pocket. These chemosensitizers can be considered as competitive inhibitors. On the other hand, several hydrophobic steroid and flavonoid modulators do not compete with substrates but bind to the high-affinity binding site in the vicinity of the ATP-binding site in the NBD domain [130].

1.4.1 P-gp inhibitors

Identifying and development of potent P-gp inhibitors has been a primary interest in drug development for decades. When P-gp inhibitors are combined with anticancer drugs, their intracellular concentration reached within MDR cancer cells is significantly higher and sensitivity to this therapeutics could thus be restored [131].

There are three generations of P-gp inhibitors. The first generation of P-gp inhibitors comprises calcium channel blocker verapamil (VRP), immunosuppressive drug cyclosporine A (CsA) and calmodulin antagonists such as trifluorperazine, chlorpromazine and prochlorperazine. All compounds of the first generation were generally drugs with their own pharmacological activity and they suffered from high toxicity and/or low efficacy at tolerable doses. The search for non-toxic P-gp modulators resulted in analogues of the first generation agents, entitled as the second generation. These modulators such as structural analogue of VRP, dex-verapamil, and analogue of CsA, valspodar (PSC-388), showed improve efficacy at low doses, but serious adverse pharmacokinetics interactions with anticancer drugs since both the drugs and the modulators are substrates for cytochrome P450. Reduced clearance of the anticancer drug led to severely increased toxicity. Third generation modulators, including zosuquidar (LY335979), tariquidar (XR9576), ontogen (OC144-09) and

elacridar (GF 120918) have low toxicity and show both increased selectivity and high potency to inhibit P-gp [65, 132].

1.4.2 Inhibitors of MRPs

In contrast to P-gp, only a few modulators have been described for MRPs. Major obstacle for finding effective modulators is probably the preference of MRPs for anionic compound as a substrates and inhibitors. Because most anionic compounds enter cells poorly, it's difficult to reach sufficient intracellular concentration of the inhibitor. Only few inhibitors have been described for MRP1 so far, including biricodar (VX-710), leukotriene D_4-receptor agonist (MK571), raloxifene analogs and tricyclic isoxazole derivatives which are very potent but exhibit low bioavailability and toxic side effects [133].

The list of currently available small molecule inhibitors of MRP2 and MRP3 is quite limited. Several inhibitors have been demonstrated to work such as PAK-10P, PSC-833 and MK571. Additionally, general organic anion transporter inhibitors such as sulfinpyrazone, benzbromarone and probenecid could inhibit MRPs to some extent [134-135].

1.4.3 Inhibitors of BCRP

The first reported inhibitor of BCRP which effectively reverse drug resistance in BCRP expressing cells was fumitremorgin C (FTC), a tremorgenic mycotoxin produced by *Aspergillus fumigatus*. FTC inhibits BCRP well below toxic concentrations and had little effect on P-gp or MRP1 mediated drug resistance. However, neurotoxic effects precluded potential clinical application, but prompted the discovery of the FTC analogue Ko143. Compounds such as elacridar identified as P-gp inhibitors also act on BCRP or even act as multifunctional inhibitors such as biricodar (VX-710) inhibiting the activity of all three efflux pumps [136-137]. The list of reported BCRP inhibitors has been growing rapidly and includes several new compounds for example novobiocin, flavonoids (silymarin, hesperetin, quercetin), genestein, naringenin, acacetin, kaempferol and other compounds [138-139].

1.5 High-molecular-weight delivery system for cancer treatment

Chemotherapy with classical low-molecular weight (LMW) anticancer drugs plays important role in treatment of cancer. However, disadvantages of using LMW drugs such as unfavourable pharmacokinetics profile and severe side toxicity resulted in development of new drug delivery systems for cancer treatment based on the principle of passive drug targeting using the biochemical and physiological differences between tumor and normal tissue (EPR effect; see chapter 1.5.1). The central components of these drug delivery systems are high-molecular-weight (HMW) carriers to which the drug may be either non-covalently or covalently linked. Many different HMW drug delivery systems have been used to improve pharmacological activity of chemotherapeutics such liposomes and nanoparticles, which non-covalently entrap their drug payload. The polymer-protein or polymer-drug conjugates and polymer micelles containing covalently bound drug [140].

Polymer-protein and polymer-drug conjugates in which bioactive agent is coupled to the macromolecular water-soluble polymer carrier were investigated as most promising approach for controlled delivery and release of drugs, peptides or proteins [141]. The first experiments with conjugation of drug to polymer carrier were initiated in the 1950s, however, the clear concept of using polymers as carriers was created 25 years later. Various polymeric carriers were used which can be categorized in several ways: according to origin (natural or synthetic polymers), biodegradability (biodegradable or non-biodegradable) and according to chemical nature.

Anticancer agents are be bound to the polymer backbone via spacers which determines together with the type of the bond between the drug and the end of spacer the site and release rate of the active anticancer drug. The polymer-drug conjugates are designated as prodrugs (by definition, the prodrugs are derivatives of drugs that are processed in the body to release the active drugs), which are able to transport inactive form of drug into targeted tissues, such as tumor tissues, and released the bioactive form of drug. One of the most promising and the most extensively studied water-soluble polymer-drug conjugates are those based on *N*-(2-hydroxypropyl)methacrylamide (HPMA) [142-144, 163].

1.5.1 HPMA copolymer-bound drug conjugates

HPMA copolymers were developed at the Institute of Macromolecular Chemistry in Prague by Kopecek and the co-workers, and they become one of the most intensively studied water-soluble polymeric carriers for drug delivery. The main reasons which makes HPMA copolymers almost ideal drug carriers are their biocompatibility, immunocompatibility and versatility. Superior water solubility may also help to solubilize even highly hydrophobic drug [145-147]. The HPMA copolymer bound drug conjugates consist of three distinct parts: water-soluble HPMA copolymer carrier, a linker and anticancer drug (Figure 1.10).

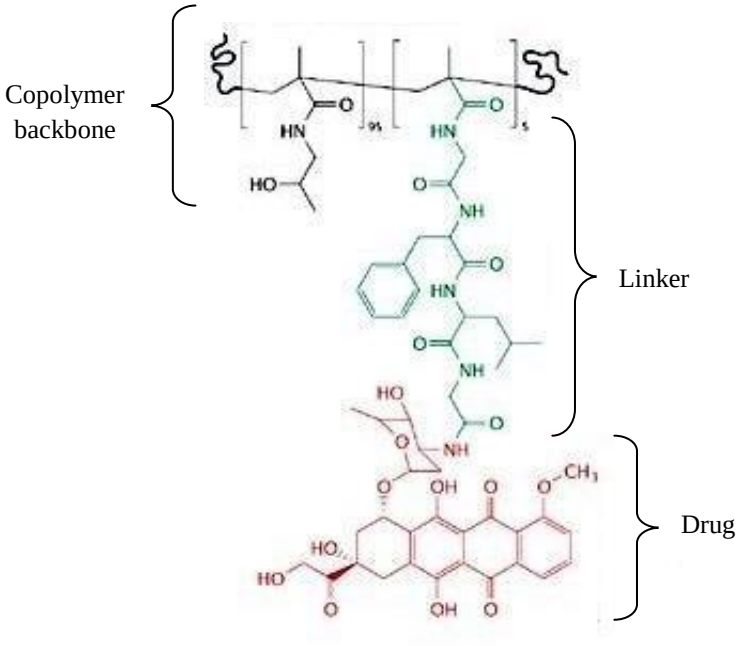

Figure 1.10: Schematic structure of HPMA copolymer-drug conjugate. The example of HPMA copolymer-drug conjugate containing doxorubicin. The polymer backbone is shown in black, linker in green and drug in red. The drug (Dox) is bound through amide bond to last amino acid (Gly) residue of the linker. Adopted from Duncan with minor changes made [148].

There are two widely used methods how drug may be bound to the HPMA copolymer. The first one is based on the use of tetrapeptide GlyPheLeuGly (GFLG) as a linker and the drug is bound to terminal Gly through amide bond (see Figure 1.10). Dox is most often used drug in this type of conjugates and it is released enzymatically (mostly by the cathepsin activity). The second type of conjugate is based on hydrazone

bond between the drug and some simple spacer (i.e. hexanoic acid) which is susceptible to pH-controlled hydrolysis. Such conjugates containing hydrazone bond are relatively stable under normal physiological pH 7.4 in the bloodstream but quickly hydrolyze in acidic environment of endosomes and lysosomes or in acidic microenvironment in tumor tissue [149-151]. Binding LMW drugs to the polymer carrier significantly improves their pharmacological features like: (i) water solubility of drugs even if the drug has highly hydrophobic nature, (ii) protecting the drug (at least partially) from binding to the serum proteins, enzymatic degradation or scavenging processes, (iii) pharmacological profile, (iv) reduced side toxicity by limiting access of the drug to the healthy tissues (v) changing the way of drug cell entry; while the LMW drug enters the cell directly via plasma membrane, the polymer-bound drug conjugate usually enters into the cell by more slowly endocytic route, and (vi) enhanced drug accumulation in solid tumors via Enhanced Permeability and Retention (EPR) effect [143].

The concept of EPR effect was formulated by Matsumura and Maeda in 1986 and was validated for almost all types of solid tumors [152]. The underlying mechanism of EPR effect is that solid tumors have poor or missing lymphatic drainage and blood vessels with defective and fenestrated endothelium with large pores up to 400 nm, depending on the anatomic localization of the tumor (Figure 1.11). This feature of tumor vasculature allows easy and rapid extravasation of macromolecules into tumor but not into normal tissues. Moreover, absence of lymphatic drainage inhibit clearance of macromolecules from tumor, so they remain in the tumor for prolonged time. The size limit for macromolecules to employ EPR effect was determined to be approximately 40 kDa. Macromolecules with lower molecular weight are cleared from tumors relatively rapidly [153-154].

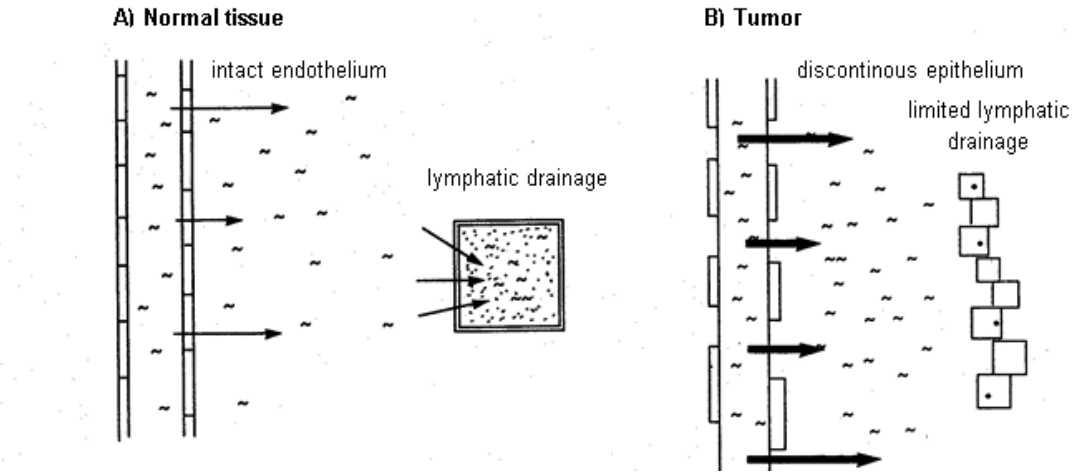

Figure 1.11: Enhanced Permeability and Retention (EPR) effect. Solid tumors exhibit passive accumulation of the macromolecules due to EPR effect which is characterized by limited lymphatic drainage and large fenestration within tumor blood vessels. These features allow increase extravasation and simultaneously inhibition of macromolecules clearance from tumors. Thus, enhanced accumulation of macromolecules in tumors is seen. Adopted from Duncan et al. [155].

Dox^{AM}-PHPMA (FC28068, also known as PK1) conjugate was the first HPMA copolymer bearing Dox bound via amide bond to the GFLG spacer. Numerous studies performed with Dox^{AM}-HPMA conjugate demonstrated that it possesses some of the key characteristics for polymer-bound prodrugs, such as prolonged circulation time in organism depending on the molecular weight of the conjugate, reduced non-specific toxicity and increased accumulation of solid tumors [156]. Moreover, anti-tumor effect of Dox^{AM}-HPMA conjugate was also demonstrated in numerous tumor models of mouse, rat and human origin both *in vitro* and *in vivo* [157-158, 164-165]. Conjugates with drug bound via pH-sensitive hydrazone bond between copolymer side chain terminus and cytostatic drug were developed later on [149]. These conjugates were described to have significant antitumor effect in variety of tumor cell lines *in vitro* as well as several experimental tumor models *in vivo* [151, 159-160, 166-167].

1.5.1.1 Actively targeted HPMA copolymer-bound drug conjugates

Presence of functional chemical groups in the side chains of HPMA copolymers enables to bind a targeting moiety and thus to actively target the whole conjugate. Variety of structures was tested as a targeting moiety ranging from lectins, saccharides,

hormones, transferrin to monoclonal antibodies. Actively targeted HPMA copolymer conjugates are taken up by the cells expressing appropriate receptor through receptor-mediated endocytosis, which could improve its therapeutic index. HPMA copolymer bound Dox conjugate targeted by galactosamine, called PK2 (Dox^{AM}-PHPMA-galactosamine or FCE28069) was the first actively targeted HPMA-based conjugate. This conjugate targeted to the cells of hepatocellular carcinoma which overexpress asialoglycoprotein receptor entered phase I/II clinical trials. However, further testing was abandoned due to the comparable accumulation in tumor site and normal liver tissues [161].

It is well known, that cancer often express an altered glycosylation pattern. This opens a possibility to use lectins as cancer-selective ligands. Thus, conjugates where wheat germ agglutinin (WGA) and peanut agglutinin (PNA) were bound to HPMA copolymer backbone and tested for binding to cells of SW620 colorectal cancer and normal colon tissue. Whereas binding of WGA-targeting conjugate was similar in normal and cancer colon tissue, conjugate containing PNA revealed higher binding to cells of colorectal cancer [171-172].

The most explored targeting structures are represented by antibodies. The research of antibody targeted HPMA copolymer conjugates led to development of two types of conjugate structures. The first one, in which the copolymer chains and primary amino groups of the IgG molecule form covalent bond, was called “classical structure”. However, this “random binding” could led to significant decrease in antibody binding activity, as the antibody binding site could be blocked by presence of copolymer chains directly linked into it or sterically hindered, if copolymers were bound to the adjacent locations. Therefore, the method of oriented binding” was developed, using oxidized carbohydrate residues located in the Fc part of the antibody molecule for binding to the polymer. However, binding activity of the most bound antibody molecules were comparable to those in “classical conjugates”. The efforts to develop actively targeted HPMA copolymer conjugates with more define structure led to invention of “star structures”, where semitelechelic HPMA copolymer chains bearing Dox bound either via GFLG linker or via the pH-sensitive hydrazone bond are linked to the central antibody molecule (Figure 1.12). These conjugates exhibited higher antitumor activity in both *in vitro* and *in vivo* in comparison to “classical conjugates” [162, 168-170].

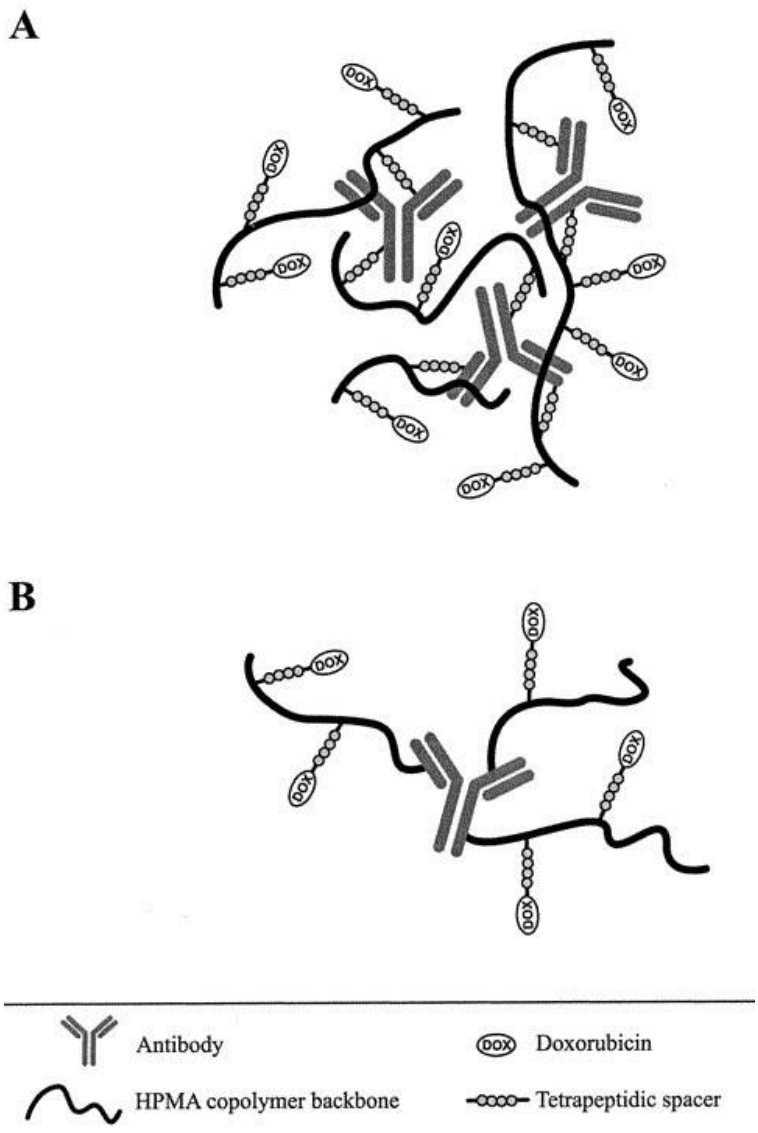

Figure 1.12: Schematic picture of classical and star structure of HPMA copolymer-bound doxorubicin conjugate. The classical structure of antibody-targeted HPMA copolymer-bound doxorubicin (A) and the star structure of antibody-targeted HPMA copolymer-bound doxorubicin conjugate (B). Adopted from Kovář et al. with minor changes made [169].

2 Aims

The aims of this study are:

1) Determination of expression of selected ABC transporters in established system of two murine leukemia cell lines, sensitive P388 and doxorubicin resistant P388/MDR cell line.
    a) To determine P-gp, MRP1 and BCRP expression, major proteins related to MDR phenotype, in both sensitive P388 and resistant P388/MDR cell lines.

2) Investigation of biological activity of selected derivatives of P-gp inhibitors reversin 121, reversin 205 and ritonavir in P388 and P388/MDR cell lines.
    a) To determine the toxicity of selected P-gp inhibitors and their derivatives in P388 and P388/MDR cell lines.
    b) To evaluate the P-gp inhibitory activity of selected P-gp inhibitors and their derivatives.
    c) To test and compare the potential of selected P-gp inhibitors and their derivatives to sensitize MDR cells to cytostatic activity of Dox.

3) Characterization of biological activity of new HPMA-based conjugates bearing P-gp inhibitor or Dox or both in sensitive P388 and resistant P388/MDR cell lines.
    a) To determine the toxicity of HPMA copolymer conjugates bearing selected P-gp inhibitor derivatives.
    b) To evaluate the P-gp inhibitory activity of HPMA copolymer conjugates bearing selected derivatives of P-gp inhibitors.
    c) To evaluate the potentiation of cytostatic and cytotoxic activity of Dox by HPMA copolymer conjugates bearing P-gp inhibitor derivatives.
    d) To determine the intracellular accumulation of Dox in the presence/absence of HPMA copolymer conjugate bearing P-gp inhibitor derivative.
    e) To figure out the cytostatic activity of HPMA copolymer conjugates bearing both Dox and P-gp inhibitor derivative.

3 Material

3.1 Solutions

Phosphate buffer saline (PBS)

9.0 g	NaCl
1.2 g	$Na_2HPO_4.12H_2O$
0.2 g	$NaH_2PO_4.2H_2O$
0.2 g	KCl

To prepare 1000 ml of 1x PBS, reagents were dissolved in 800 ml of distilled H_2O. The pH was adjusted to 7.4 with HCl. Distilled H_2O was added to total volume of 1000 ml.

Flow cytometry buffer

	PBS
2mM	EDTA (Invitrogen)
2%	fetal calf serum (FCS, Invitrogen)

Annexin binding buffer (10x)

100 mM	HEPES
1400 mM	NaCl
25 mM	$CaCl_2$

To prepare 10x Annexin binding buffer all reagents were dissolved in 500 ml of distilled water and pH was adjusted to 7.4. Before use, the 1x Annexin binding buffer was prepared by adding 1 volume of 10x Annexin binding buffer to 9 volumes of distilled H_2O. Annexin binding buffer may be stored at 2 - 8 °C in the dark for up to 6 months.

Tris buffer solution (TBS; 10x)

24.2 g	Tris (tris-(hydroxymethyl)-aminomethan)
80.0 g	NaCl

The solution was completed to a final volume of 1000 ml with distilled H_2O and pH was adjusted to 7.6 with HCl.

SDS-PAGE running solution (10x)

30.3 g	Tris
144 g	glycine (Sigma-Aldrich)
10.0 g	SDS (sodium dodecyl sulphate)

The solution was completed to a final volume of 1000 ml with distilled H_2O and pH was adjusted to 7.6 with HCl.

Cell lysis buffer

0.02 ml	Nonidet P-40 (Pierce)
0.20 ml	Na_3VO_4 (Sigma-Aldrich)
0.0074 g	$Na_2EDTA.2H_2O$ (Invitrogen)
0.0152 g	EGTA
0.0084 g	NaF (Lachema)
0.0031 g	DTT (Sigma-Aldrich)
0.05 ml	PMSF (Sigma-Aldrich)
1.0 ml	Protease inhibitors mix

(AEBSF, 4-(2-aminoethyl)benzensulfonyl fluoride; pepstatin A; E-64; bestatin; leupeptin; aprotinin; Sigma-Aldrich)

The solution was completed to a final volume of 20 ml with distilled H_2O and pH was adjusted to 7.4 with HCl.

SDS-PAGE sample buffer (3x)

0.0985 g	Tris
0.60 g	SDS
0.030 g	Bromophenol Blue
3 ml	glycerol
0.23 g	DTT (5M)

The solution was completed to a final volume of 10 ml with distilled H_2O.

Western blot transfer buffer

5.82 g	Tris
2.93 g	glycine
0.375 g	SDS
200 ml	methanol (Lachema)

The solution was completed to a final volume of 1000 ml with distilled H_2O.

Western blot washing buffer (TBS/T)

1x	Tris buffer solution (TBS)
0.1% v/v	Tween-20 (Sigma-Aldrich)

The 1x TBS solutions was prepared by adding 1 volume of 10x TBS to 9 volumes of distilled H_2O.

Western blot blocking buffer

1x	Tris buffer solution (TBS)
2% w/v	BSA (bovine serum albumin)
0.1% v/v	Tween-20

The 1x TBS solutions was prepared by adding 1 volume of 10x TBS to 9 volumes of distilled H_2O.

Antibody dilution buffer

1x	TBS/T
5% w/v	BSA or low-fat milk

5 g of low-fat milk or BSA per 100 ml 1x TBS/T buffer was added. Final solution was mixed using magnetic stirrer.

Running gel solution (10% acrylamide)

4.0 ml	distilled H_2O
3.3 ml	acrylamide / Bis-acrylamide
2.5 ml	1.5M Tris (pH 8.8)
0.1 ml	SDS (10% w/v)
0.15 ml	APS (ammonium persulfate)
0.006 ml	TEMED

Polymerization reagents were added before gel pouring. After adding TEMED and APS, gel was polymerized fairly quickly. All reagents were mixed to a final volume 10 ml.

Running gel solution (8% acrylamide)

4.60 ml	distilled H_2O
2.70 ml	acrylamide / Bis-acrylamide
2.50 ml	1.5M Tris (pH 8.8)
0.10 ml	SDS (10% w/v)
0.15 ml	APS (ammonium persulfate)
0.006 ml	TEMED

Polymerization reagents were added before gel pouring. After adding TEMED and APS, gel was polymerized fairly quickly. All reagents were mixed to a final volume 10 ml.

Stacking gel solution (4% acrylamide)

2.70 ml	distilled H_2O
0.67 ml	acrylamide / Bis-acrylamide
0.50 ml	0.5M Tris (pH 8.8)
0.10 ml	SDS (10% w/v)
0.15 ml	APS (ammonium persulfate)
0.006 ml	TEMED

Polymerization reagents were added before gel pouring. After adding TEMED and APS, gel was polymerized fairly quickly. All reagents were mixed to a final volume 4 ml.

3.2 Antibodies

3.2.1 Antibodies for western blot immunoassay

Following anti-mouse primary antibodies were used for western blot immunoassay. All primary antibodies were diluted in a ration 1:300 in antibody dilution buffer.

Polyclonal goat anti-mouse ABCB1 (C-19, Santa Cruz Biotechnology)
Polyclonal rabbit anti-mouse ABCC1 (H-70, Santa Cruz Biotechnology)
Polyclonal rabbit anti-mouse ABCG2 (B-25, Santa Cruz Biotechnology)
Monoclonal biotinylated anti-mouse β-actin (C-4, Santa Cruz Biotechnology)
Biotinylated protein ladder (Cell Signaling)

Following secondary antibodies were used for western blot immunoassay. All secondary antibodies are conjugated to horseradish peroxidase (HRP) and were diluted in western blot blocking buffer.

Anti-goat IgG-HRP (1.10,000; Santa Cruz Biotechnology)
Anti-rabbit IgG-HRP (1:10,000; Cell Signaling)
Anti-biotin IgG-HRP (1:10,000; Cell Signaling)

3.3 Cell lines

The murine monocytic leukemia cell line P388 and its doxorubicin-resistant sub-line P388/MDR were obtained from Prof. I. Lefkovits (Basel Institute for Immunology, Basel, Switzerland). The highly tumorigenic lymphoblastic lymphoma P388 cell (parental cell line) was originally derived from chemically induced lymphoblastic leukemia in DBA/2 mice by painting the skin with methylcholanthrene.

3.4 Derivatives of ABC transporter inhibitors

Following low-molecular weight derivatives of ABC transporter inhibitors were synthetized and characterized at Institute of Macromolecular Chemistry of AS CR, v.v.i. (ICM).

3.4.1 Derivatives of reversin 121

The synthesis of all derivatives of reversin 121 was performed on ICM. The synthetic scheme of reversin 121 derivatives is shown in Scheme 3.1.

Reversin 121

Reversin 121 (R121) is an aspartyl lysine (Asp-Lys) dipeptide with molecular weight (Mw) 641.7. Reversin 121 was prepared by the reaction of Boc-Asp(OBzl)-OH (*N*-α-t.-Boc-L-aspartic acid β-benzyl ester; Novobiochem) with H-Lys(Z)-OtBu.HCl (*N*-ε-CBZ-L-lysine t.-butyl ester hydrochloride; Novabiochem). The product was purified chromatographically and characterized by HPLC (high-performance liquid chromatography).

4-oxopentanoyl (Lev) reversin 121

Synthesis of derivative 4-oxopentanoyl reversin 121 (OPe-R121) with molecular weight 639.74 was performed by reaction of OPe-Asp(OBzl)-COOH (*N*-α-4-oxopentanoyl-L-aspartic acid β-benzoyl acid) with H-Lys(Z)-otBu.HCl in the presence of HOBT (1-hydroxybenzotriazole hydrate; Sigma-Aldrich), DMF (*N*,*N*-dimethyl formamide; Sigma-Aldrich) and EDC (*N*-ethyl-N′-(3-dimethylaminopropyl)carbodiimide hydrochloride; Sigma-Aldrich). The product was purified chromatographically and characterized by HPLC.

6-oxoheptanoyl reversin 121

Synthesis of derivative 6-oxoheptanoyl reversin 121 (OHe-R121) with molecular weight 667.79 was performed by reaction of OHe-Asp(OBzl)-COOH (*N*-α-6-oxoheptanoyl-L-aspartic acid β-benzoyl acid) with H-Lys(Z)-otBu.HCl in the presence of NaHCO3 (sodium bicarbonate; Sigma-Aldrich). The product was purified chromatographically and characterized by HPLC.

5-methyl-4-oxohexanoyl reversin 121

Synthesis of derivative 5-methyl-4-oxohexanoyl reversin 121 (MeOHe-R121) with molecular weight 667.79 was performed by reaction of MeOHe-Asp(OBzl)-COOH (*N*-α-5-methyl-4-oxohexanoyl-L-aspartic acid β-benzoyl acid) with H-Lys(Y)-OtBu.HCl in the presence of HOBT, DIPEA (*N*,*N*-diisopropylethylamine; Sigma-Aldrich) and EDC. The product was purified chromatographically and characterized by HPLC.

4-(2-oxopropyl)benzoyl reversin 121

Synthesis of 4-(2-oxopropyl)benzoyl reversin 121 (OPB-R121) with molecular weight 881.12 was performed by reaction of OPB-Asp(OBzl)-COOH (*N*-α-4-(2oxopropyl)benzoyl-L-aspartic acid β-benzoyl acid) with H-Lys(Y)-OtBu.HCl in the presence of HOBT, DIPEA and EDC. The product was purified chromatographically and characterized by HPLC.

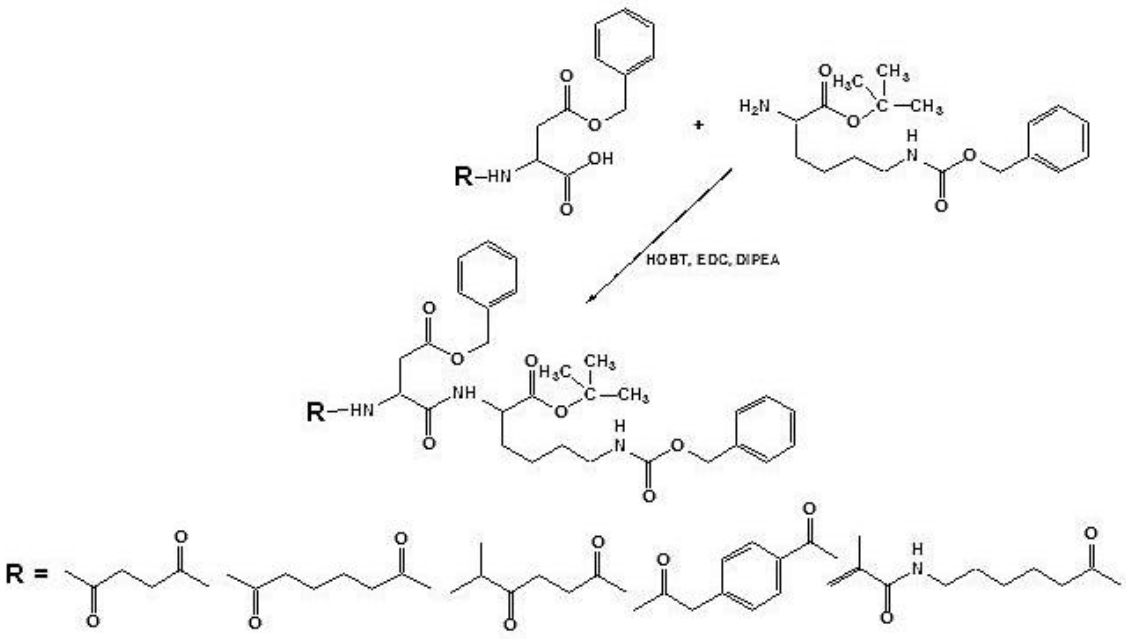

Scheme 3.1: Synthesis of reversin 121 derivatives

Scheme was obtained from ICM.

3.4.2 Derivatives of ritonavir

The synthesis of all derivatives of ritonavir (RIT) was performed on ICM. The synthetic scheme of ritonavir derivatives is shown in Scheme 3.2.

6-oxoheptanoyl ritonavir

6-oxoheptanoyl ritonavir (OHe-RIT) was prepared by esterification of ritonavir (ChemPacific Corp.) with 6-oxoheptanoic acid. RIT and 6-oxoheptanoic acids were dissolved in DCM (dichloromethane; Sigma-Aldrich) and EDC was added. The reaction was catalyzed by DMAP (4-(dimethylamino)pyridine; Sigma-Aldrich). The product was purified chromatographically and characterized by HPLC.

5-methyl-4-oxohexanoyl ritonavir

5-methyl-4-oxohexanoyl ritonavir (MeOHe-RIT) was prepared by esterification of ritonavir with 5-methyl-4-oxohexanoic acid catalyzed by DMAP. RIT. DMAP and 5-methyl-4-oxohexanoic acid were dissolved in DCM and EDC was added. The product was purified chromatographically and characterized by HPLC.

4-(2-oxopropyl)-benzoyl ritonavir

4-(2-oxopropyl)-benzoyl ritonavir was prepared by esterification of ritonavir with 4-(2-oxopropyl)-benzoic acid in the presence of EDC. Reaction was catalyzed by DMAP. The product was purified chromatographically and characterized by HPLC.

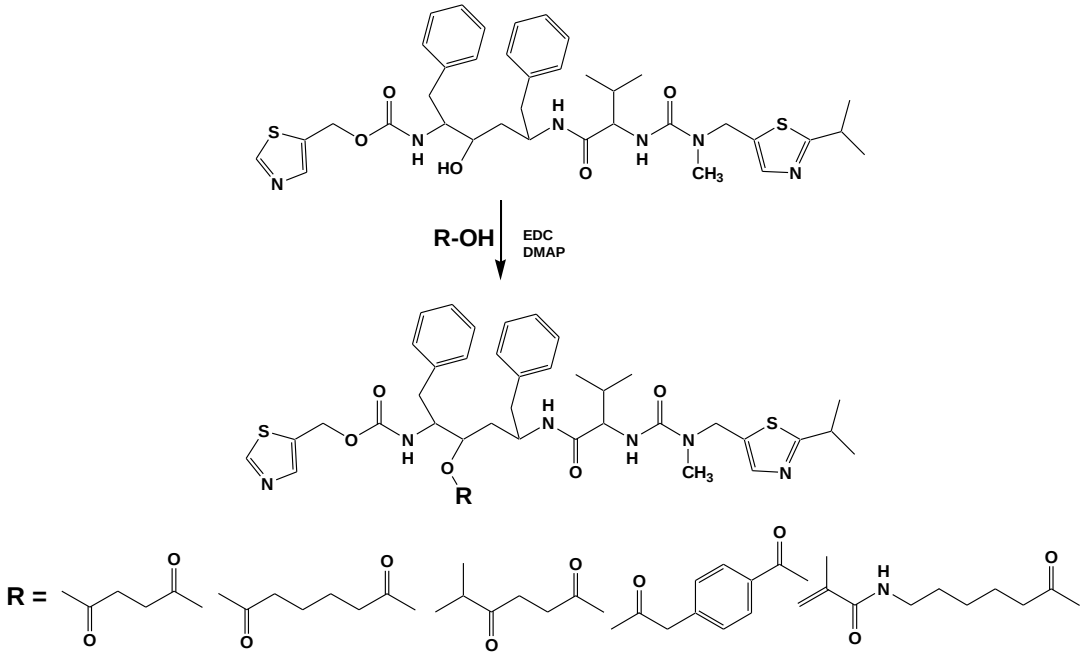

Scheme 3.2: Synthesis of ritonavir derivatives

Scheme was obtained from ICM.

3.4.3 Derivatives of reversin 205

The synthesis of derivative of reversin 205 (R205) was performed on ICM.

5-methyl-4-oxohexanoyl reversin 205

5-methyl-4-oxohexanoyl reversin 205 (MeOHe-R205) was synthetized through manual solid phase peptide synthesis using a standard Fmoc (9-fulorenylmethyloxycarbonyl) strategy with 4-Fmoc-hydrazinobenzoyl AM Nove Gel™ (Novabiochem), PyBOP ((benzotriazol-1-yloxy)tripyrrolidinophosphonium hexafluorophosphate; Sigma-Aldrich), HOBT and DIPEA in DMF. The product was purified chromatographically and characterized by HPLC.

3.5 HPMA copolymer-bound inhibitor conjugates

Following HPMA (*N*-(2-hydroxypropyl)methacrylamide) copolymer-bound derivatives of ABC transporter inhibitors and/or drugs were synthetized and characterized at Institute of Macromolecular Chemistry of AS CR, v.v.i.

3.5.1 HPMA copolymer-bound derivatives of reversin 121

P-Ahx-NH-N=MeOHe-R121

Linear HPMA-based copolymer bearing 5-methyl-4-oxohexanoyl derivative of reversin 121 via pH-sensitive hydrazone bond.

Mw = 33,100 g/mol; Mw/Mn = 1.12

8.6 wt% of 5-methyl-4-oxohexanoyl derivative of reversin 121

P-Ahx-NH-NH-MeOHe-R121

HPMA copolymer conjugate bearing 5-methyl-4-oxohexanoyl derivative of reversin 121 via non-degradable bond.

Mw = 35,800 g/mol; Mw/Mn = 1.12

9.5 wt% of 5-methyl-4-oxohexanoyl derivative of reversin 121

P-Ahx-R121

HPMA copolymer conjugate bearing reversin 121 via non-degradable bond.

Mw = 27,700 g/mol; Mw/Mn = 1.15

5.3 wt% of reversin 121

P-Ahx-NH-N=MeOHe-R121(Dox)

HPMA copolymer conjugate bearing 5-methyl-4-oxohexanoyl derivative of reversin 121 and doxorubicin via pH-sensitive hydrazone bond.

Mw = 33,100 g/mol; Mw/Mn = 1.12

11.1 wt% of 5-methyl-4-oxohexanoyl derivative of reversin 121

10.73 wt% of doxorubicin

P-Ahx-NH-N=MeOHe-R121(Dox)

HPMA copolymer conjugate bearing 5-methyl-4-oxohexanoyl derivative of reversin 121 and doxorubicin via pH-sensitive hydrazone bond.

Mw = 33,100 g/mol; Mw/Mn = 1.12

15.74 wt% of 5-methyl-4-oxohexanoyl derivative of reversin 121

3.96 wt% of doxorubicin

P-Ahx-NH-N=MeOHe-R121(Dox)

HPMA copolymer conjugate bearing 5-methyl-4-oxohexanoyl derivative of reversin 121 and doxorubicin via pH-sensitive hydrazone bond.

Mw = 33 100 g/mol; Mw/Mn = 1.12

3.83 wt% of 5-methyl-4-oxohexanoyl derivative of reversin 121

12.02 wt% of doxorubicin

3.5.2 HPMA copolymer-bound derivatives of ritonavir

P-Ahx-NH-N=MeOHe-RIT

HPMA copolymer conjugate bearing 5-methyl-4-oxohexanoyl derivative of ritonavir via pH-sensitive hydrazone bond.

Mw = 30,700 g/mol; Mw/Mn = 1.06

8.3 wt% of 5-methyl-4-oxohexanoyl derivative of ritonavir

P-Ahx-NH-NH-MeOHe-RIT

HPMA copolymer conjugate bearing 5-methyl-4-oxohexanoyl derivative of ritonavir via non-degradable bond.

Mw = 31 900 g/mol; Mw/Mn = 1.09

7.3 wt% of 5-methyl-4-oxohexanoyl derivative of ritonavir

3.5.3 HPMA copolymer-bound drugs

P-Ahx-NH-N=Dox

HPMA copolymer conjugate bearing doxorubicin via degradable hydrazone bond.

Mw = 27 000 g/mol; Mw/Mn = 1.80

9.8 wt% of doxorubicin

4 Methods

4.1 Cell lines propagation

The murine monocytic leukemia cell line P388 (parental cell line) and its doxorubicin-resistant sub-line P388/MDR (cell line overexpressing P-gp) were obtained from Prof. I. Lefkovits (Basel Institute for Immunology, Basel, Switzerland). Both cell lines were propagated in RPMI-1640 medium supplemented with heat-inactivated 10% fetal calf serum (FCS), 2mM glutamine, 100 U/ml penicillin, 1 mM sodium pyruvate, 100 µg/ml streptomycin and 5 ml non-essential amino acids (Sigma-Aldrich, Czech Republic). The P388/MDR cells were continuously grown in the presence of 750 ng/ml doxorubicin to maintain the MDR-phenotype. One day before each experiment, cells were grown in doxorubicin-free culture medium. Both cell lines were propagated at 37 °C in a 5% CO_2 atmosphere. The cell lines were tested for mycoplasma infection (MycoAlert Mycoplasma Detection kit, Lonza, Switzerland).

4.2 Cellular drug sensitivity assay

To test the cytostatic effect of the drugs in the presence or absence of chemosensitizers, cell growth inhibition was determined using the [^{3}H]-thymidine incorporation assay. The cells (1 x 10^4 per well) were seeded into 96-well flat bottom (FB) tissue culture plates (Nunc, Denmark). Different concentrations of samples were added to the wells to reach a final volume of 250 µl. Triplicate wells were used for each test condition. The plates were incubated in 5% CO_2 at 37 °C for 72 h. After cultivation, each well was pulsed with 1 µCi (37 kBq) of [^{3}H]-thymidine for 6 h. The cells were then collected on glass fibre filters (Filtermat, Wallac, Finland) using a cell harvester (Tomtec, U.S.A) and the radioactivity of the samples was measured in scintillation counter (1450 MicroBeta TriLux, Wallac, Finland). Cells cultivated in a fresh medium were used as controls. The inhibition of tumor cell growth was expressed as IC_{50} i.e., as the concentration of Dox (or equivalent) inhibiting the cells growth by 50%. All IC_{50} values were a mean of at least three independent experiments. The resistant ratio was calculated by dividing the IC_{50} value for P388/MDR cell line by corresponding value in P388 cells.

4.3 Calcein efflux assay

Calcein assay was performed using 96-well round bottom (U-base) tissue culture plates (TPP, Switzerland). All incubation steps were conducted in 5% CO_2 at 37 °C. Drug-sensitive and drug-resistance cells were seeded at a concentration of 1 x 10^5 cells per well (100 µl per well) in culture medium. Cells were then incubated with tested compounds or controls (in duplicates) for 30 min. After pre-incubation, calcein^{AM} was added (final concentration 0.1 µM per well) and the cells were incubated for another 20 min in the dark. After 20 min incubation, the uptake of calcein^{AM} was stopped by centrifugation (200 x g, 5 min, and 4 °C). Cell pellets were washed and centrifuged twice with 200 µl and resuspended in 100 µl cold FACS (fluorescence-activated cell sorter) buffer (PBS with 2% FCS, 2 mmol EDTA). Flow cytometric analysis was performed on LSRII (BD Biosciences, U.S.A), and the data were analyzed using FlowJo software (Tree Star, Inc., Ashland). Non living cells were detected and gated out by Hoechst 33258 staining (Sigma-Aldrich, Czech Republic). Each experiment was performed at least three times.

4.4 Statistical analysis

Data from different experiments were reported as mean ± S.D. For statistical analysis, Student´s t-test for independent measurements was used. A value of $P < 0.05$ was considered significant.

4.5 Western blot immunoassay

Sensitive P388 and doxorubicin resistant cells P388/MDR were washed twice with ice-cold Tris-buffered saline (TBS) and centrifuged (4,000×g, 5 min, and 4°C). They were then resuspended in a cell lysis buffer composed of 1% Nonidet P-40 (Pierce), 1 mM Na_3VO_4, 1 mM EDTA, 2 mM EGTA, 10 mM NaF, 1 mM dithiothreitol (DTT), 5% Protease mix (Sigma-Aldrich), 1 mM phenylmethylsulfonyl fluoride (PMSF), and TBS of pH 7.4 and passed ten times through a syringe needle (25–30 G) for complete lysis. After 60 min of incubation at 4°C, cell lysates were centrifuged

(14,000×g, 4°C) and protein concentration in aspirated supernatants was determined by the bicinchoninic acid assay (Sigma-Aldrich). Twenty micrograms of protein aliquots (final protein load per lane) was mixed 2:1 with 3× sample buffer composed of 62.5 mM TRIS, 30% glycerol, 20.8 μM sodium dodecyl sulfate (SDS), 50 mM DTT, and 0.03% (w/v) bromophenol blue and stored at -20°C until needed. Then, standard electrophoresis (SDS-PAGE) was performed using polyacrylamide gel (8% PAG for ABCB1 and ABCC1, and 10% PAG for ABCG2) followed by a standard blotting semidry procedure with a nitrocellulose membrane. Five microliters of biotinylated protein ladder (Cell Signaling) was used to estimate the molecular weight of the protein bands. The membrane was washed in 25 ml of TBS and blocked with blocking buffer for 60 min consists with 5% low-fat milk in TBS at room temperature before overnight incubation with 1:300 primary goat anti-mouse ABCB1 (Santa Cruz Biotechnology), rabbit anti-mouse ABCC1 (Santa Cruz Biotechnology) and rabbit anti-mouse ABCG2 (Santa Cruz Biotechnology) at 4°C in antibody dilution buffer composed of TBS with 0.1% Tween-20 and 5% bovine serum albumin (BSA). Proper washing with TBS, containing 0.1% Tween-20 (TBS/T), preceded 60–120 min of incubation with anti-goat IgG-HRP (1:10 000; Santa Cruz Biotechnology), anti-rabbit IgG-HRP (1:10 000; Cell Signaling) and anti-biotin horseradish peroxidase (HRP)-linked IgG (1:10 000; Cell Signaling) in 5% low-fat milk or 2% BSA in TBS at room temperature. Finally, the membranes were washed in TBS/T, developed by a chemiluminescence reaction. Signal was detected on a LAS-1000 CCD camera (Fujifilm) or by film exposure (Kodak).

4.6 Detection of apoptosis

The pattern of cell death (externalization of phosphatidylserine (PS) and membrane integrity) was determined using flow cytometry by simultaneous staining with Annexin V-Dyomics 647 (Apronnex, Czech Republic) and Hoechst 33258 (Invitrogen, USA). Drug sensitive P388 and drug-resistance P388/MDR were seeded at a concentration of 1 x 10^5 cells per well in 100 μl of culture media (RPMI-1640 medium supplemented with heat-inactivated 10% fetal calf serum (FCS), 2mM glutamine, 100 U/ml penicillin, 1 mM sodium pyruvate, 100 μg/ml streptomycin and 5 ml non-essential amino acids) using 96-well round bottom (U-base) tissue culture plates (TPP, Switzerland). Subsequently, 50 μl of desired concentrations of inhibitors and

drugs were added to final volume 200 µl. Cells were then incubated with tested compounds or controls (in duplicates) 5% CO_2 at 37 °C for 24 hours. After incubation cells were collected by centrifugation (200 x g, 5 min, and 4 °C), transferred into 96-well culture tissue plates with conical bottom (Nunc, Denmark) and washed twice with 200 µl of 1x Annexin binding buffer (10 mM HEPES buffer, 140 mM NaCl, 2.0 mM $CaCl_2$, pH 7.4). Cells were then resuspended in 10 µl of 1x Annexin binding buffer containing Annexin V-Dyomics 647 (1:100) and incubated for 15 min at room temperature in the dark. After incubation 90 µl of 1x Annexin binding buffer and 10 µl of Hoechst 33258 (0.1 µg/ml) were added and immediately analyzed. The percentage of apoptotic/necrotic cells was measured on LSRII (BD Biosciences, U.S.A) flow cytometer. At least 10,000 cells were analyzed for each sample. Negative control represents cells incubated in fresh medium and as a positive control was taken cells incubate with free non-modified drug using highest used concentration. Data were analyzed using FlowJo software (Tree Star, Inc., Ashland). Positioning of quadrants on Annexin V-Dyomics 647/Hoechst 33258 dot-plots was performed to distinguish living cells (Annexin V negative/Hoechst negative), apoptotic cells (Annexin V positive/Hoechst negative) and necrotic cells (Annexin V negative/Hoechst positive).

5 Results

The most promising and widely studied strategy to overcome MDR phenotype so far seems to be the use of low-molecular-weight inhibitors of ABC transporters. Three generations of ABC inhibitors have been described, in which the inhibitors of third generation effectively blocked efflux function of ABC transporters in nanomolar concentrations. However, low-molecular-weight inhibitors are mainly hydrophobic molecules suffering by low solubility and they may possess severe side effects.

Here we focused on evaluation of biological activity of novel polymeric therapeutics based on water-soluble HPMA copolymers bearing an anticancer drug doxorubicin (Dox), inhibitor of ABC transporters or both bound to a polymeric carrier via pH-sensitive hydrazone bond. Conjugation of the Dox and P-gp inhibitor to the water-soluble HPMA copolymer should significantly increase their solubility, prolonged their half-life in circulation, improved biodistribution and overcome nonspecific side effects on healthy tissue due to passive accumulation in solid tumors via EPR effect.

Three ABC transporter inhibitors were selected, namely reversin 121 (R121), reversin 205 (R205) and ritonavir (RIT). Reversins are short peptides consisting of di- or tripeptide derivatives that share common physicochemical and structural features. Reversin 121 is an aspartyl lysine (Asp-Lys) dipeptide derivative and reversin 205 is a bis(glutamyl)lysine (bis[Glu]-Lys) tripeptide derivative. Selection of ritonavir as a third P-gp inhibitor for this work was based on two reasons. First, numerous studies proved that protease inhibitors such as lopinavir or ritonavir are highly effective in reversing resistance against cytostatic drugs. The second reason is that RIT molecule is suitable for derivatization. All three selected compounds exhibit sufficient inhibitory activity for P-gp. However, none of these compounds contain any suitable functional group for covalent attachment to the HPMA copolymer via hydrazone bond. Hence, we derivatized reversin 121, reversin 205 and ritonavir with 4-oxopentanoyl (OPe), 6-oxoheptanoyl (OHe), 5-methyl-4-oxohexanoyl (MeOHe) and 4-(2-oxopropyl)benzoyl (OPB) functional group. All these derivatives possess carbonyl group necessary for their binding to HPMA copolymer through pH-sensitive hydrazone bond.

5.1 Expression of selected ABC transporters in model cell lines

Murine leukemia cell line P388 (parental cell line) and its doxorubicin-resistant sub-line P388/MDR (for detailed characteristic see Materials) were used in this study. P388 cell line is sensitive to Dox while the P388/MDR cell line is highly resistant. Doxorubicin represents well characterized substrate for all three most important ABC transporters related to MDR phenotype, P-gp, MRP1 and BCRP. Thus, we first determined the expression of these proteins in both P388 and P388/MDR cell line by western blot analysis. Whole cell lysates of both cell lines were used for analysis.

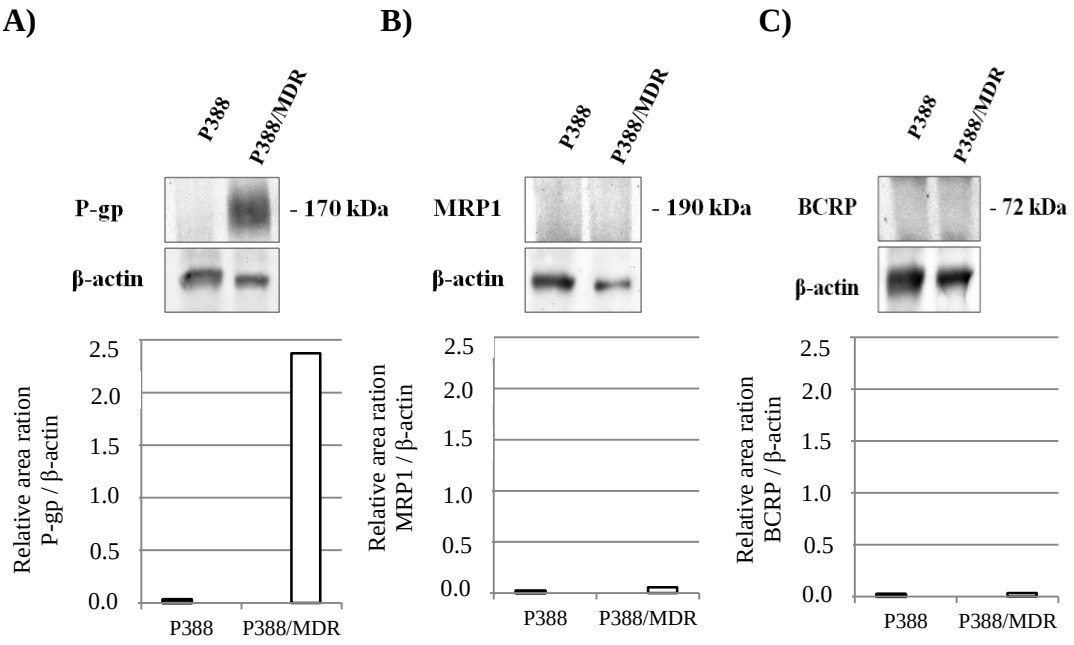

Figure 5.1: Expression of P-gp (A), MRP1 (B) and BCRP (C) in sensitive P388 and Dox resistant P388/MDR cells. Expressions of P-gp, MRP1 and BCRP in P388 and P388/MDR cell line were analyzed by western blotting. 3 day cell cultures were harvested and the whole cell lysates were prepared. Equal amounts (20 µg of proteins) of cell lysates were separated onto 8% SDS-polyacrylamide gel containing for P-gp and MRP1 separation and 10% SDS-polyacrylamide gel for BCRP, than transferred onto nitrocellulose membrane and immunoblotted with polyclonal anti-Pgp, anti-MRP1 and anti-BCRP antibodies. Membranes were then washed and incubated with secondary antibody anti-goat IgG-HRP and anti-rabbit IgG-HRP for 2 hours. Detection of proteins expression was performed using enzyme-linked chemiluminescence system. Cytosolic protein β-actin was used as a control. The proteins expression were quantified by ImageJ software and plotted as P-gp/β-actin, MRP1/β-actin and BCRP/β-actin ratio.

We have demonstrated that P388/MDR cell line express high levels of P-gp (Figure 5.1A). However, we did not detect any MRP1 (Figure 5.1B) and BCRP (Figure 5.1C) and thus we assumed that resistance of P388/MDR cells is mediated only by overexpression of P-gp. Expression levels of P-gp, MRP1 and BCRP were undetectable in parental P388 cell line.

5.2 *In vitro* cytostatic activity of free and HPMA copolymer-bound Dox

P388 cells are relatively sensitive to doxorubicin, a cytostatic drug used in our study, which shows an IC_{50} of approximately 0.01 μM. On the other hand, P388/MDR cells, the Dox-resistance sub-line which overexpress P-gp as we described previously, showed an IC_{50} of approximately 5.9 μM. Thus, the P388/MDR cells are approximately 600 times less sensitive to Dox than the parental P388 cell line. A similar situation was observed when the P-Ahx-NH-N=Dox conjugate was used instead of free Dox. The IC_{50} concentrations for the P388 and P388/MDR cell were 0.024 μM and 92 μM, respectively. The calculated resistant ratio, determined as ratio of IC_{50} of resistant cell line P388/MDR to IC_{50} of sensitive cell line P388, for P-Ahx-NH-N=Dox is approximately 3,800 and thus even higher than that for free Dox (Table 5.1).

Table 5.1: IC_{50} values determined in sensitive P388 and multidrug resistant P388/MDR cell lines for Dox and HPMA copolymer conjugate P-Ahx-NH-N=Dox.

Type of drug	P388 IC_{50} (μM)[a]	P388/MDR IC_{50} (μM)	Resistance ratio
Dox	0.0098 ± 0.001	5.86 ± 0.41	598
P-Ahx-NH-N=Dox	0.024 ± 0.001	91.7 ± 11.8	3821

[a] IC_{50} (μM) values were calculated as concentration of doxorubicin which inhibits after 72 hours of cultivation (see Methods) the incorporation of [^{3}H]-thymidine by exposed cells to 50 % of the controls. The activity of control cells was always higher than 50 000 cpm/well. Experiments were repeated 5-9 times and average value ± SE is shown. The resistance ratio was calculated by dividing the IC_{50} value for P388/MDR cell line by corresponding value in P388 cells. Dox: doxorubicin; P-Ahx-NH-N=Dox: HPMA copolymer-bound Dox.

5.3 Toxicity of selected P-gp inhibitors and their derivatives *in vitro*

The P-gp inhibitors and their derivatives were intended to induce sensitization of the MDR cancer cells to the cytostatic effect of Dox. However, it was important that the concentration used not affect the proliferation of MDR cells *per se*. Thus, both P388 and P388/MDR cells were incubated with titrated concentrations of the tested compounds for 72 hours, and the IC_{50}s were determined by standard [^{3}H]-thymidine incorporation assay (for more detailed description see Methods). The results are summarized in Table 5.2.

Table 5.2: IC_{50} values of different inhibitors of P-gp determined in sensitive P388 and multidrug resistant P388/MDR cell lines.

P-gp inhibitor and derivatives	P388 IC_{50} (µM)[a]	P388/MDR IC_{50} (µM)
Reversin 121	12.1 ± 1.45	5.5 ± 0.74
OPe-R121	> 32	> 32
OHe-R121	11.9 ± 1.65	21.5 ± 1.00
MeOHe-R121	10.6 ± 1.75	15.3 ± 2.66
OBP-R121	23.0 ± 0.50	14.1 ± 2.03
Reversin 205	3.9 ± 0.25	22.7 ± 0.20
MeOHe-R205	13.2 ± 0.60	34.3 ± 0.80
Ritonavir	7.2 ± 0.72	24.9 ± 1.02
OHe-RIT	11.1 ± 0.76	14.2 ± 0.56
MeOHe-RIT	9.1 ± 0.82	12.4 ± 1.40
OPB-RIT	11.5 ± 1.50	43.0 ± 1.00

[a] IC_{50} (µM) values were calculated as concentration of tested P-gp inhibitor or its derivative which inhibited the incorporation of [^{3}H]-thymidine into exposed cells to 50 % of the controls after 72 hours of culture (see Methods). The activity of control cells was always higher than 50 000 cpm/well. The experiments were repeated 2-6 times, and average values ± SE are shown.

All R121 derivatives except for OPe-R121, which showed no toxicity in either cell line within the concentration range used, exerted toxicity comparable to unmodified reversin 121 in the P388 cell line. However, MeOHe-R121, OHe-R121 and OPB-R121 showed approximately 2.5-4 times lower toxicity than unmodified reversin 121 in the P388/MDR cell line. Notably, reversin 121 had more than two-fold higher toxicity to the P388/MDR cells than to the P388 cells. Conversely, reversin 205 was almost six times less toxic to the P388/MDR cells than the P388 cells. MeOHe-R205 was less toxic than parent compound in both cell lines. However, the decrease in toxicity was more pronounced in the P388 cells (approximately 6 times versus approximately 1.5 times). Ritonavir, the last P-gp inhibitor tested, was approximately 3.5 times less toxic to the P388/MDR cells than to the P388 cells. All ritonavir esters were shown to have comparable or only slightly lower toxicity in the P388 cell line. On the other hand, OHe-RIT and MeOHe-RIT showed two-fold higher toxicity and OPB-RIT showed two-fold lower toxicity than the unmodified ritonavir in the P388/MDR cell line.

5.4 Inhibitory activity of selected P-gp inhibitors and their derivatives

All compounds described above were tested for their potential to inhibit the drug efflux function of P-gp using calcein assay. This method is based on calcein^{AM} which is able to cross the cytoplasmic membrane. However, it is cleaved by intracellular esterases to calcein, which become fluorescently active, and unable to cross cell membrane. Moreover, calcein is very good substrate for P-gp which leads to decrease of intracellular fluorescence in P-gp expressing cells. Thus, cells with strongly expressed P-gp remain negative when exposed to calcein^{AM}, while normal P-gp negative cells are highly positive. The P388/MDR cells were incubated with titrated concentrations of P-gp inhibitors or their derivatives for the 30 minutes before calcein^{AM} was added. Cells were incubated for another 20 minutes and analyzed by flow cytometry. P388/MDR cells incubated with 10 μM cyclosporine A (CsA) and P388 cells were used as positive controls.

5.4.1 Reversin 121 and its derivatives

To identify the promising candidate compound for future conjugation to HPMA copolymer carrier, four derivatives of reversin 121 were tested for their inhibitory activity in P388/MDR cells using calcein assay. MeOHe-R121 showed exceptionally high inhibitory activity of all derivatives of reversin 121 tested (Figure 5.2). Actually, MeOHe-R121 derivative was found to be even more potent P-gp inhibitor than unmodified reversin 121. Of note, MeOHe-R121 was found to be approximately 3 times less toxic than unmodified reversin 121 in P388/MDR cells. Moreover, MeOHe-R121 showed highest inhibitory activity at a concentration of 8 µM, which is far below its IC_{50} in these cells. MeOHe-R121 derivative is thus the first promising candidate as potent P-gp inhibitor with the ability to be conjugated to HPMA copolymer via hydrazone bond.

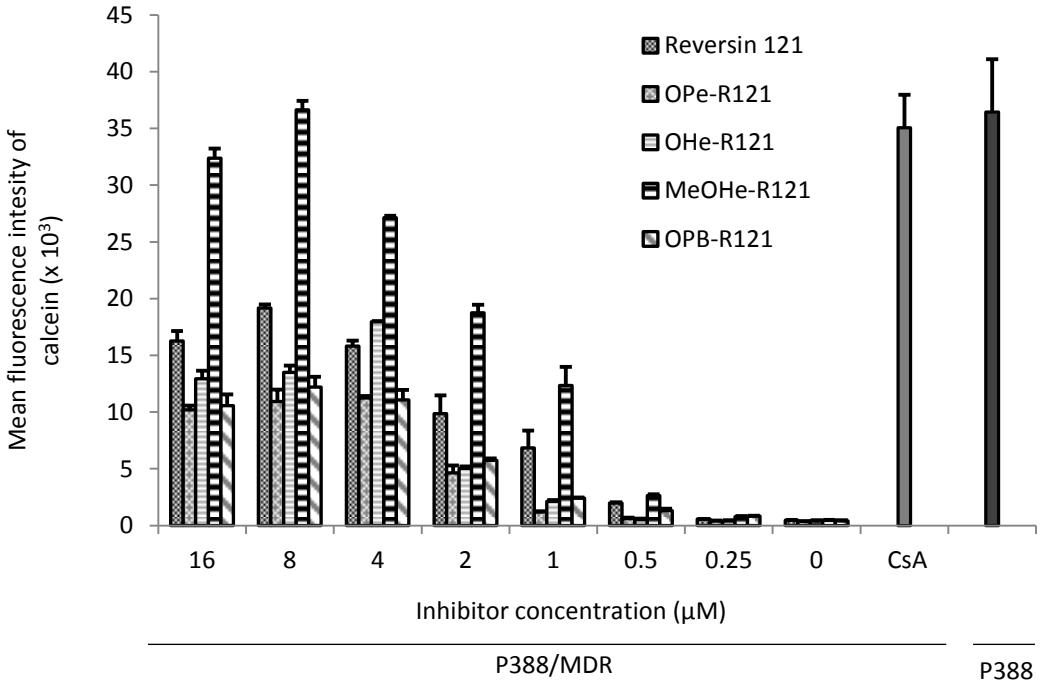

Figure 5.2: Inhibition of P-gp function by reversin 121 and its derivatives in P388/MDR cells. The P388/MDR cells were incubated with titrated concentrations of the P-gp inhibitors or their derivatives for 30 min under standard culture conditions. Calcein^{AM} was then added and the cells were incubated for another 20 min. The cells were analyzed by flow cytometry for calcein fluorescence, and the dead cells were gated out using Hoechst 33258. P388/MDR cells incubated with 10 µM cyclosporine A (CsA) and P388 cells incubated with calcein^{AM} only were used as positive controls. The values shown are the averages of 3-6 experiments ± SD.

5.4.2 Reversin 205 and its derivatives

Similarly to reversin 121, reversin 205 and only one derivative, reversin 205 modified with 5-methyl-4-oxohexanoyl group (MeOHe-R205), were tested as an another potential inhibitors of P-gp by calcein assay. MeOHe-R205 showed virtually no P-gp inhibitory activity at all, despite the fact that this kind of modification resulted in increasing P-gp blocking activity in reversin 121 (Figure 5.3).

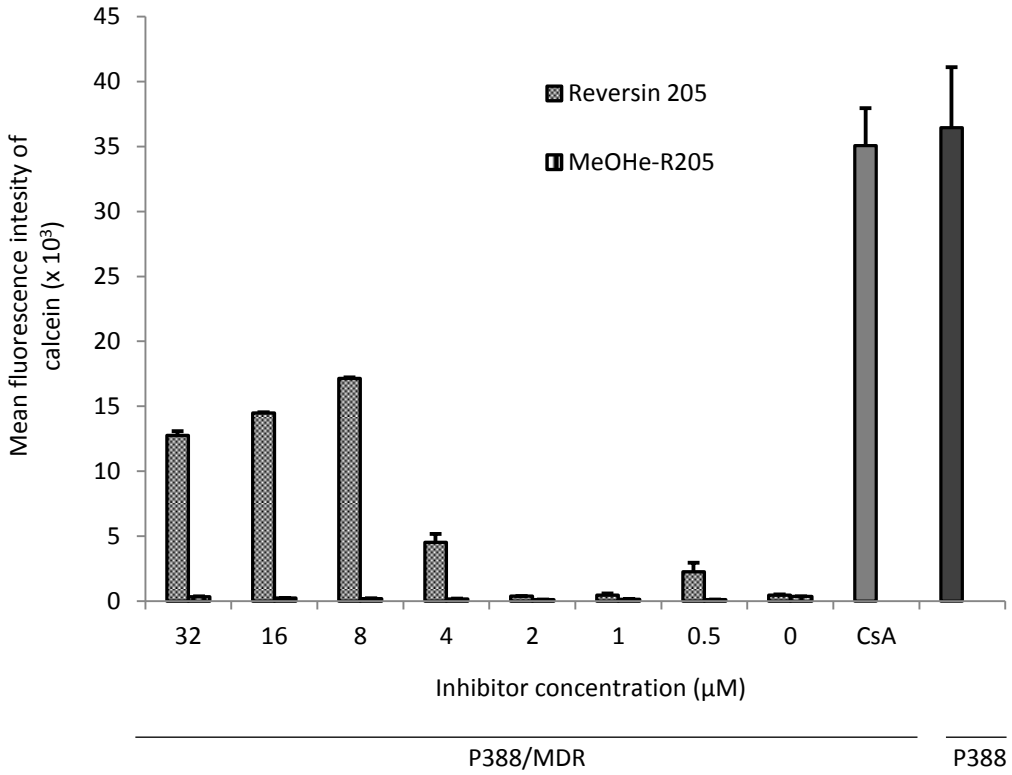

Figure 5.3: Inhibition of P-gp function by reversin 205 and MeOHe-R205 derivative in P388/MDR cells. The P388/MDR cells were incubated with titrated concentrations of the P-gp inhibitors or their derivatives for 30 min under standard culture conditions. Calcein^{AM} was then added and the cells were incubated for another 20 min. The cells were analyzed by flow cytometry for calcein fluorescence, and the dead cells were gated out using Hoechst 33258. P388/MDR cells incubated with 10 µM cyclosporine A (CsA) and P388 cells incubated with calcein^{AM} only were used as positive controls. The values shown are the averages of 3-6 experiments ± SD.

5.4.3 Ritonavir and its derivatives

Ritonavir and its three derivatives shown in Table 5.2 were tested for their potential to block P-gp. Only MeOHe-RIT showed good activity in the inhibition of P-gp, while others derivatives were significantly less potent or comparable with unmodified ritonavir. Moreover, MeOHe-RIT was also found to be considerably more potent as a P-gp inhibitor than unmodified ritonavir (Figure 5.4). However, the toxicity observed in MeOHe-RIT was slightly higher and P-gp inhibitory activity is somewhat lower than that found for MeOHe-R121. Anyway, MeOHe-RIT was selected as another candidate for further studies. Interestingly, both selected candidates were obtained through modification with 5-methyl-4-oxohexanoic acid.

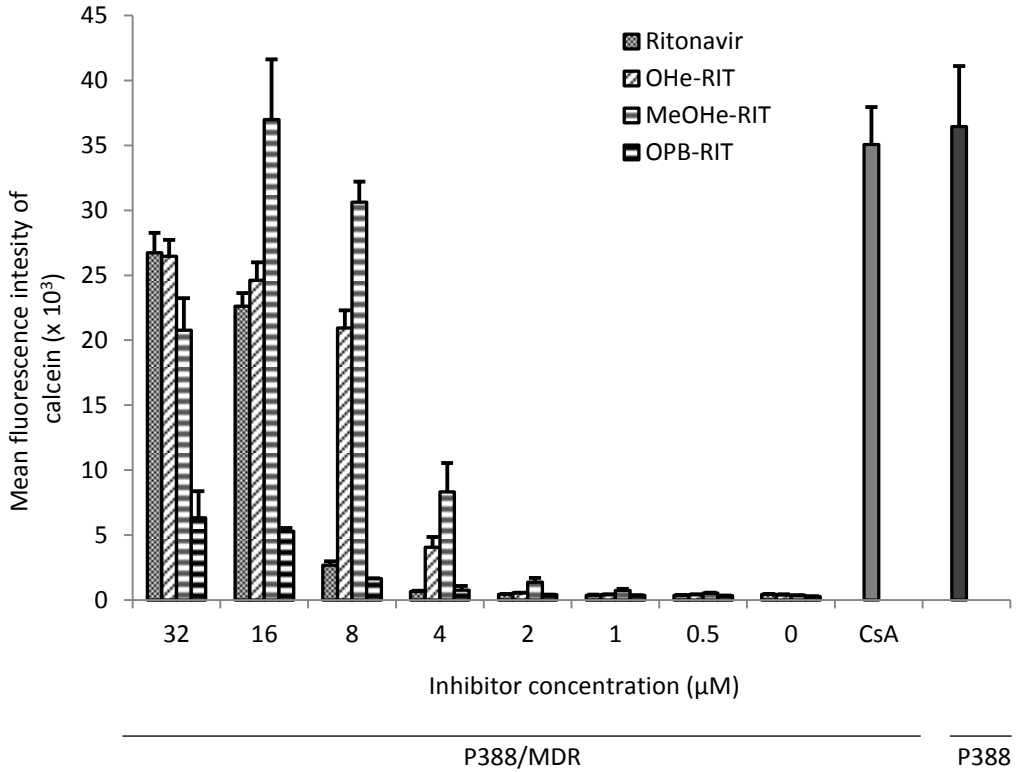

Figure 5.4: Inhibition of P-gp function by ritonavir and its derivative in P388/MDR cells. The P388/MDR cells were incubated with titrated concentrations of the P-gp inhibitors or their derivatives for 30 min under standard culture conditions. Calcein^{AM} was then added and the cells were incubated for another 20 min. The cells were analyzed by flow cytometry for calcein fluorescence, and the dead cells were gated out using Hoechst 33258. P388/MDR cells incubated with 10 µM cyclosporine A (CsA) and P388 cells incubated with calcein^{AM} only were used as positive controls. The values shown are the averages of 3-6 experiments ± SD.

5.5 Sensitization of P388/MDR cells to cytostatic activity of Dox by selected P-gp inhibitors and their derivatives

To evaluate the potential of selected P-gp inhibitors and their derivatives to overcome multidrug resistance in the P-gp overexpressing P388/MDR cells, the cytostatic activity of Dox was determined by the use of [^{3}H]-thymidine assay. P388/MDR cells were exposed to titrated concentrations of Dox, either alone or with constant concentration of P-gp inhibitors or their derivatives.

5.5.1 Sensitization of P388/MDR cells by the reversin 121 and its derivatives

Four derivatives of reversin 121 mentioned above, containing the functional group enabling their further binding to HPMA copolymer carrier, were tested for their capability to increase the cytostatic activity of Dox. Among all R121 derivatives, MeOHe-R121 showed the highest capacity to sensitize P388/MDR cells to Dox. The MeOHe-R121 derivative showed gradually increasing capacity to sensitize the P388/MDR cells from approximately 5-fold increase at 0.5 μM to almost complete inhibition of proliferation at 4 μM (Figure 5.5D). Other three derivatives OPe-R121 (Figure 5.5B), OHe-R121 (Figure 5.5C) and OPB-R121 (Figure 5.5E) were much less potent than unmodified reversin 121 (Figure 5.5A) as demonstrated by very low inhibition of proliferation at all tested concentrations. Of note, comparing the efficacy of MeOHe-R121 derivative with reversin 121 on equitoxic dose of 4 μM, which is considered as a non-toxic, the pharmacological activity of both compounds were comparable. The IC_{50} values for Dox in the presence of titrated concentrations of reversin 121 and its derivatives are summarized in Table 5.3. Overall, the results obtained from sensitization of P388/MDR cells to Dox is in good agreement with the results from measurement of the inhibitory activity by the calcein assay and identifies MeOHe-R121 derivative again as a most promising candidate for subsequent conjugation to the HPMA copolymer carrier.

A)

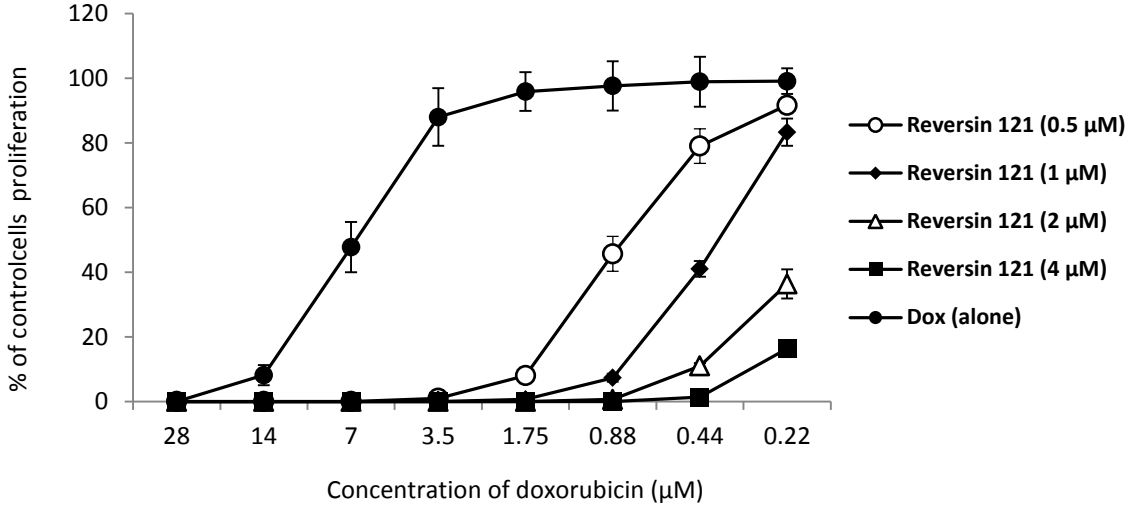
120
100
80
60
40
20
0
% of controlcells proliferation
28
14
7
3.5
1.75
0.88
0.44
0.22
Concentration of doxorubicin (µM)
Reversin 121 (0.5 µM)
Reversin 121 (1 µM)
Reversin 121 (2 µM)
Reversin 121 (4 µM)
Dox (alone)

B)

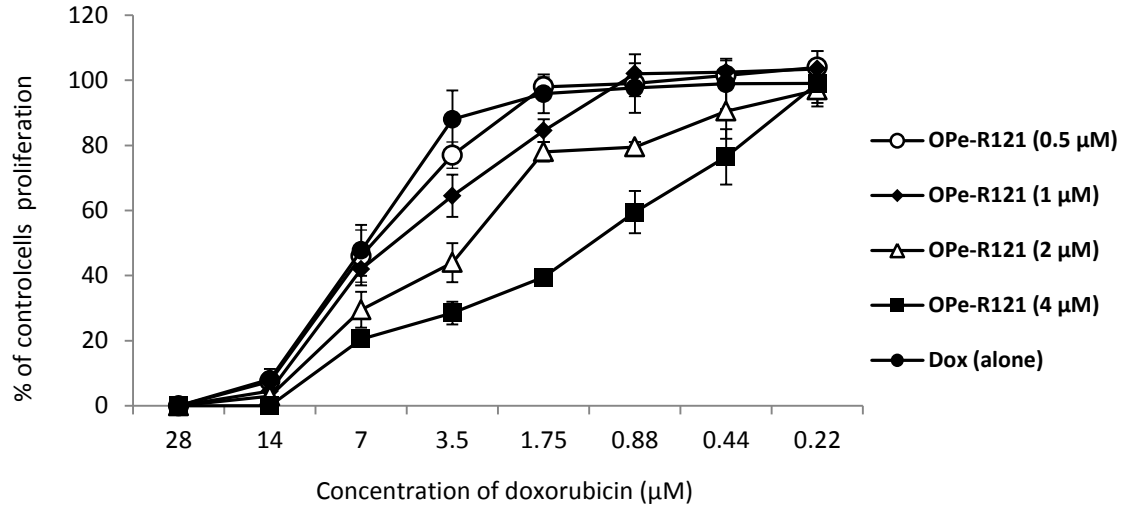
120
100
80
60
40
20
0
% of controlcells proliferation
28
14
7
3.5
1.75
0.88
0.44
0.22
Concentration of doxorubicin (µM)
OPe-R121 (0.5 µM)
OPe-R121 (1 µM)
OPe-R121 (2 µM)
OPe-R121 (4 µM)
Dox (alone)

C)

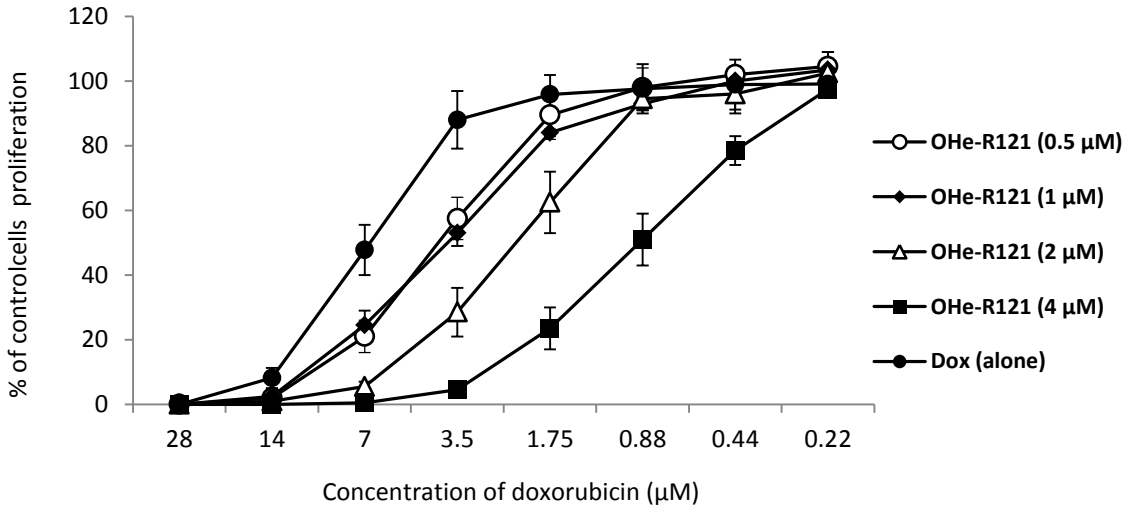
120
100
80
60
40
20
0
% of controlcells proliferation
28
14
7
3.5
1.75
0.88
0.44
0.22
Concentration of doxorubicin (µM)
OHe-R121 (0.5 µM)
OHe-R121 (1 µM)
OHe-R121 (2 µM)
OHe-R121 (4 µM)
Dox (alone)

D)

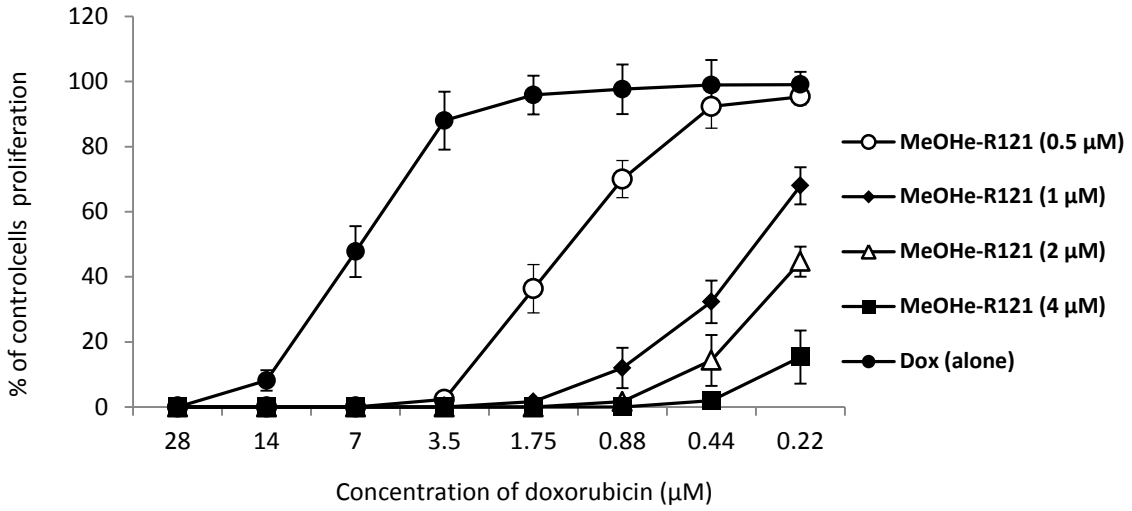

E)

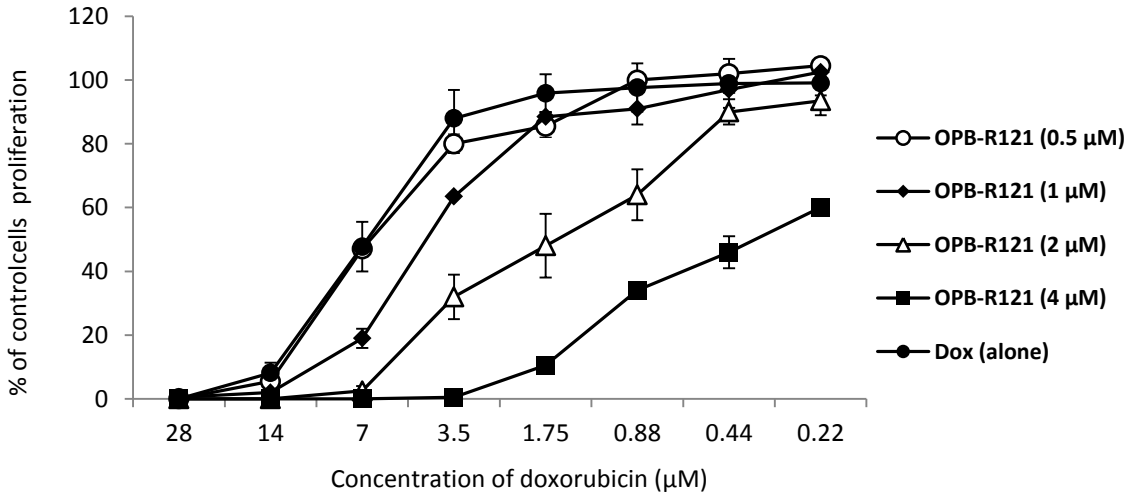

Figure 5.5: Sensitization of P388/MDR cells to the cytostatic effect of Dox by R121 (A), OPe-R121 (B), OHe-R121 (C), MeOHe-R121 (D) and OPB-R121 (E). P388/MDR cells were incubated with titrated concentrations of Dox and a constant concentration of P-gp inhibitor for 72 h under standard culture conditions. The cell proliferation was assessed by [^{3}H]-thymidine incorporation by adding this tracer to the cultures for last 6 h of incubation. The results are shown as the inhibition of the proliferation of the exposed cells relative to the controls (cells incubated in medium only). The activity of the control cells was always greater than 50 000 cpm/well. Each experimental point is the average of 3 experiments ± SD.

Table 5.3: IC_{50} values determined in multidrug resistance P388/MDR cell line for Dox in presence of different concentrations of reversin 121 or its derivatives.[a]

	Type of inhibitor				
	Reversin 121	OPe-R121	OHe-R121	MeOHe-R121	OPB-R121
Dox + inhibitor 4 μM	< 0.20	1.09 ± 0.52	0.93 ± 0.21	< 0.10	0.59 ± 0.38
Dox + inhibitor 2 μM	0.24 ± 0.01	3.14 ± 1.81	2.33 ± 0.45	0.17 ± 0.01	1.88 ± 0.86
Dox + inhibitor 1 μM	0.43 ± 0.05	4.88 ± 1.71	3.86 ± 0.47	0.39 ± 0.10	5.10 ± 1.29
Dox + inhibitor 0.5 μM	0.72 ± 0.03	6.69 ± 3.65	4.21 ± 1.12	1.17 ± 0.22	6.53 ± 1.71

[a] IC_{50} (μM) values were calculated as concentration of doxorubicin which inhibits after 72 hours of cultivation (see Materials and Methods) the incorporation of [^{3}H]-thymidine by exposed cells to 50 % of the controls. The activity of control cells was always higher than 50 000 cpm/well. Experiments were repeated 5-9 times and average value ± SE is shown.

5.5.2 Sensitization of P388/MDR cells by the reversin 205 and its derivative

Similarly, reversin 205 and its derivative MeOHe-R205 were tested for their potential to increase sensitivity of P388/MDR cells to Dox. As shown in Figure 5.6A, reversin 205 showed similar potency to that of reversin 121 in sensitization of P388/MDR cells. However, its derivative MeOHe-R205 was found to have virtually no effect on cytostatic activity of Dox (Figure 5.6B). The IC_{50} values for Dox in the presence of titrated concentrations of reversin 205 and MeOHe-R205 are summarized in Table 5.4.

A)

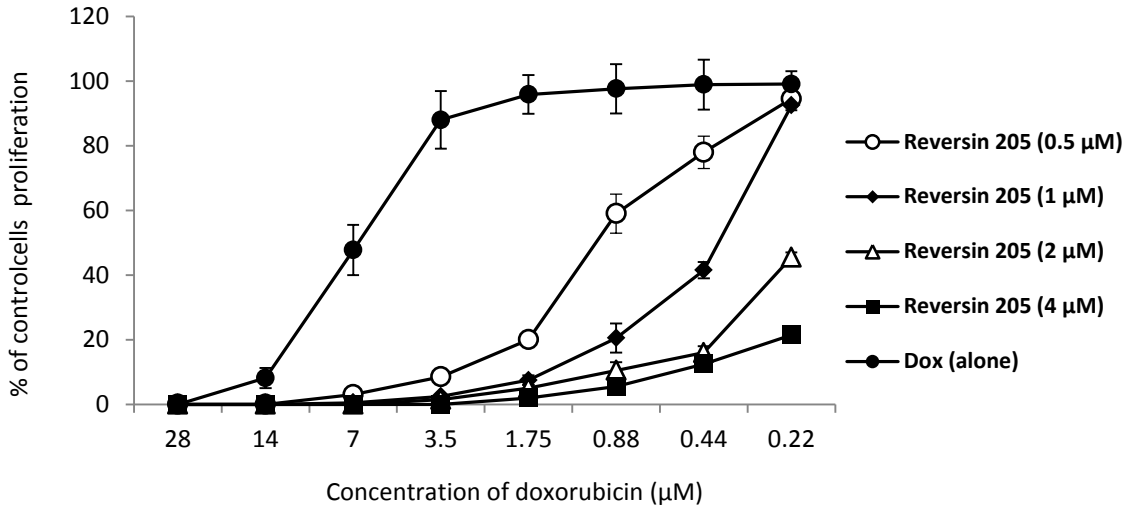

B)

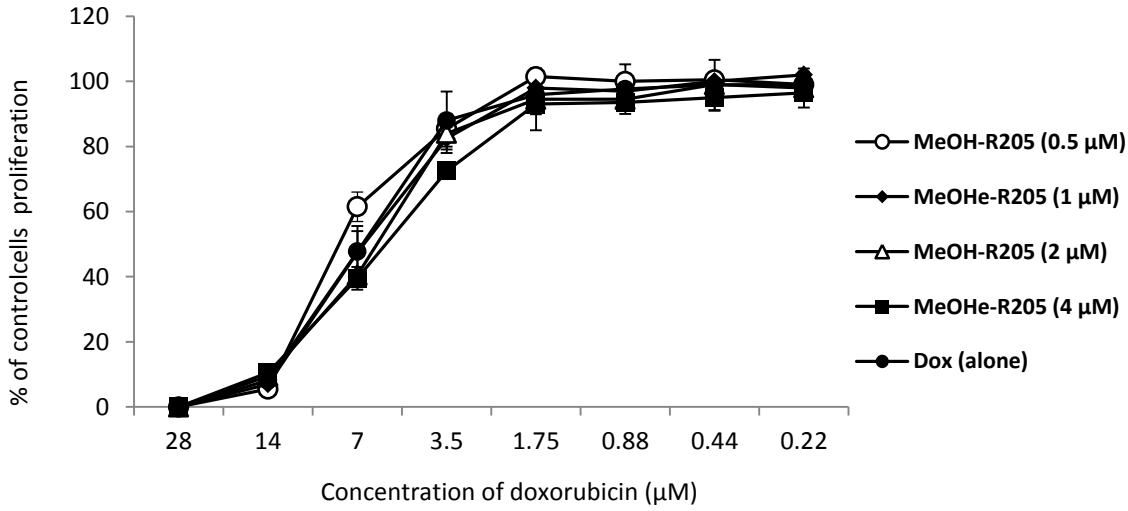

Figure 5.6: Sensitization of P388/MDR cells to the cytostatic effect of Dox by reversin 205 (A) and MeOHe-R205 (B). P388/MDR cells were incubated with titrated concentrations of Dox and a constant concentration of P-gp inhibitor for 72 h under standard culture conditions. The cell proliferation was assessed by [^{3}H]-thymidine incorporation by adding this tracer to the cultures for last 6 h of incubation. The results are shown as the inhibition of the proliferation of the exposed cells relative to the controls (cells incubated in medium only). The activity of the control cells was always greater than 50 000 cpm/well. Each experimental point is the average of 3 experiments ± SD.

Table 5.4: IC_{50} values determined in multidrug resistance P388/MDR cell line for Dox in presence of different concentrations of reversin 205 and MeOH-R205.[a]

	Type of inhibitor	
	Reversin 205	MeOHe-R205
Dox + inhibitor 4 μM	0.24 ± 0.03	5.86 ± 0.34
Dox + inhibitor 2 μM	0.47 ± 0.05	5.00 ± 0.34
Dox + inhibitor 1 μM	0.62 ± 0.03	4.74 ± 0.60
Dox + inhibitor 0.5 μM	1.03 ± 0.03	5.94 ± 1.12

[a] IC_{50} (μM) values were calculated as concentration of doxorubicin which inhibits after 72 hours of cultivation (see Materials and Methods) the incorporation of [^{3}H]-thymidine by exposed cells to 50 % of the controls. The activity of control cells was always higher than 50 000 cpm/well. Experiments were repeated 5-9 times and average value ± SE is shown.

5.5.3 Sensitization of P388/MDR cells by the ritonavir and its derivatives

We determined the potential of P-gp inhibitor ritonavir and its three derivatives to increase the cytostatic activity of Dox in P-gp overexpressing P388/MDR cells. Generally, ritonavir was much less efficient in sensitizing the P388/MDR cells to Dox (Figure 5.7) in comparison to reversin 121. Nevertheless, one of the tested derivative, MeOHe-RIT, showed superior activity in comparison to all other tested derivatives of ritonavir, and surprisingly, also in comparison to unmodified RIT. It increased cytostatic activity of Dox more than 20 times in comparison to less than 2 times increase in the case of unmodified RIT at 5 μM concentration (Table 5.5). Thus, MeOHe-RIT was shown to be almost 15 times more potent than unmodified ritonavir. MeOHe-RIT was found to have slightly higher toxicity than the parent compound ritonavir (Table. 5.2), but we compared their inhibitory activity at 5 μM concentration which is considered as a non-toxic. Thus, this result reflects data of the calcein assay, where this derivative was found to most efficiently block P-gp activity. Interestingly, the OPB-RIT was also found to be more potent inhibitor than unmodified RIT in sensitization of P388/MDR cells to Dox. However, the potential of OPB-RIT was much lower than that of MeOHe-RIT. OHe-RIT derivative was much less potent than unmodified ritonavir or other derivatives, which is demonstrated by the very little

potency to increase cytostatic activity of Dox (Figure 5.7B). The IC_{50} values for Dox in the presence of titrated concentrations of ritonavir and its derivatives are summarized in Table 5.5.

A)

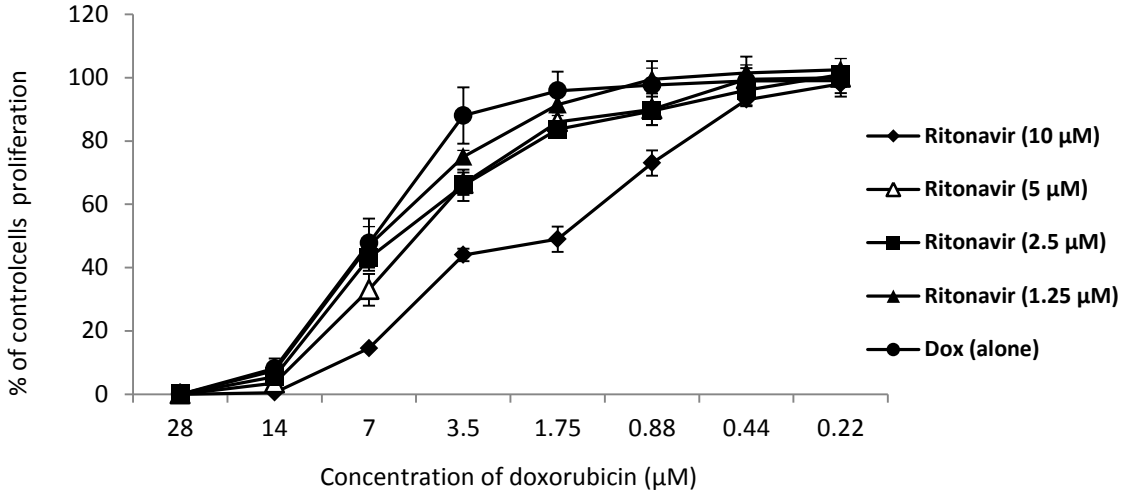

B)

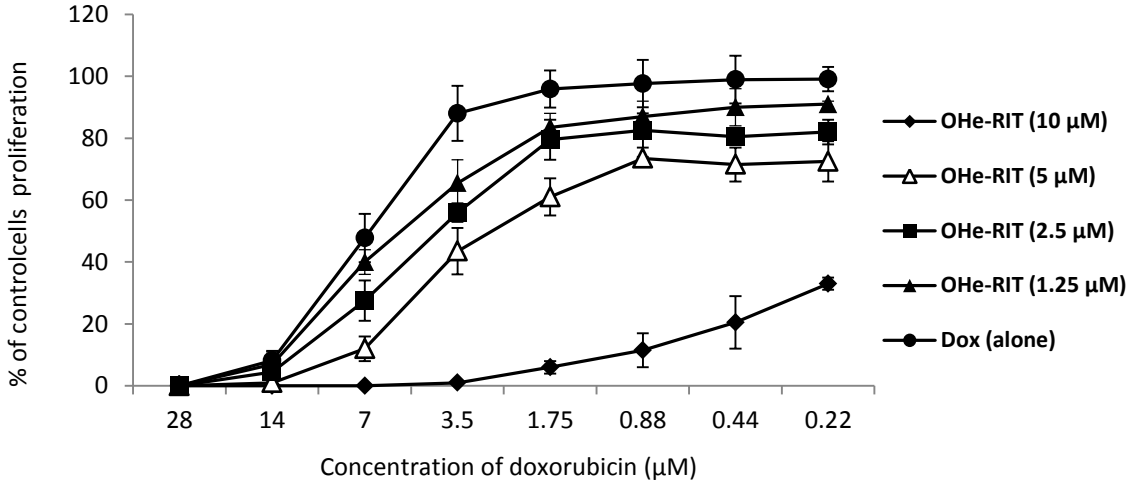

C)

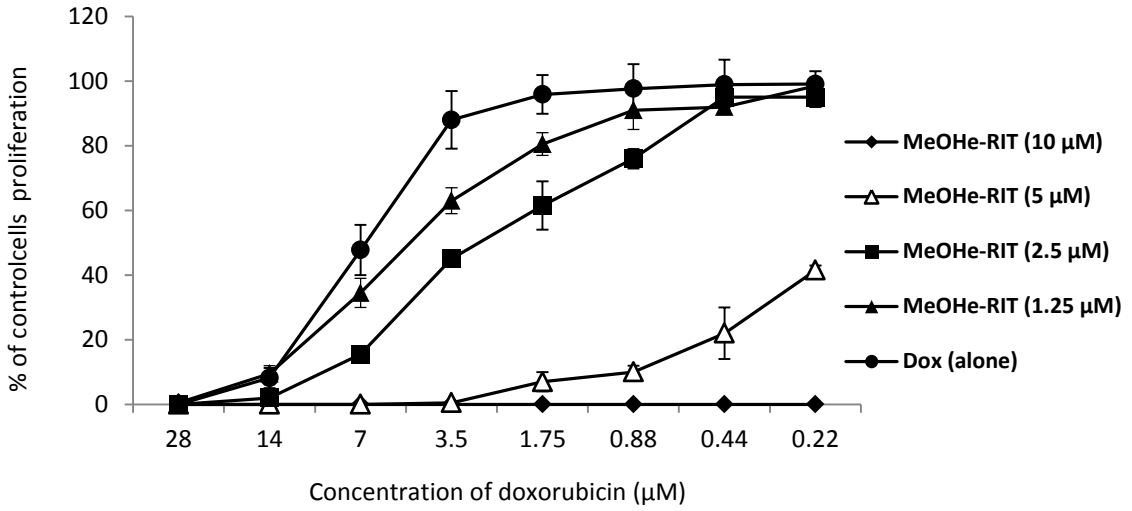

D)

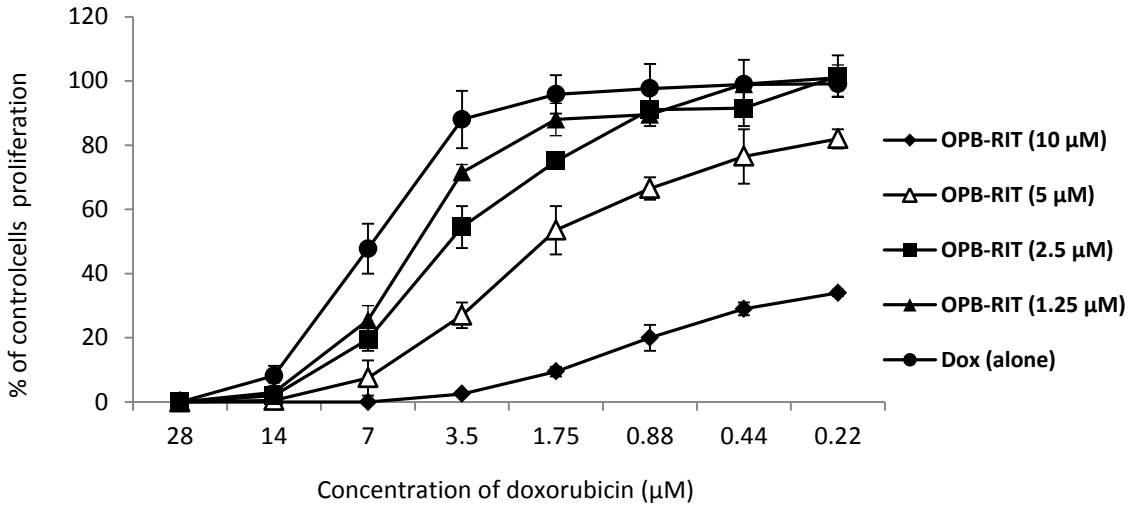

Figure 5.7: Sensitization of P388/MDR cells to the cytostatic effect of Dox by ritonavir (A), OHe-RIT (B), MeOHe-RIT (C) and MeOHe-RIT (D). P388/MDR cells were incubated with titrated concentrations of Dox and a constant concentration of P-gp inhibitor for 72 h under standard culture conditions. The cell proliferation was assessed by [^{3}H]-thymidine incorporation by adding this tracer to the cultures for last 6 h of incubation. The results are shown as the inhibition of the proliferation of the exposed cells relative to the controls (cells incubated in medium only). The activity of the control cells was always greater than 50 000 cpm/well. Each experimental point is the average of 3 experiments ± SD.

Table 5.5: IC_{50} values determined in multidrug resistance P388/MDR cell line for Dox in presence of different concentrations of ritonavir and its derivatives.[a]

	Type of inhibitor			
	Ritonavir	OHe-RIT	MeOHe-RIT	OPB-RIT
Dox + inhibitor 10 μM	2.53 ± 0.47	< 0.20	< 0.20	< 0.20
Dox + inhibitor 5 μM	4.34 ± 0.78	2.83 ± 1.00	0.27 ± 0.07	1.72 ± 0.69
Dox + inhibitor 2.5 μM	5.21 ± 0.64	4.36 ± 1.52	2.81 ± 0.40	3.71 ± 0.43
Dox + inhibitor 1.25 μM	5.81 ± 0.74	5.81 ± 1.26	3.62 ± 0.86	4.48 ± 0.86

[a] IC_{50} (μM) values were calculated as concentration of doxorubicin which inhibits after 72 hours of cultivation (see Materials and Methods) the incorporation of [^{3}H]-thymidine by exposed cells to 50 % of the controls. The activity of control cells was always higher than 50 000 cpm/well. Experiments were repeated 5-9 times and average value ± SE is shown.

5.6 *In vitro* toxicity of HPMA copolymer-bound MeOHe-R121 and MeOHe-RIT

In the effort of finding a novel polymeric therapeutics based on water soluble HPMA copolymer bearing an inhibitor of P-gp, new HPMA copolymer conjugate containing MeOHe-R121 (P-Ahx-NH-N=MeOHe-R121) was synthesized. Moreover, conjugates containing MeOHe-R121 (P-Ahx-NH-NH-MeOHe-R121) and unmodified R121 (P-Ahx-R121) bound through stable non-biodegradable bond were used as controls. The toxicity of the conjugates was tested by the use of [^{3}H]-thymidine incorporation assay in the same way as used for low-molecular weight P-gp inhibitors and their derivatives. Conjugate P-Ahx-NH-N=MeOHe-R121 was found to have no toxicity up to 24 μM and only very mild toxicity was observed at 48 μM (Figure 5.8). Moreover, the P-Ahx-R121 and P-Ahx-NH-NH-MeOHe-R121 conjugates containing P-gp inhibitor bound to the HPMA copolymer carrier via non-biodegradable bond exhibited no toxicity at all. All tested polymeric conjugates had no toxicity in P388 cells up to 48 μM, probably reflecting lower toxicity of reversin 121 in these cells.

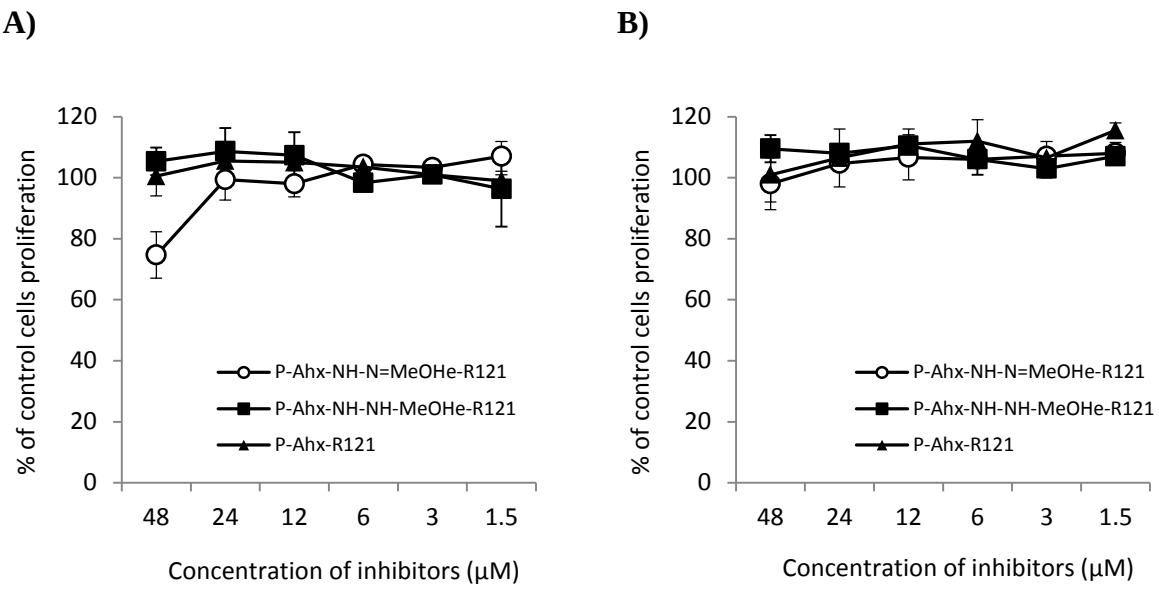

Figure 5.8: Toxicity of conjugates P-Ahx-NH-N=MeOHe-R121, P-Ahx-NH-NH-MeOHe-R121 and P-Ahx-R121 in P388/MDR (A) and P388 (B) cells. The P388/MDR or P388 cells were incubated with titrated concentrations of conjugates P-Ahx-NH-N=MeOHe-R121, P-Ahx-NH-NH-MeOHe-R121, P-Ahx-R121 for 72 h under standard culture conditions. Cell proliferation was assessed using [^{3}H]-thymidine incorporation by adding this tracer to the cultures for last 6 h of incubation. The results shown are the inhibition of the proliferation of the exposed cells relative to the controls (cells incubated in medium only). The activity of control cells was always greater than 50 000 cpm/well. Each experimental point is the average of 3 experiments ± SD.

Next, the toxicity of polymer conjugate P-Ahx-NH-N=MeOHe-RIT was tested (Figure 5.9). Similarly to conjugate containing MeOHe-R121, conjugate P-Ahx-NH-NH-MeOHe-RIT was used as control. Polymeric conjugate P-Ahx-NH-N=MeOHe-RIT exhibited significant toxicity at concentrations 24 µM and 48 µM in both P388 and P388/MDR cell lines. The polymer conjugate P-Ahx-NH-NH-MeOHe-RIT containing MeOHe-RIT derivative bound to HPMA copolymer carrier via non-biodegradable bond showed no toxicity up to 48 µM in P388/MDR cells. However, this control conjugate had significant toxicity at 48 µM in P388 cells. Since, the MeOHe-RIT is not released from this conjugate at tissue culture condition, P-Ahx-NH-NH-MeOHe-RIT probably possess toxicity *per se*.

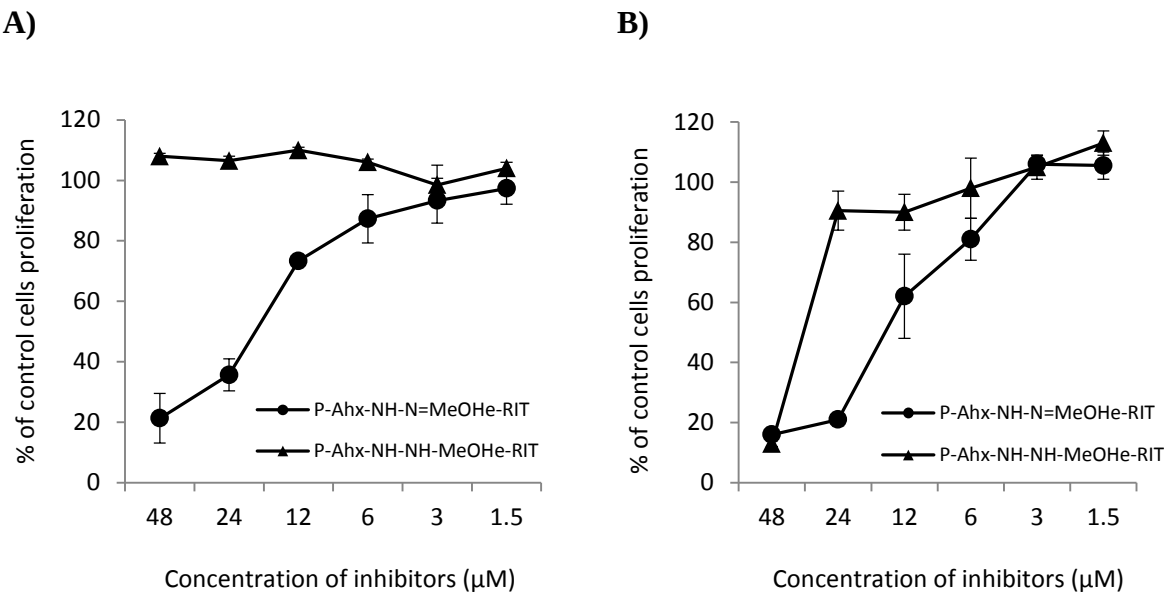

Figure 5.9: Toxicity of conjugates P-Ahx-NH-N=MeOHe-RIT and P-Ahx-NH-NH-MeOHe-RIT in P388/MDR (A) and P388 (B) cells. The P388/MDR or P388 cells were incubated with titrated concentrations of conjugates P-Ahx-NH-N=MeOHe-RIT and P-Ahx-NH-NH-MeOHe-RIT for 72 h under standard culture conditions. Cell proliferation was assessed using [^{3}H]-thymidine incorporation by adding this tracer to the cultures for last 6 h of incubation. The results shown are the inhibition of the proliferation of the exposed cells relative to the controls (cells incubated in medium only). The activity of control cells was always greater than 50 000 cpm/well. Each experimental point is the average of 3 experiments ± SD.

5.7 P-gp inhibitory activity of HPMA copolymer-bound MeOHe-R121 and MeOHe-RIT

P-Ahx-NH-N=MeOHe-R121 and P-Ahx-NH-N=MeOHe=RIT were tested for their capability to inhibit P-gp function by the use of calcein assay. Both tested HPMA copolymer conjugates are relatively stable at physiological pH 7.4 while pharmacological active derivatives MeOHe-R121 and MeOHe-RIT are released at pH 5.0. The *in vitro* release experiments with conjugates P-Ahx-NH-N=MeOHe-R121 and P-Ahx-NH-N=MeOHe-RIT showed that after 24 hour of incubation at pH 5.0 almost 95% of MeOHe-R121 derivative was released from the conjugate, while 85% of MeOHe-RIT derivative was released already after 5 hour (data not shown). Accordingly, the potential of both conjugates to inhibit the drug-efflux function of P-gp were tested after 16 hours of incubation.

P388/MDR cells were preincubated with P-Ahx-NH-N=MeOHe-R121, for 16 hours and then calcein assay was performed. The P-Ahx-NH-NH-MeOHe-R121 and P-Ahx-R121 conjugates with MeOHe-R121 derivative and reversin 121 bound via non-biodegradable bond were used as controls. The P-Ahx-NH-N=MeOHe-R121 effectively and gradually inhibited P-gp activity up to 48 μM, the highest tested concentration. This conjugate was even able to inhibit the intracellular calcein accumulation to the level seen in positive control at 48 μM. Moreover, none of the control conjugates showed any activity (Figure 5.10A). Since P-Ahx-NH-N=MeOHe-R121 showed no toxicity in P388 and P388/MDR cells at the same concentration range (Figure 5.8), we can hypothesized that therapeutic window of this conjugate is wider than that for free MeOHe-R121 derivative.

Similarly to the R121 derivative-bearing conjugate the P-Ahx-NH-N=MeOHe-RIT and P-Ahx-NH-NH-MeOHe-RIT were tested for their capability to inhibit P-gp function in P388/MDR cells. P-Ahx-NH-N=MeOHe-RIT was very effective in P-gp inhibition (Figure 5.10B), 12 μM concentration was able to inhibit the calcein efflux to the level seen with CsA (positive control). The P-Ahx-NH-NH-MeOHe-RIT used as a control conjugate showed no activity.

A)

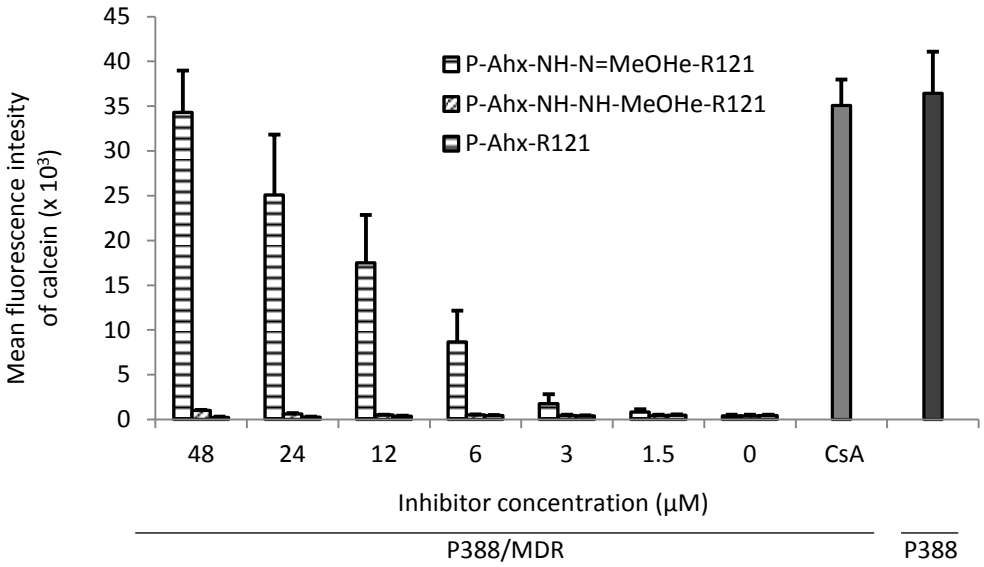

B)

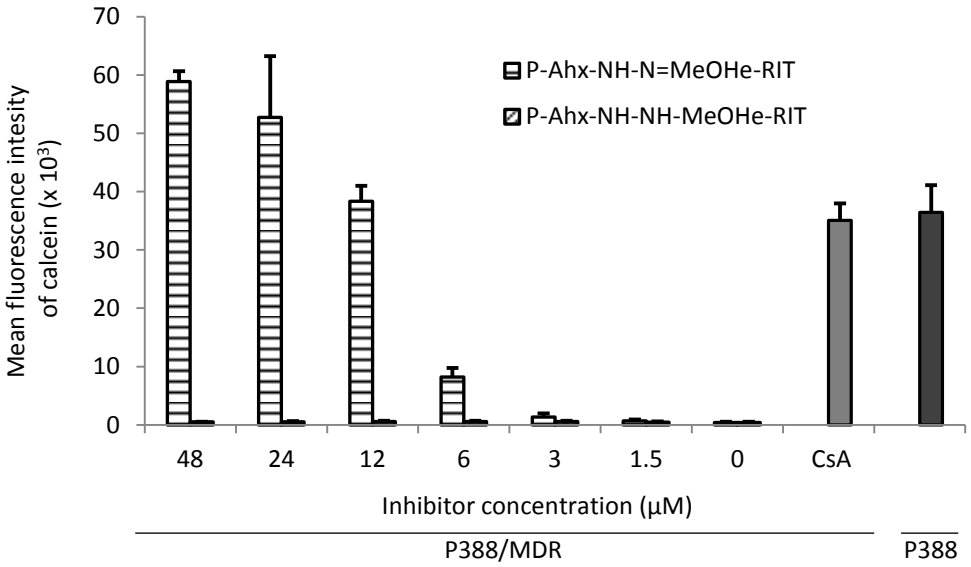

Figure 5.10: Ability of conjugates P-Ahx-NH-N=MeOHe-R121, P-Ahx-NH-NH-MeOHe-R121 and P-Ahx-R121 (A) and conjugates P-Ahx-NH-N=MeOHe-RIT and P-Ahx-NH-NH-MeOHe-RIT (B) to inhibit P-gp function in the P388/MDR cells. P388/MDR cells were incubated with titrated concentrations of conjugates P-Ahx-NH-N=MeOHe-R121, P-Ahx-NH-NH-MeOHe-R121, P-Ahx-R121, P-Ahx-NH-N=MeOHe-RIT and P-Ahx-NH-NH-MeOHe-RIT for 16 h under standard culture conditions. Calcein^{AM} was then added, and cells were incubated for another 30 min. The cells were analyzed by flow cytometry for calcein fluorescence, and the dead cells were gated out using Hoechst 33258. P-388/MDR cells incubated with 10 µM cyclosporine A (CsA) and P388 cells incubated with calcein^{AM} only were used as positive controls. The values shown are the averages of 3 experiments ± SD.

5.8 Sensitization of P388/MDR cells to the cytostatic activity of Dox by the HPMA copolymer conjugates bearing MeOHe-R121 or MeOHe-RIT

To evaluate the potential of polymer conjugates P-Ahx-NH-N=MeOHe-R121 and P-Ahx-NH-N=MeOHe-RIT for sensitization of P388/MDR cells to cytostatic effect of Dox we employed standard [^{3}H]-thymidine assay. The P388/MDR cells were incubated with titrated concentrations of Dox plus fixed concentration of polymer conjugates.

We decide that highest tested concentration of conjugate P-Ahx-NH-N=MeOHe-R121, should be 24 μM, because higher concentrations exhibited modest toxicity. As shown in Figure 5.11A, the P-Ahx-NH-N=MeOHe-R121 conjugate showed a gradually increasing capacity to sensitize the P388/MDR cells to Dox beginning at 1.5 μM and approximately 50-fold increase of cytostatic activity of Dox was observed at concentration 24 μM. The P-Ahx-NH-NH-MeOHe-R121 and P-Ahx-R121 conjugates, bearing MeOHe-R121 and R121 bound via non-biodegradable bond, were used as control compounds and showed no activity in sensitization of P388/MDR cells (Figure 5.11A).

P-Ahx-NH-N=MeOHe-RIT and P-Ahx-NH-NH-MeOHe-RIT (control compound) were tested for their potential to increase cytostatic activity of Dox in P388/MDR cells (Figure 5.11B). The highest concentration used was 12 μM, due the observed toxicity in higher concentrations. The P-Ahx-NH-N=MeOHe-RIT conjugate was not able to sensitize the P388/MDR cells to cytostatic activity of Dox up to 3 μM, and only moderate activity was observed at 6 μM. However, concentration of 12 μM provided 50-fold sensitization, which was comparable activity to the 24 μM of P-Ahx-NH-N=MeOHe-R121 conjugate. Nevertheless, there was still moderate level of toxicity seen at 12 μM of this conjugate (see Figure 5.9), which could be the reason of unexpectedly high sensitization.

A)

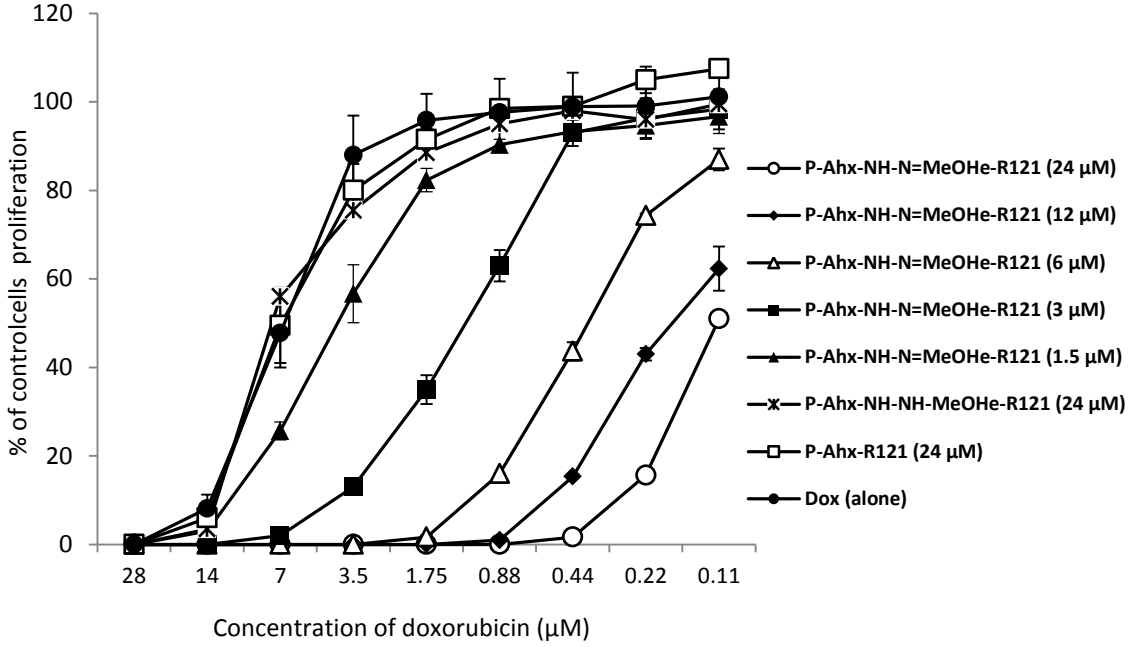

B)

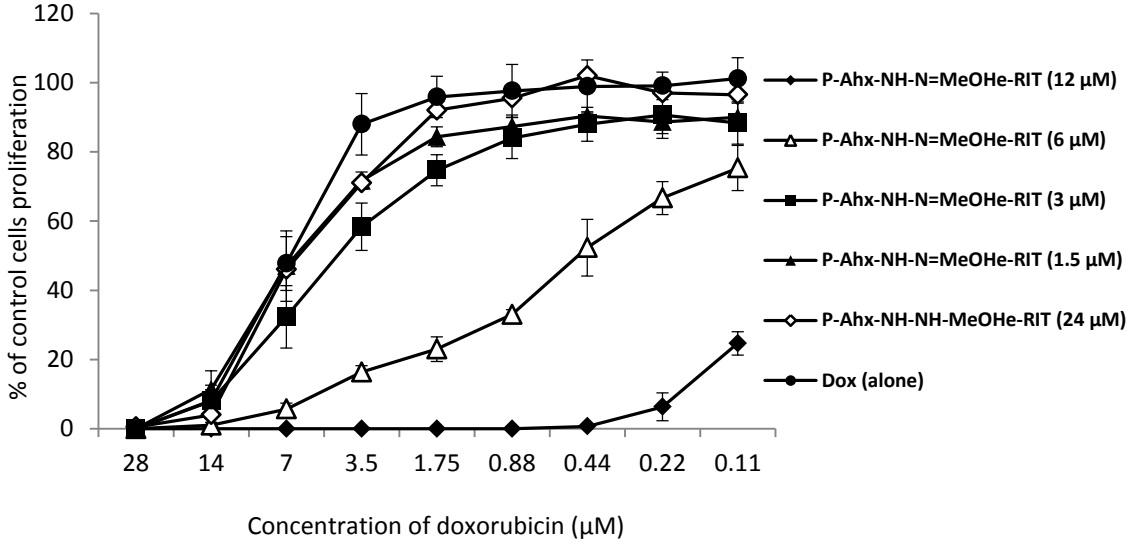

Figure 5.11: Sensitization of P388/MDR cells to the cytostatic effect of doxorubicin by the conjugates P-Ahx-NH-N=MeOHe-R121, P-Ahx-NH-NH-MeOHe-R121 and P-Ahx-R121 (A), and conjugates P-Ahx-NH-N=MeOHe-RIT and P-Ahx-NH-NH-MeOHe-RIT (B). P388/MDR cells were incubated with titrated concentrations of conjugates P-Ahx-NH-N=MeOHe-R121, P-Ahx-NH-NH-MeOHe-R121, P-Ahx-R121, P-Ahx-NH-N=MeOHe-RIT or P-Ahx-NH-NH-MeOHe-RIT at the indicated concentration of Dox for 72 h under standard culture conditions. Cell proliferation was assessed using [^{3}H]-thymidine incorporation by adding this tracer to the cultures for last 6 h of incubation. The results are shown as the inhibition of the proliferation of the exposed cells relative to controls (cells incubated in medium only). The activity of the control cells was always greater than 50 000 cpm/well. Each experimental point is the average of 3 experiments ± SD.

5.9 Evaluation of cytotoxic activity in P388/MDR cell line exposed to the Dox and HPMA copolymer conjugate P-Ahx-NH-N=MeOHe-R121

To evaluate the potential of the conjugate P-Ahx-NH-N=MeOHe-R121 to sensitize P388/MDR cells to cytotoxic activity of Dox, apoptotic induction was determined in P388/MDR cell line by Annexin V apoptotic assay (for more detail see Methods). The P388/MDR cells were incubated with fixed concentration of Dox alone or with titrated concentrations of P-Ahx-NH-N=MeOHe-R121 conjugate. Cells were incubated at these conditions for 24 hours and fraction of live (Annexin V^-/Hoechst 33258^-), apoptotic (Annexin V^+/Hoechst 33258^-) and dead cells (Annexin V^-/Hoechst 33258^+) were determined

When P388/MDR cells were incubated with Dox at concentration 7 μM (comparable to IC_{50} of Dox), no cytotoxic activity was observed as fraction of live cells was comparable with cells incubated without Dox (Figure 5.12). Incubation of Dox with P-Ahx-NH-N=MeOHe-R121 from 1.5 μM up to the 24 μM showed gradually increasing cytotoxic activity of Dox in all tested concentrations, demonstrated by decreasing percentage of fraction of live cells and simultaneously increasing percentage of apoptotic and dead cells fraction. All tested concentrations of P-Ahx-NH-N=MeOHe-R121 conjugate alone showed no cytotoxicity. These results indicate that P-Ahx-NH-N-MeOHe-R121 is able to significantly increase the cytotoxic activity at concentrations when it has no cytotoxicity *per se*.

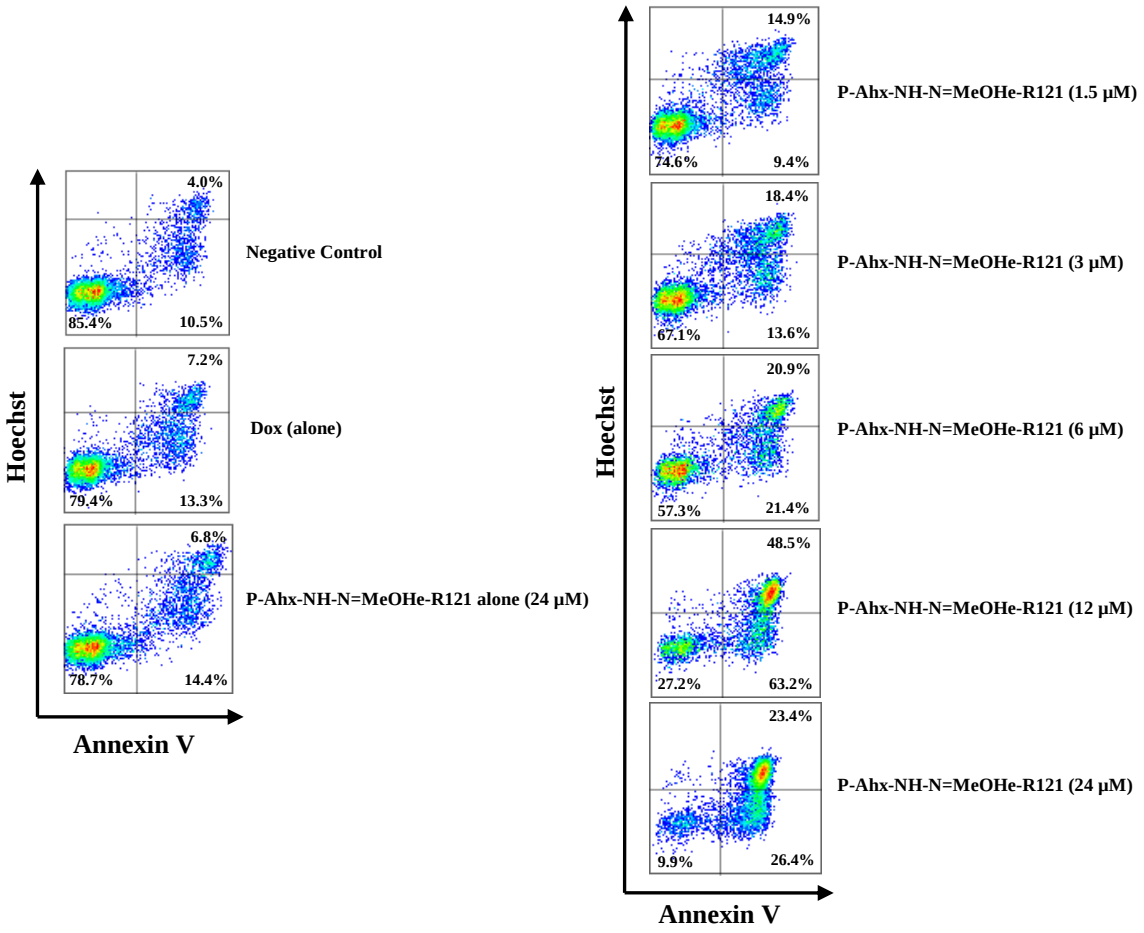

Figure 5.12: Sensitization of P388/MDR cells to the cytotoxic activity of Dox by the P-Ahx-NH-N=MeOHe-R121 conjugate. P388/MDR cells were incubated with titrated concentration of P-Ahx-NH-N=MeOHe-R121 and a constant concentration of Dox (7 µM) alone or with polymeric conjugate for 24 h under standard culture conditions. Cells were than stained with Annexin V-Dy647/Hoechst 33258 and the percentage of live (Annexin V^-/Hoechst 33258^-), apoptotic (Annexin V^+/Hoechst 33258^-) and dead (Annexin V^-/Hoechst 33258^+) fraction was determined by flow cytometry. Cell incubated in medium only were used as a negative controls. Experiments were repeated 3 times.

5.10 Intracellular accumulation of Dox in P388/MDR cell line exposed to Dox and P-Ahx-NH-N=MeOHe-R121 conjugate

To evaluate the potential of conjugate P-Ahx-NH-N=MeOHe-R121 to increase the intracellular accumulation of Dox, P388/MDR cells were incubated with fixed concentration of Dox alone or with titrated concentrations of P-Ahx-NH-N=MeOHe-R121 conjugate for 24 hours (Figure 5.13).

Incubation of Dox with P-Ahx-NH-N=MeOHe-R121 in concentration range from 1.5 µM to 24 µM showed gradually increase of intracellular Dox accumulation.

These results shows that P-Ahx-NH-N=MeOHe-R121 is capable to markedly increase the intracellular accumulation of Dox in P388/MDR cells and thus likely to sensitize these cells to Dox.

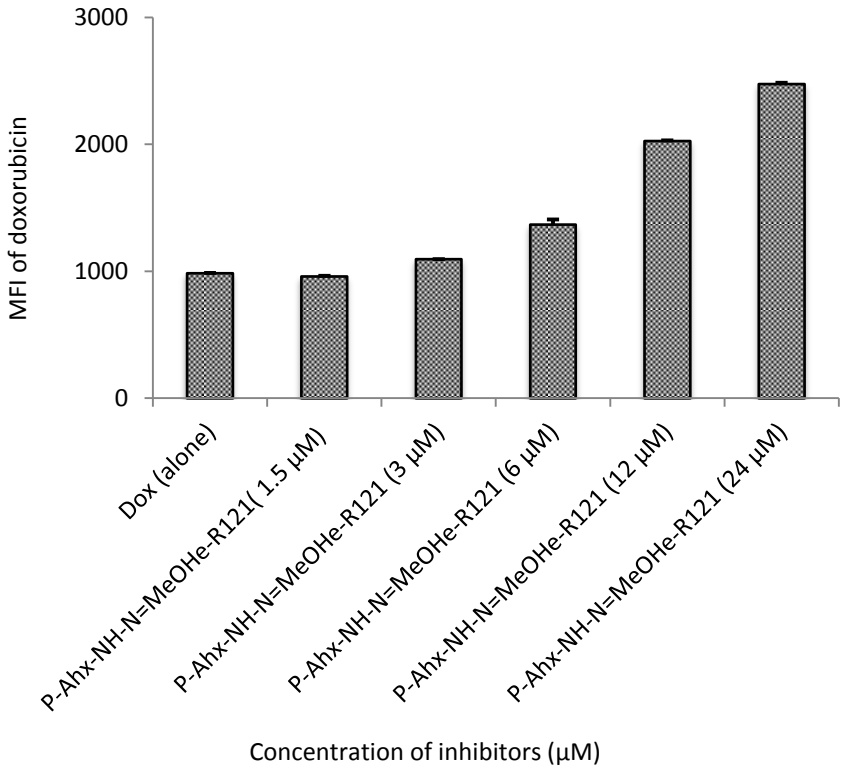

Figure 5.13: Intracellular accumulation of Dox in P388/MDR cells. P388/MDR cells were incubated with constant concentration of Dox (7 µM) alone or with titrated concentrations of P-Ahx-NH-N=MeOHe-R121 conjugate for 24 h under standard culture conditions. Cells were analyzed by flow cytometry and the dead cells were gated out using Hoechst 33258. Experiments were repeated 3 times. The representative graph is shown.

5.11 Cytostatic activity of the HPMA copolymer conjugates containing both MeOHe-R121 and Dox or MeOHe-RIT and Dox

Finally, the cytostatic activity of the HPMA copolymer conjugates P-Ahx-NH-N=MeOHe-R121(Dox) containing both Dox and P-gp inhibitor MeOHe-R121 both bound via hydrazone bonds at the molar ratio 1:1, 1:2 and 2:1 were compared to that of the mixture of the conjugates P-Ahx-NH-N=MeOHe-R121 and P-Ahx-NH-N=Dox in the P388/MDR cell line.

While IC_{50} for conjugate P-Ahx-NH-N=Dox alone was calculated to be almost 92 μM, co-incubation with the P-Ahx-NH-N=MeOHe-R121 (at molar ratio Dox: MeOHe-R121) resulted in the almost 30-fold increase of cytostatic activity. Moreover, the conjugate P-Ahx-NH-N=MeOHe-R121(Dox) containing both Dox and MeOHe-R121 at the molar ratio 1:1 had higher cytostatic activity than conjugate P-Ahx-NH-N=Dox with IC_{50} more than 30 times lower, and about 2 times lower than mixture of the conjugates P-Ahx-NH-N=MeOHe-R121 and P-Ahx-NH-N=Dox discussed above (Figure 5.14).

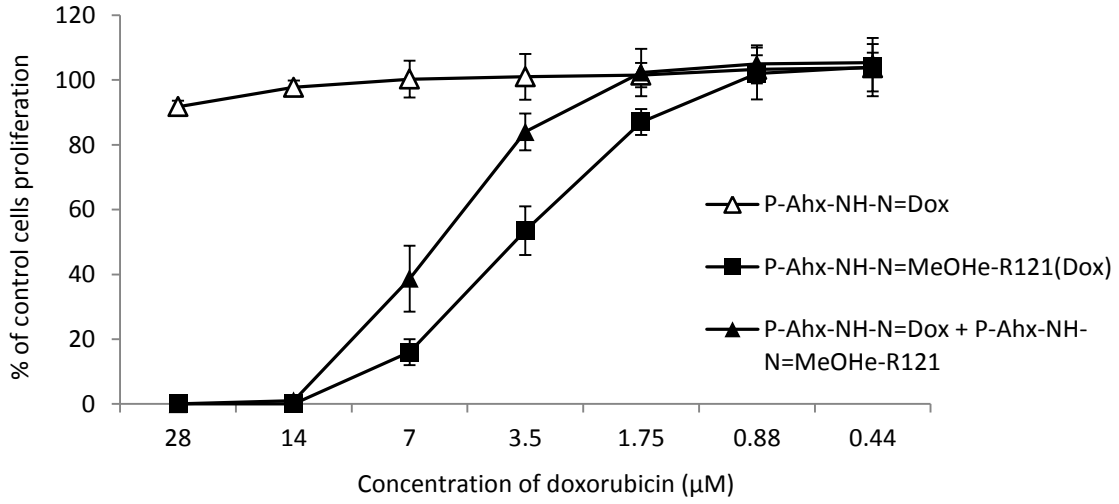

Figure 5.14: Overcoming MDR by simultaneous delivery of conjugates P-Ahx-NH-N=Dox and P-Ahx-NH-N=MeOHe-R121 in an equimolar drug/inhibitor ratio, or by the conjugate P-Ahx-NH-N=MeOHe-R121(Dox) bearing both Dox and MeOHe-R121 in the same ratio. P388/MDR cells were incubated with titrated concentrations of P-Ahx-NH-N=Dox, mixture of P-Ahx-NH-N=Dox and P-Ahx-NH-N=MeOHe-R121 or P-Ahx-NH-N=MeOHe-R121(Dox) for 72 h at standard cultivation conditions. The concentration of MeOHe-R121 was proportional to Dox concentration with the ratio 1:1 throughout the experiment. Cell proliferation was assessed by [^{3}H]-thymidine incorporation which was added to the cultures for last 6 h of incubation. Results are shown as inhibition of proliferation of exposed cell relative to controls (cells incubated in medium only). The activity of control cells was always higher than 50 000 cpm/well. Each experimental point is average of 3 experiments ± SD.

Similarly, the cytostatic activity was determined also for conjugate P-Ahx-NH-N=MeOHe-R121(Dox) containing Dox and MeOHe-R121 at the molar ratio ~ 2:1 (i.e. the excess of MeOHe-R121). This conjugate possess remarkably high cytostatic activity in comparison to conjugate P-Ahx-NH-N=Dox as the calculated IC_{50} was approximately 45 times lower. Furthermore, P-Ahx-NH-N=MeOHe-R121(Dox)

exhibited almost 3 times higher cytostatic activity than the comparable mixture of the conjugates P-Ahx-NH-N=MeOHe-R121 and P-Ahx-NH-N=Dox (Figure 5.15).

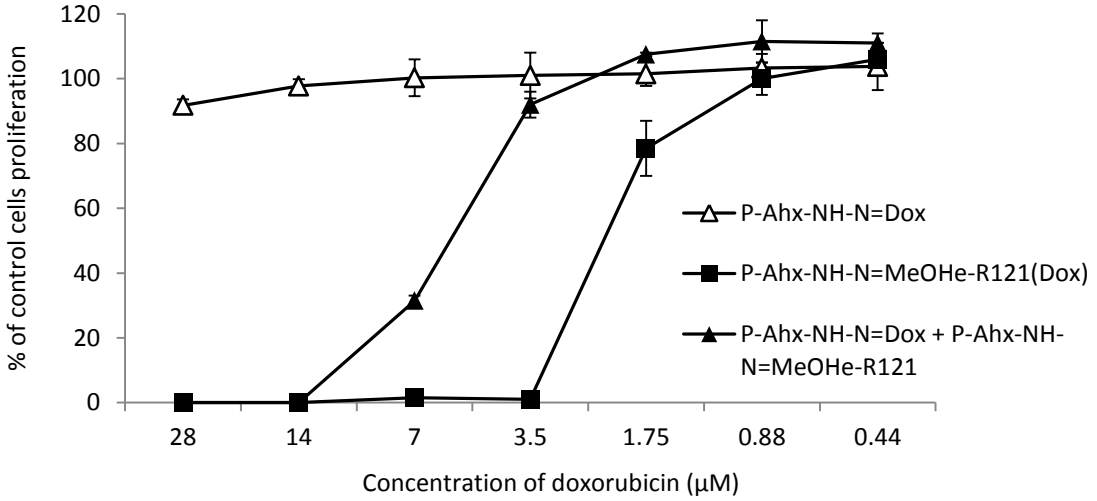

Figure 5.15: Overcoming MDR by simultaneous delivery of conjugates P-Ahx-NH-N=Dox and P-Ahx-NH-N=MeOHe-R121, or by the conjugate P-Ahx-NH-N=MeOHe-R121(Dox) bearing both Dox and MeOHe-R121 at a ratio 2:1 (i.e. excess of MeOHe-R121). P388/MDR cells were incubated with titrated concentrations of P-Ahx-NH-N=Dox, mixture of P-Ahx-NH-N=Dox and P-Ahx-NH-N=MeOHe-R121 or P-Ahx-NH-N=MeOHe-R121(Dox) for 72 h at standard cultivation conditions. The concentration of MeOHe-R121 was proportional to Dox concentration with the ratio 2:1 throughout the experiment. Cell proliferation was assessed by [^{3}H]-thymidine incorporation which was added to the cultures for last 6 h of incubation. Results are shown as inhibition of proliferation of exposed cell relative to controls (cells incubated in medium only). The activity of control cells was always higher than 50 000 cpm/well. Each experimental point is average of 3 experiments ± SD.

Next, we determined also cytostatic activity of conjugate P-Ahx-NH-N=MeOHe-R121(Dox) containing Dox and MeOHe-R121 at the molar ratio ~ 1:2 (i.e. the excess of Dox) in P388/MDR cells. Unlike above conjugates with the molar ratios of Dox and MeOHe-R121 1:1 and 2:1, this conjugate exert only 7 times higher cytostatic activity than P-Ahx-NH-N=Dox. Moreover, this conjugate had slightly lower cytostatic activity than mixture of P-Ahx-NH-N=MeOHe-R121 and P-Ahx-NH-N=Dox (Figure 5.16).

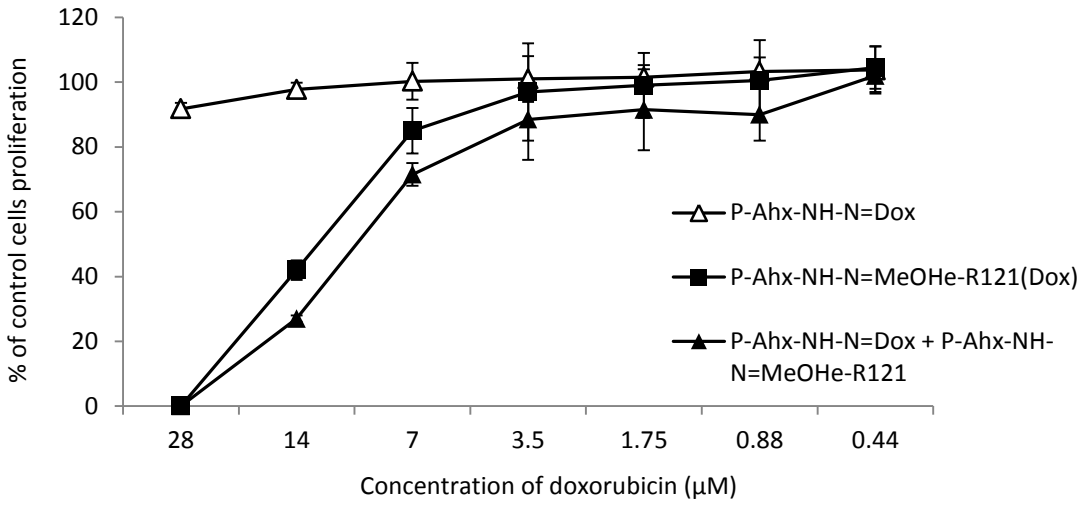

Figure 5.16: Overcoming MDR by simultaneous delivery of conjugates P-Ahx-NH-N=Dox and P-Ahx-NH-N=MeOHe-R121, or by the conjugate P-Ahx-NH-N=MeOHe-R121(Dox) bearing both Dox and MeOHe-R121 at a ratio 1:2 (i.e. excess of Dox). P388/MDR cells were incubated with titrated concentrations of P-Ahx-NH-N=Dox, mixture of P-Ahx-NH-N=Dox and P-Ahx-NH-N=MeOHe-R121 or P-Ahx-NH-N=MeOHe-R121(Dox) for 72 h at standard cultivation conditions. The concentration of MeOHe-R121 was proportional to Dox concentration with the ratio 1:2 throughout the experiment. Cell proliferation was assessed by [^{3}H]-thymidine incorporation which was added to the cultures for last 6 h of incubation. Results are shown as inhibition of proliferation of exposed cell relative to controls (cells incubated in medium only). The activity of control cells was always higher than 50 000 cpm/well. Each experimental point is average of 3 experiments ± SD.

Finally, the cytostatic activity of the P-Ahx-NH-N=MeOHe-RIT(Dox) conjugate containing both Dox and MeOHe-RIT in equimolar ratio was determined. The P-Ahx-NH-N=MeOHe-RIT(Dox) exert almost 10 times higher cytostatic activity than P-Ahx-NH-N=Dox, however, it showed about 1.5 times lower cytostatic activity in comparison to the mixture of P-Ahx-NH-N=MeOHe-RIT and P-Ahx-NH-N=Dox at the same Dox: MeOHe-RIT ration (Figure 5.17).

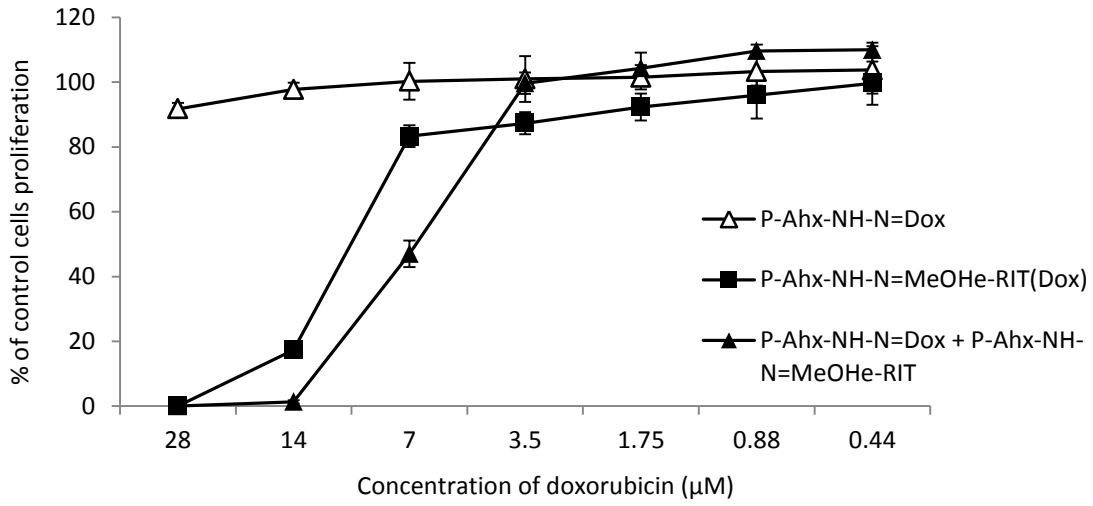

Figure 5.17: Overcoming MDR by simultaneous delivery of conjugates P-Ahx-NH-N=Dox and P-Ahx-NH-N=MeOHe-RIT, or by the conjugate P-Ahx-NH-N=MeOHe-RIT(Dox) bearing both Dox and MeOHe-RIT at a ratio 1:1.

P388/MDR cells were incubated with titrated concentrations of P-Ahx-NH-N=Dox, mixture of P-Ahx-NH-N=Dox and P-Ahx-NH-N=MeOHe-RIT or P-Ahx-NH-N=MeOHe-RIT(Dox) for 72 h at standard cultivation conditions. The concentration of MeOHe-RIT was proportional to Dox concentration with the ratio 1:1 throughout the experiment. Cell proliferation was assessed by [^{3}H]-thymidine incorporation which was added to the cultures for last 6 h of incubation. Results are shown as inhibition of proliferation of exposed cell relative to controls (cells incubated in medium only). The activity of control cells was always higher than 50 000 cpm/well. Each experimental point is average of 3 experiments ± SD.

6 Discussion

Chemotherapy using low-molecular weight drugs is one of the three principal approaches for the cancer treatment. However, using low-molecular weight drugs is associated with several disadvantages, such as severe side toxicity. Moreover, the effectiveness of chemotherapy is also limited by the drug resistance, when even originally very sensitive tumors become resistant to cytostatic/cytotoxic action of multiple, structurally dissimilar and functionally unrelated chemotherapeutic drugs after several treatment cycles. This phenomenon, called MDR is most often related to overexpression of ABC transporters, mainly P-glycoprotein [1-4, 6-7].

Several distinct approaches were developed to reverse MDR phenotype. Most promising and widely studied strategy to overcome MDR so far seems to be the use of low-molecular weight inhibitors of ABC transporters. Inhibitors of ABC transporters, also called chemosensitizers, show the same diversity of chemical structures as substrates and therefore they suffer from similar disadvantages as anticancer drugs [129]. There are three generations of P-gp inhibitors. The first generation was identified in early 1980s by Tsuruo and co-workers, who first demonstrated the ability of the calcium channel blocker, verapamil, to reverse MDR [173]. Subsequent studies revealed that this MDR reversing property is shared by many other calcium channel blockers [174-175]. Thus these agents were classified as first generation of P-gp inhibitors. However, almost all inhibitors of the first generation possess their own therapeutic activity and they reverse MDR at much higher concentrations than those required for their individual therapeutic activity. In view of these limitations the second generation of P-gp inhibitors was synthetized. Unfortunately, albeit these compounds including valspodar or dex-verapamil showed improve efficacy, they also exert serious adverse pharmacokinetics interactions with anticancer drugs [176-177]. To avoid the limitations of the first and second generation of P-gp inhibitors, third generation have been recently developed. These agents are effective in MDR reversing within nanomolar concentrations. However, their limited solubility in aqueous solutions is relevant factor influences their bioavailability.

Many studies emphasize the promising potential of nanocarriers to overcome MDR. The binding of P-gp inhibitor polymer carrier could reduce the adverse effects and improve solubility and bioavailability at the pharmacological sites of action. For example, recently study performed by Binkhathlan et al. showed that methoxy-

poly(ethylene oxide)-block-poly(e-caprolactone) micelles improve valspodar solubility and its pharmacological activity upon intravenous administration [178]. One of the most recent studies described a system to co-encapsulate a third generation of P-gp inhibitor tariquidar and paclitaxel in long circulating liposomes. Antitumor activity of paclitaxel was observed in paclitaxel-resistant human ovarian adenocarcinoma SKOV3/TR at the dose that was ineffective in the absence tariquidar. Co-loaded liposomes had 100-fold higher cytostatic activity than paclitaxel loaded liposomes alone [179]. Another approach combined doxorubicin and verapamil encapsulated in liposomes actively targeted with transferrin. This study demonstrated that liposome containing Dox and verapamil showed 3-fold lower IC_{50} than transferrin liposome loaded doxorubicin alone in doxorubicin resistant chronic human leukemia K562/Dox [180]. In contrast, Krishna et al. showed that anticancer drug encapsulated into liposome was more effective when co-administered with free P-gp inhibitor than liposome loaded with both anticancer drug and P-gp inhibitor in P388/ADR leukemia [181].

Moreover, many studies demonstrated that conjugation of low-molecular weight anticancer drug to a water-soluble polymeric carrier substantially increase solubility of high hydrophobic drugs, improves their biodistribution, pharmacokinetics and decrease their side toxicity. The results obtained by Minko et al. indicate that HPMA copolymer containing Dox bound via the lysosomally degradable GlyPheLeuGly spacer are partially able to avoid the P-gp mediated efflux of Dox in the Dox-resistant A2780/ADR human ovarian carcinoma [182-184]. Moreover, hydrolytically degradable hydrogels based on HPMA loaded with Dox and CsA were used in combined therapy against the mouse P388/MDR leukemia. The synergistic effect of the anticancer drug and P-gp inhibitor was observed. The tumor volumes were reduced to approximately 50% of the controls when HPMA hydrogel containing four times the maximum tolerated dose (MTD) of Dox and CsA was implanted [185].

Amphiphilic structure appears to be a predominant condition for the modulation of the P-gp efflux. Amphiphilic polymers have shown promising potential for the inhibition of the P-gp. Pluronic P85 loaded with daunorubicin was studied in the P-gp overexpressing human carcinoma SKVLB and non-MDR SKOV3 cells. A dramatic increase in the daunorubicin cytotoxic activity (up to 700 times) was observed in the presence of copolymer in SKVLB cells.

In this study, we investigated the potential of polymeric therapeutics based on water-soluble HPMA copolymer conjugates bearing either anticancer drug doxorubicin

or inhibitor of ABC transporters or both bound to the polymeric carrier through pH-sensitive bond. P-gp inhibitors reversin 121, reversin 205 and ritonavir were selected for the study. They are highly hydrophobic and do not possess any carbonyl residue necessary for binding to HPMA copolymer through hydrazone bond. Several oxoacid analogues of these inhibitors were thus synthetized to enable their further binding to polymeric carrier and their capacity to inhibit P-gp function in P388/MDR cells was evaluated.

P388/MDR cells are approximately 600 times less sensitive to Dox than the parental P388 cell line. However, resistance of P388/MDR cells to P-Ahx-NH-N=Dox is approximately 3,800 times higher in comparison to P388 cells and thus even higher than that for free Dox. These results are not in accordance with literature. Higher resistance ratio found for P-Ahx-NH-N=Dox than for free Dox may be theoretically explained by slow/inefficient intracellular release of Dox from P-Ahx-NH-N-Dox in case that P388/MDR cells have lower content of acidic compartments like endosomes/lysosomes than P388 cells which are required for Dox release.

Interestingly, we found that the same derivatization (using MeOHe) potentiates P-gp inhibitory activity of R121 but completely abrogates P-gp inhibitory activity of R205. This shows that R121 and R205 are probably bound to P-gp in different way although they have similar structure.

The several studies performed by Minko et al. proposed that polymer-drug conjugates delivered to membrane-limited organelles along the endocytic pathway is protected from the action of P-gp pump [186-187]. However, our results are not in accordance with such conclusion and thus shows that at least in the case of Dox bound to HPMA copolymer via hydrazone bond this is not the case.

7 Conclusions

The conclusions of this study are:

1) We determined P-gp, MRP1 and BCRP expression in both sensitive P388 and doxorubicin-resistant P388/MDR cell lines.
   a) The P388/MDR cells express P-gp at very high level. The protein expression of MRP1 and BCRP were undetectable in P388/MDR cells. The P388 cell line showed no expression of P-gp, MRP1 and BCRP.

In conclusion, P388 and P388/MDR murine leukemia cell lines have been proved to be suitable for further testing of P-gp inhibitors, their derivatives and HPMA copolymer-bound counterparts.

2) We evaluated the biological activity of selected P-gp inhibitors and their derivatives in P388 and P388/MDR cells.
   a) All R121 derivatives, except OPe-R121, showed comparable toxicity to R121 in P388 cell line. MeOHe-R121, OHe-R121 and OPB-R121 showed 2.5-4 lower toxicity than R121 in P388/MDR cells, in which R121 had more than 2-fold higher toxicity than in P388 cells. MeOHe-R205 was approximately 1.5 times and 6 times less toxic than R205 in P388/MDR and P388, respectively. OHe-RIT and MeOHe-RIT showed 2-fold higher toxicity than RIT in P388/MDR cells. In contrast, OPB-RIT was 2 times less toxic. All RIT derivatives had comparable toxicity in P388 cell line.
   b) All R121 derivatives, except MeOHe-R121, exhibited lower or comparable P-gp inhibitory activity in P388/MDR cells. MeOHe-R121 derivative was found to be considerably more potent P-gp inhibitor than R121. R205 was found to be as potent inhibitor as R121. In contrast, MeOHe-R205 showed no P-gp inhibitory activity at all. Only MeOHe-RIT showed good activity in the inhibition of P-gp out of all RIT derivatives.
   c) Among all derivatives of R121, MeOHe-R121 showed gradually increasing capacity to sensitize the P388/MDR cells to Dox beginning approximately with 5-fold increase at 0.5 μM and more than 40-fold increase was achieved at 4 μM. OPe-R121, OHe-R121 and OPB-R121 were much less potent than R121. R205 showed similar potency to that of R121 in sensitization of P388/MDR cells.

However, MeOHe-R205 showed no effect on cytostatic activity of Dox in P388/MDR cells. MeOHe-RIT showed far best activity to increase the cytostatic effect of Dox in P388/MDR cells out of all RIT derivatives.

Results from sensitization of P388/MDR cells to cytostatic activity of Dox are in accordance with the P-gp inhibitory activity. Thus, we identified MeOHe-R121 and MeOHe-RIT as suitable candidates for subsequent conjugation to the HPMA polymer carrier.

3) We characterized the biological activity of new HPMA copolymer conjugates bearing selected P-gp inhibitor or Dox or both in sensitive P388 and resistant P388/MDR cell lines.
   a) The polymeric conjugate P-Ahx-NH-N=MeOHe-R121 exhibited no toxicity up to 24 μM in both cell lines and only slight toxicity was observed at 48 μM in P388/MDR cells. The P-Ahx-NH-N=MeOHe-RIT showed no or negligible toxicity up to 12μM in P388/MDR cells but only up to 6 μM in P388 cells. Higher concentrations showed significant toxicity in both cell lines.
   b) The P-Ahx-NH-N=MeOHe-R121 conjugate was very effective in the inhibition of P-gp activity already at 12 μM and it was even able to inhibit the P-gp activity that calcein MFI was comparable to level seen in positive control at 48 μM. The P-Ahx-NH-N=MeOHe-RIT was also very effective in P-gp inhibition, 12 μM concentration nearly completely block P-gp activity.
   c) The P-Ahx-NH-N=MeOHe-R121 gradually increased cytotoxic activity of Dox in concentration range from 1.5 μM to 24 μM in which it has no cytotoxic activity *per se*. Approximately 50-fold increase of cytostatic activity of Dox was observed at 24 μM. The P-Ahx-NH-N=MeOHe-RIT was not able to sensitize the P388/MDR cells to cytostatic activity of Dox up to 3 μM and only moderate activity was observed at 6 μM. However, 12 μM concentration showed approximately 50-fold increase in sensitization of P388/MDR.
   d) P-Ahx-NH-N=MeOHe-R121 exerted the potential to increase intracellular accumulation of Dox in P388/MDR cells in concentration dependent manner.
   e) Conjugate P-Ahx-NH-N=MeOHe-R121(Dox) with molar ratio of drugs 1:1 had more than 30 times higher cytostatic activity than P-Ahx-NH-N=Dox and 2 times higher than mixture of the conjugates P-Ahx-NH-N=MeOHe-R121 and P-Ahx-NH-N=Dox. P-Ahx-NH-N=MeOHe-R121(Dox) with the molar ratio of

drugs 2:1 was even more cytostatic than previous one, calculated IC_{50} was about 45 times lower than P-Ahx-NH-N=Dox and almost 3 times lower than comparable mixture of conjugates P-Ahx-NH-N=MeOHe-R121 and P-Ahx-NH-N=Dox. The P-Ahx-NH-N=MeOHe-R121(Dox) with the molar ratio of drugs 1:2 showed lower cytostatic activity in comparison to previously mentioned conjugates. The P-Ahx-NH-N=MeOHe-RIT(Dox) conjugate in equimolar ratio of drugs had 10 times higher cytostatic activity than P-Ahx-NH-N=Dox but less than twice lower in comparison to the comparable mixture of P-Ahx-NH-N=MeOHe-RIT and P-Ahx-NH-N=Dox.

Our results showed that simultaneous delivery of cytostatic drug and P-gp inhibitor in the form of HPMA copolymer-bound conjugates is a promising strategy to overcome MDR in cancer cells.

8 References

[1] D. B. Longley and P. G. Johnston, "Molecular mechanisms of drug resistance," *J Pathol,* vol. 205, pp. 275-92, Jan 2005.

[2] V. Nosková, M. Hajdúch, V. Mihál, and K. Cwiertka, "Mechanismy mnohočetné lékové rezistence a jejich význam pro klinickou praxi II. Atypická MDR Mechanisms of multidrug resistance and their clinical implications II. Atypical MDR."

[3] M. M. Gottesman, "How cancer cells evade chemotherapy: sixteenth Richard and Hinda Rosenthal Foundation Award Lecture," *Cancer Res,* vol. 53, pp. 747-54, Feb 15 1993.

[4] S. Puig, J. Lee, M. Lau, and D. J. Thiele, "Biochemical and genetic analyses of yeast and human high affinity copper transporters suggest a conserved mechanism for copper uptake," *J Biol Chem,* vol. 277, pp. 26021-30, Jul 19 2002.

[5] H. Thomas and H. M. Coley, "Overcoming multidrug resistance in cancer: an update on the clinical strategy of inhibiting p-glycoprotein," *Cancer Control,* vol. 10, pp. 159-65, Mar-Apr 2003.

[6] S. V. Ambudkar, S. Dey, C. A. Hrycyna, M. Ramachandra, I. Pastan, and M. M. Gottesman, "Biochemical, cellular, and pharmacological aspects of the multidrug transporter," *Annu Rev Pharmacol Toxicol,* vol. 39, pp. 361-98, 1999.

[7] R. Krishna and L. D. Mayer, "Multidrug resistance (MDR) in cancer. Mechanisms, reversal using modulators of MDR and the role of MDR modulators in influencing the pharmacokinetics of anticancer drugs," *Eur J Pharm Sci,* vol. 11, pp. 265-83, Oct 2000.

[8] A. A. Stavrovskaya, "Cellular mechanisms of multidrug resistance of tumor cells," *Biochemistry (Mosc),* vol. 65, pp. 95-106, Jan 2000.

[9] D. W. McMillin, J. M. Negri, and C. S. Mitsiades, "The role of tumour-stromal interactions in modifying drug response: challenges and opportunities," *Nat Rev Drug Discov,* vol. 12, pp. 217-28, Mar 2013.

[10] M. M. Gottesman, T. Fojo, and S. E. Bates, "Multidrug resistance in cancer: role of ATP-dependent transporters," *Nat Rev Cancer,* vol. 2, pp. 48-58, Jan 2002.

[11] C. Holohan, S. Van Schaeybroeck, D. B. Longley, and P. G. Johnston, "Cancer drug resistance: an evolving paradigm," *Nat Rev Cancer,* vol. 13, pp. 714-26, Oct 2013.

[12] C. C. McIlwain, D. M. Townsend, and K. D. Tew, "Glutathione S-transferase polymorphisms: cancer incidence and therapy," *Oncogene,* vol. 25, pp. 1639-48, Mar 13 2006.

[13] D. M. Townsend and K. D. Tew, "The role of glutathione-S-transferase in anti-cancer drug resistance," *Oncogene,* vol. 22, pp. 7369-75, Oct 20 2003.

[14] A. Sharma, B. Patrick, J. Li, R. Sharma, P. V. Jeyabal, P. M. Reddy, *et al.*, "Glutathione S-transferases as antioxidant enzymes: small cell lung cancer (H69) cells transfected with hGSTA1 resist doxorubicin-induced apoptosis," *Arch Biochem Biophys,* vol. 452, pp. 165-73, Aug 15 2006.

[15] A. G. Hall, P. Autzen, A. R. Cattan, A. J. Malcolm, M. Cole, J. Kernahan, *et al.*, "Expression of mu class glutathione S-transferase correlates with event-free survival in childhood acute lymphoblastic leukemia," *Cancer Res,* vol. 54, pp. 5251-4, Oct 15 1994.

[16] V. Adler, Z. Yin, S. Y. Fuchs, M. Benezra, L. Rosario, K. D. Tew, *et al.*, "Regulation of JNK signaling by GSTp," *EMBO J,* vol. 18, pp. 1321-34, Mar 1 1999.

[17] D. Hanahan and R. A. Weinberg, "The hallmarks of cancer," *Cell,* vol. 100, pp. 57-70, Jan 7 2000.

[18] J. C. Reed, "Regulation of apoptosis by bcl-2 family proteins and its role in cancer and chemoresistance," *Curr Opin Oncol,* vol. 7, pp. 541-6, Nov 1995.

[19] T. C. Fisher, A. E. Milner, C. D. Gregory, A. L. Jackman, G. W. Aherne, J. A. Hartley, *et al.*, "bcl-2 modulation of apoptosis induced by anticancer drugs: resistance to thymidylate stress is independent of classical resistance pathways," *Cancer Res,* vol. 53, pp. 3321-6, Jul 15 1993.

[20] S. Kitada, J. Andersen, S. Akar, J. M. Zapata, S. Takayama, S. Krajewski, *et al.*, "Expression of apoptosis-regulating proteins in chronic lymphocytic leukemia: correlations with In vitro and In vivo chemoresponses," *Blood,* vol. 91, pp. 3379-89, May 1 1998.

[21] M. Dean, A. Rzhetsky, and R. Allikmets, "The human ATP-binding cassette (ABC) transporter superfamily," *Genome Res,* vol. 11, pp. 1156-66, Jul 2001.

[22] G. L. Scheffer, P. L. Wijngaard, M. J. Flens, M. A. Izquierdo, M. L. Slovak, H. M. Pinedo, *et al.*, "The drug resistance-related protein LRP is the human major vault protein," *Nat Med,* vol. 1, pp. 578-82, Jun 1995.

[23] A. van Zon, M. H. Mossink, R. J. Scheper, P. Sonneveld, and E. A. Wiemer, "The vault complex," *Cell Mol Life Sci,* vol. 60, pp. 1828-37, Sep 2003.

[24] M. A. Izquierdo, G. L. Scheffer, M. J. Flens, A. B. Schroeijers, P. van der Valk, and R. J. Scheper, "Major vault protein LRP-related multidrug resistance," *Eur J Cancer,* vol. 32A, pp. 979-84, Jun 1996.

[25] M. L. den Boer, R. Pieters, K. M. Kazemier, M. M. Rottier, C. M. Zwaan, G. J. Kaspers, *et al.*, "Relationship between major vault protein/lung resistance protein, multidrug resistance-associated protein, P-glycoprotein expression, and drug resistance in childhood leukemia," *Blood,* vol. 91, pp. 2092-8, Mar 15 1998.

[26] A. Sauerbrey, A. Voigt, S. Wittig, R. Hafer, and F. Zintl, "Messenger RNA analysis of the multidrug resistance related protein (MRP1) and the lung resistance protein (LRP) in de novo and relapsed childhood acute lymphoblastic leukemia," *Leuk Lymphoma,* vol. 43, pp. 875-9, Apr 2002.

[27] A. C. Siva, S. Raval-Fernandes, A. G. Stephen, M. J. LaFemina, R. J. Scheper, V. A. Kickhoefer, *et al.*, "Up-regulation of vaults may be necessary but not sufficient for multidrug resistance," *Int J Cancer,* vol. 92, pp. 195-202, Apr 15 2001.

[28] M. H. Mossink, A. van Zon, R. J. Scheper, P. Sonneveld, and E. A. Wiemer, "Vaults: a ribonucleoprotein particle involved in drug resistance?," *Oncogene,* vol. 22, pp. 7458-67, Oct 20 2003.

[29] Z. H. Siddik, "Cisplatin: mode of cytotoxic action and molecular basis of resistance," *Oncogene,* vol. 22, pp. 7265-79, Oct 20 2003.

[30] S. W. Johnson, P. B. Laub, J. S. Beesley, R. F. Ozols, and T. C. Hamilton, "Increased platinum-DNA damage tolerance is associated with cisplatin resistance and cross-resistance to various chemotherapeutic agents in unrelated human ovarian cancer cell lines," *Cancer Res,* vol. 57, pp. 850-6, Mar 1 1997.

[31] I. S. Song, N. Savaraj, Z. H. Siddik, P. Liu, Y. Wei, C. J. Wu, *et al.*, "Role of human copper transporter Ctr1 in the transport of platinum-based antitumor agents in cisplatin-sensitive and cisplatin-resistant cells," *Mol Cancer Ther,* vol. 3, pp. 1543-9, Dec 2004.

[32] M. Komatsu, T. Sumizawa, M. Mutoh, Z. S. Chen, K. Terada, T. Furukawa, *et al.*, "Copper-transporting P-type adenosine triphosphatase (ATP7B) is associated with cisplatin resistance," *Cancer Res,* vol. 60, pp. 1312-6, Mar 1 2000.

[33] K. Nakayama, A. Kanzaki, K. Terada, M. Mutoh, K. Ogawa, T. Sugiyama, *et al.*, "Prognostic value of the Cu-transporting ATPase in ovarian carcinoma patients receiving cisplatin-based chemotherapy," *Clin Cancer Res,* vol. 10, pp. 2804-11, Apr 15 2004.

[34] M. Ohbu, K. Ogawa, S. Konno, A. Kanzaki, K. Terada, T. Sugiyama, *et al.*, "Copper-transporting P-type adenosine triphosphatase (ATP7B) is expressed in human gastric carcinoma," *Cancer Lett,* vol. 189, pp. 33-8, Jan 10 2003.

[35] M. Dean and R. Allikmets, "Complete characterization of the human ABC gene family," *J Bioenerg Biomembr,* vol. 33, pp. 475-9, Dec 2001.

[36] B. Sarkadi, L. Homolya, G. Szakacs, and A. Varadi, "Human multidrug resistance ABCB and ABCG transporters: participation in a chemoimmunity defense system," *Physiol Rev,* vol. 86, pp. 1179-236, Oct 2006.

[37] M. Dean, Y. Hamon, and G. Chimini, "The human ATP-binding cassette (ABC) transporter superfamily," *J Lipid Res,* vol. 42, pp. 1007-17, Jul 2001.

[38] L. W. Hung, I. X. Wang, K. Nikaido, P. Q. Liu, G. F. Ames, and S. H. Kim, "Crystal structure of the ATP-binding subunit of an ABC transporter," *Nature,* vol. 396, pp. 703-7, Dec 17 1998.

[39] K. P. Hopfner, A. Karcher, D. S. Shin, L. Craig, L. M. Arthur, J. P. Carney, *et al.*, "Structural biology of Rad50 ATPase: ATP-driven conformational control in DNA double-strand break repair and the ABC-ATPase superfamily," *Cell,* vol. 101, pp. 789-800, Jun 23 2000.

[40] P. C. Smith, N. Karpowich, L. Millen, J. E. Moody, J. Rosen, P. J. Thomas, *et al.*, "ATP binding to the motor domain from an ABC transporter drives formation of a nucleotide sandwich dimer," *Mol Cell,* vol. 10, pp. 139-49, Jul 2002.

[41] J. Zaitseva, S. Jenewein, T. Jumpertz, I. B. Holland, and L. Schmitt, "H662 is the linchpin of ATP hydrolysis in the nucleotide-binding domain of the ABC transporter HlyB," *EMBO J,* vol. 24, pp. 1901-10, Jun 1 2005.

[42] P. M. Jones and A. M. George, "Subunit interactions in ABC transporters: towards a functional architecture," *FEMS Microbiol Lett,* vol. 179, pp. 187-202, Oct 15 1999.

[43] S. C. Hyde, P. Emsley, M. J. Hartshorn, M. M. Mimmack, U. Gileadi, S. R. Pearce, *et al.*, "Structural model of ATP-binding proteins associated with cystic fibrosis, multidrug resistance and bacterial transport," *Nature,* vol. 346, pp. 362-5, Jul 26 1990.

[44] P. M. Jones and A. M. George, "Molecular-dynamics simulations of the ATP/apo state of a multidrug ATP-binding cassette transporter provide a structural and mechanistic basis for the asymmetric occluded state," *Biophys J,* vol. 100, pp. 3025-34, Jun 22 2011.

[45] L. Cuthbertson, V. Kos, and C. Whitfield, "ABC transporters involved in export of cell surface glycoconjugates," *Microbiol Mol Biol Rev,* vol. 74, pp. 341-62, Sep 2010.

[46] R. J. Dawson and K. P. Locher, "Structure of a bacterial multidrug ABC transporter," *Nature,* vol. 443, pp. 180-5, Sep 14 2006.

[47] P. M. Jones and A. M. George, "Opening of the ADP-bound active site in the ABC transporter ATPase dimer: evidence for a constant contact, alternating sites model for the catalytic cycle," *Proteins,* vol. 75, pp. 387-96, May 1 2009.

[48] J. E. Walker, M. Saraste, M. J. Runswick, and N. J. Gay, "Distantly related sequences in the alpha- and beta-subunits of ATP synthase, myosin, kinases and other ATP-requiring enzymes and a common nucleotide binding fold," *EMBO J,* vol. 1, pp. 945-51, 1982.

[49] N. Karpowich, O. Martsinkevich, L. Millen, Y. R. Yuan, P. L. Dai, K. MacVey, *et al.*, "Crystal structures of the MJ1267 ATP binding cassette reveal an induced-fit effect at the ATPase active site of an ABC transporter," *Structure,* vol. 9, pp. 571-86, Jul 3 2001.

[50] P. M. Jones and A. M. George, "Mechanism of ABC transporters: a molecular dynamics simulation of a well characterized nucleotide-binding subunit," *Proc Natl Acad Sci U S A,* vol. 99, pp. 12639-44, Oct 1 2002.

[51] J. Zaitseva, C. Oswald, T. Jumpertz, S. Jenewein, A. Wiedenmann, I. B. Holland, *et al.*, "A structural analysis of asymmetry required for catalytic activity of an ABC-ATPase domain dimer," *EMBO J,* vol. 25, pp. 3432-43, Jul 26 2006.

[52] E. Procko, I. Ferrin-O'Connell, S. L. Ng, and R. Gaudet, "Distinct structural and functional properties of the ATPase sites in an asymmetric ABC transporter," *Mol Cell,* vol. 24, pp. 51-62, Oct 6 2006.

[53] P. M. Jones and A. M. George, "Role of the D-loops in allosteric control of ATP hydrolysis in an ABC transporter," *J Phys Chem A,* vol. 116, pp. 3004-13, Mar 22 2012.

[54] J. D. Campbell, S. S. Deol, F. M. Ashcroft, I. D. Kerr, and M. S. Sansom, "Nucleotide-dependent conformational changes in HisP: molecular dynamics simulations of an ABC transporter nucleotide-binding domain," *Biophys J,* vol. 87, pp. 3703-15, Dec 2004.

[55] A. C. Hobson, R. Weatherwax, and G. F. Ames, "ATP-binding sites in the membrane components of histidine permease, a periplasmic transport system," *Proc Natl Acad Sci U S A,* vol. 81, pp. 7333-7, Dec 1984.

[56] C. F. Higgins, I. D. Hiles, K. Whalley, and D. J. Jamieson, "Nucleotide binding by membrane components of bacterial periplasmic binding protein-dependent transport systems," *EMBO J,* vol. 4, pp. 1033-9, Apr 1985.

[57] A. E. Senior, M. K. al-Shawi, and I. L. Urbatsch, "The catalytic cycle of P-glycoprotein," *FEBS Lett,* vol. 377, pp. 285-9, Dec 27 1995.

[58] J. Chen, G. Lu, J. Lin, A. L. Davidson, and F. A. Quiocho, "A tweezers-like motion of the ATP-binding cassette dimer in an ABC transport cycle," *Mol Cell,* vol. 12, pp. 651-61, Sep 2003.

[59] A. A. Aleksandrov, X. Chang, L. Aleksandrov, and J. R. Riordan, "The non-hydrolytic pathway of cystic fibrosis transmembrane conductance regulator ion channel gating," *J Physiol,* vol. 528 Pt 2, pp. 259-65, Oct 15 2000.

[60] R. Yang, L. Cui, Y. X. Hou, J. R. Riordan, and X. B. Chang, "ATP binding to the first nucleotide binding domain of multidrug resistance-associated protein plays a regulatory role at low nucleotide concentration, whereas ATP hydrolysis at the second plays a dominant role in ATP-dependent leukotriene C4 transport," *J Biol Chem,* vol. 278, pp. 30764-71, Aug 15 2003.

[61] I. L. Urbatsch, G. A. Tyndall, G. Tombline, and A. E. Senior, "P-glycoprotein catalytic mechanism: studies of the ADP-vanadate inhibited state," *J Biol Chem,* vol. 278, pp. 23171-9, Jun 20 2003.

[62] C. F. Higgins and K. J. Linton, "The ATP switch model for ABC transporters," *Nat Struct Mol Biol,* vol. 11, pp. 918-26, Oct 2004.

[63] A. E. Senior and S. Bhagat, "P-glycoprotein shows strong catalytic cooperativity between the two nucleotide sites," *Biochemistry,* vol. 37, pp. 831-6, Jan 20 1998.

[64] B. Verhalen and S. Wilkens, "P-glycoprotein retains drug-stimulated ATPase activity upon covalent linkage of the two nucleotide binding domains at their C-terminal ends," *J Biol Chem,* vol. 286, pp. 10476-82, Mar 25 2011.

[65] G. Szakacs, J. K. Paterson, J. A. Ludwig, C. Booth-Genthe, and M. M. Gottesman, "Targeting multidrug resistance in cancer," *Nat Rev Drug Discov,* vol. 5, pp. 219-34, Mar 2006.

[66] T. Litman, T. E. Druley, W. D. Stein, and S. E. Bates, "From MDR to MXR: new understanding of multidrug resistance systems, their properties and clinical significance," *Cell Mol Life Sci,* vol. 58, pp. 931-59, Jun 2001.

[67] R. L. Juliano and V. Ling, "A surface glycoprotein modulating drug permeability in Chinese hamster ovary cell mutants," *Biochim Biophys Acta,* vol. 455, pp. 152-62, Nov 11 1976.

[68] S. V. Ambudkar, C. Kimchi-Sarfaty, Z. E. Sauna, and M. M. Gottesman, "P-glycoprotein: from genomics to mechanism," *Oncogene,* vol. 22, pp. 7468-85, Oct 20 2003.

[69] J. E. Chin, R. Soffir, K. E. Noonan, K. Choi, and I. B. Roninson, "Structure and expression of the human MDR (P-glycoprotein) gene family," *Mol Cell Biol,* vol. 9, pp. 3808-20, Sep 1989.

[70] L. A. Mickley, J. S. Lee, Z. Weng, Z. Zhan, M. Alvarez, W. Wilson, *et al.*, "Genetic polymorphism in MDR-1: a tool for examining allelic expression in normal cells, unselected and drug-selected cell lines, and human tumors," *Blood,* vol. 91, pp. 1749-56, Mar 1 1998.

[71] Y. Kurata, I. Ieiri, M. Kimura, T. Morita, S. Irie, A. Urae, *et al.*, "Role of human MDR1 gene polymorphism in bioavailability and interaction of digoxin, a substrate of P-glycoprotein," *Clin Pharmacol Ther,* vol. 72, pp. 209-19, Aug 2002.

[72] Z. P. Jiang, Y. R. Wang, P. Xu, R. R. Liu, X. L. Zhao, and F. P. Chen, "Meta-analysis of the effect of MDR1 C3435T polymorphism on cyclosporine pharmacokinetics," *Basic Clin Pharmacol Toxicol,* vol. 103, pp. 433-44, Nov 2008.

[73] C. Pauli-Magnus and D. L. Kroetz, "Functional implications of genetic polymorphisms in the multidrug resistance gene MDR1 (ABCB1)," *Pharm Res,* vol. 21, pp. 904-13, Jun 2004.

[74] Y. Li, H. Yuan, K. Yang, W. Xu, W. Tang, and X. Li, "The structure and functions of P-glycoprotein," *Curr Med Chem,* vol. 17, pp. 786-800, 2010.

[75] T. W. Loo and D. M. Clarke, "Correction of defective protein kinesis of human P-glycoprotein mutants by substrates and modulators," *J Biol Chem,* vol. 272, pp. 709-12, Jan 10 1997.

[76] T. W. Loo and D. M. Clarke, "The human multidrug resistance P-glycoprotein is inactive when its maturation is inhibited: potential for a role in cancer chemotherapy," *FASEB J,* vol. 13, pp. 1724-32, Oct 1999.

[77] J. J. Gribar, M. Ramachandra, C. A. Hrycyna, S. Dey, and S. V. Ambudkar, "Functional characterization of glycosylation-deficient human P-glycoprotein using a vaccinia virus expression system," *J Membr Biol,* vol. 173, pp. 203-14, Feb 1 2000.

[78] M. F. Rosenberg, R. Callaghan, S. Modok, C. F. Higgins, and R. C. Ford, "Three-dimensional structure of P-glycoprotein: the transmembrane regions adopt an asymmetric configuration in the nucleotide-bound state," *J Biol Chem,* vol. 280, pp. 2857-62, Jan 28 2005.

[79] S. G. Aller, J. Yu, A. Ward, Y. Weng, S. Chittaboina, R. Zhuo, *et al.*, "Structure of P-glycoprotein reveals a molecular basis for poly-specific drug binding," *Science,* vol. 323, pp. 1718-22, Mar 27 2009.

[80] P. M. Jones and A. M. George, "A new structural model for P-glycoprotein," *J Membr Biol,* vol. 166, pp. 133-47, Nov 15 1998.

[81] G. D. Eytan, R. Regev, G. Oren, and Y. G. Assaraf, "The role of passive transbilayer drug movement in multidrug resistance and its modulation," *J Biol Chem,* vol. 271, pp. 12897-902, May 31 1996.

[82] F. J. Sharom, "Complex Interplay between the P-Glycoprotein Multidrug Efflux Pump and the Membrane: Its Role in Modulating Protein Function," *Front Oncol,* vol. 4, p. 41, 2014.

[83] C. Cordon-Cardo, J. P. O'Brien, D. Casals, L. Rittman-Grauer, J. L. Biedler, M. R. Melamed, *et al.*, "Multidrug-resistance gene (P-glycoprotein) is expressed by endothelial cells at blood-brain barrier sites," *Proc Natl Acad Sci U S A,* vol. 86, pp. 695-8, Jan 1989.

[84] D. Fu, M. Bebawy, E. P. Kable, and B. D. Roufogalis, "Dynamic and intracellular trafficking of P-glycoprotein-EGFP fusion protein: Implications in multidrug resistance in cancer," *Int J Cancer,* vol. 109, pp. 174-81, Mar 20 2004.

[85] D. Fu and B. D. Roufogalis, "Actin disruption inhibits endosomal traffic of P-glycoprotein-EGFP and resistance to daunorubicin accumulation," *Am J Physiol Cell Physiol,* vol. 292, pp. C1543-52, Apr 2007.

[86] D. Fu, E. M. van Dam, A. Brymora, I. G. Duggin, P. J. Robinson, and B. D. Roufogalis, "The small GTPases Rab5 and RalA regulate intracellular traffic of P-glycoprotein," *Biochim Biophys Acta,* vol. 1773, pp. 1062-72, Jul 2007.

[87] K. Katayama, K. Noguchi, and Y. Sugimoto, "FBXO15 regulates P-glycoprotein/ABCB1 expression through the ubiquitin--proteasome pathway in cancer cells," *Cancer Sci,* vol. 104, pp. 694-702, Jun 2013.

[88] P. D. Eckford and F. J. Sharom, "ABC efflux pump-based resistance to chemotherapy drugs," *Chem Rev,* vol. 109, pp. 2989-3011, Jul 2009.

[89] A. van Helvoort, A. J. Smith, H. Sprong, I. Fritzsche, A. H. Schinkel, P. Borst, *et al.*, "MDR1 P-glycoprotein is a lipid translocase of broad specificity, while MDR3 P-glycoprotein specifically translocates phosphatidylcholine," *Cell,* vol. 87, pp. 507-17, Nov 1 1996.

[90] S. Harmsen, I. Meijerman, C. L. Febus, R. F. Maas-Bakker, J. H. Beijnen, and J. H. Schellens, "PXR-mediated induction of P-glycoprotein by anticancer drugs in a human colon adenocarcinoma-derived cell line," *Cancer Chemother Pharmacol,* vol. 66, pp. 765-71, Sep 2010.

[91] S. Mani, H. Huang, S. Sundarababu, W. Liu, G. Kalpana, A. B. Smith, *et al.*, "Activation of the steroid and xenobiotic receptor (human pregnane X receptor) by nontaxane microtubule-stabilizing agents," *Clin Cancer Res,* vol. 11, pp. 6359-69, Sep 1 2005.

[92] C. Zhou, S. Verma, and B. Blumberg, "The steroid and xenobiotic receptor (SXR), beyond xenobiotic metabolism," *Nucl Recept Signal,* vol. 7, p. e001, 2009.

[93] R. G. Deeley, C. Westlake, and S. P. Cole, "Transmembrane transport of endo- and xenobiotics by mammalian ATP-binding cassette multidrug resistance proteins," *Physiol Rev,* vol. 86, pp. 849-99, Jul 2006.

[94] S. P. Cole, G. Bhardwaj, J. H. Gerlach, J. E. Mackie, C. E. Grant, K. C. Almquist, *et al.*, "Overexpression of a transporter gene in a multidrug-resistant human lung cancer cell line," *Science,* vol. 258, pp. 1650-4, Dec 4 1992.

[95] B. D. Stride, G. Valdimarsson, J. H. Gerlach, G. M. Wilson, S. P. Cole, and R. G. Deeley, "Structure and expression of the messenger RNA encoding the murine multidrug resistance protein, an ATP-binding cassette transporter," *Mol Pharmacol,* vol. 49, pp. 962-71, Jun 1996.

[96] N. Godinot, P. W. Iversen, L. Tabas, X. Xia, D. C. Williams, A. H. Dantzig, *et al.*, "Cloning and functional characterization of the multidrug resistance-associated protein (MRP1/ABCC1) from the cynomolgus monkey," *Mol Cancer Ther,* vol. 2, pp. 307-16, Mar 2003.

[97] L. Ma, S. E. Pratt, J. Cao, A. H. Dantzig, R. E. Moore, and C. A. Slapak, "Identification and characterization of the canine multidrug resistance-associated protein," *Mol Cancer Ther,* vol. 1, pp. 1335-42, Dec 2002.

[98] K. Nunoya, C. E. Grant, D. Zhang, S. P. Cole, and R. G. Deeley, "Molecular cloning and pharmacological characterization of rat multidrug resistance protein 1 (mrp1)," *Drug Metab Dispos,* vol. 31, pp. 1016-26, Aug 2003.

[99] S. Conrad, H. M. Kauffmann, K. Ito, E. M. Leslie, R. G. Deeley, D. Schrenk, *et al.*, "A naturally occurring mutation in MRP1 results in a selective decrease in organic anion transport and in increased doxorubicin resistance," *Pharmacogenetics*, vol. 12, pp. 321-30, Jun 2002.

[100] A. Rajagopal and S. M. Simon, "Subcellular localization and activity of multidrug resistance proteins," *Mol Biol Cell*, vol. 14, pp. 3389-99, Aug 2003.

[101] S. R. Wright, A. H. Boag, G. Valdimarsson, D. R. Hipfner, B. G. Campling, S. P. Cole, *et al.*, "Immunohistochemical detection of multidrug resistance protein in human lung cancer and normal lung," *Clin Cancer Res*, vol. 4, pp. 2279-89, Sep 1998.

[102] J. M. Brechot, I. Hurbain, A. Fajac, N. Daty, and J. F. Bernaudin, "Different pattern of MRP localization in ciliated and basal cells from human bronchial epithelium," *J Histochem Cytochem*, vol. 46, pp. 513-7, Apr 1998.

[103] M. V. St-Pierre, M. A. Serrano, R. I. Macias, U. Dubs, M. Hoechli, U. Lauper, *et al.*, "Expression of members of the multidrug resistance protein family in human term placenta," *Am J Physiol Regul Integr Comp Physiol*, vol. 279, pp. R1495-503, Oct 2000.

[104] I. Leier, G. Jedlitschky, U. Buchholz, S. P. Cole, R. G. Deeley, and D. Keppler, "The MRP gene encodes an ATP-dependent export pump for leukotriene C4 and structurally related conjugates," *J Biol Chem*, vol. 269, pp. 27807-10, Nov 11 1994.

[105] D. F. Robbiani, R. A. Finch, D. Jager, W. A. Muller, A. C. Sartorelli, and G. J. Randolph, "The leukotriene C(4) transporter MRP1 regulates CCL19 (MIP-3beta, ELC)-dependent mobilization of dendritic cells to lymph nodes," *Cell*, vol. 103, pp. 757-68, Nov 22 2000.

[106] D. W. Loe, R. G. Deeley, and S. P. Cole, "Characterization of vincristine transport by the M(r) 190,000 multidrug resistance protein (MRP): evidence for cotransport with reduced glutathione," *Cancer Res*, vol. 58, pp. 5130-6, Nov 15 1998.

[107] T. Hegedus, L. Orfi, A. Seprodi, A. Varadi, B. Sarkadi, and G. Keri, "Interaction of tyrosine kinase inhibitors with the human multidrug transporter proteins, MDR1 and MRP1," *Biochim Biophys Acta*, vol. 1587, pp. 318-25, Jul 18 2002.

[108] K. Nooter, A. M. Westerman, M. J. Flens, G. J. Zaman, R. J. Scheper, K. E. van Wingerden, *et al.*, "Expression of the multidrug resistance-associated protein (MRP) gene in human cancers," *Clin Cancer Res*, vol. 1, pp. 1301-10, Nov 1995.

[109] H. Burger, J. A. Foekens, M. P. Look, M. E. Meijer-van Gelder, J. G. Klijn, E. A. Wiemer, *et al.*, "RNA expression of breast cancer resistance protein, lung resistance-related protein, multidrug resistance-associated proteins 1 and 2, and multidrug resistance gene 1 in breast cancer: correlation with chemotherapeutic response," *Clin Cancer Res*, vol. 9, pp. 827-36, Feb 2003.

[110] C. C. Paulusma, M. Kool, P. J. Bosma, G. L. Scheffer, F. ter Borg, R. J. Scheper, *et al.*, "A mutation in the human canalicular multispecific organic anion transporter gene causes the Dubin-Johnson syndrome," *Hepatology,* vol. 25, pp. 1539-42, Jun 1997.

[111] A. D. Mottino, T. Hoffman, L. Jennes, J. Cao, and M. Vore, "Expression of multidrug resistance-associated protein 2 in small intestine from pregnant and postpartum rats," *Am J Physiol Gastrointest Liver Physiol,* vol. 280, pp. G1261-73, Jun 2001.

[112] T. P. Schaub, J. Kartenbeck, J. Konig, O. Vogel, R. Witzgall, W. Kriz, *et al.*, "Expression of the conjugate export pump encoded by the mrp2 gene in the apical membrane of kidney proximal tubules," *J Am Soc Nephrol,* vol. 8, pp. 1213-21, Aug 1997.

[113] M. Kool, M. de Haas, G. L. Scheffer, R. J. Scheper, M. J. van Eijk, J. A. Juijn, *et al.*, "Analysis of expression of cMOAT (MRP2), MRP3, MRP4, and MRP5, homologues of the multidrug resistance-associated protein gene (MRP1), in human cancer cell lines," *Cancer Res,* vol. 57, pp. 3537-47, Aug 15 1997.

[114] R. Evers, M. de Haas, R. Sparidans, J. Beijnen, P. R. Wielinga, J. Lankelma, *et al.*, "Vinblastine and sulfinpyrazone export by the multidrug resistance protein MRP2 is associated with glutathione export," *Br J Cancer,* vol. 83, pp. 375-83, Aug 2000.

[115] T. Kawabe, Z. S. Chen, M. Wada, T. Uchiumi, M. Ono, S. Akiyama, *et al.*, "Enhanced transport of anticancer agents and leukotriene C4 by the human canalicular multispecific organic anion transporter (cMOAT/MRP2)," *FEBS Lett,* vol. 456, pp. 327-31, Aug 6 1999.

[116] K. Koike, T. Kawabe, T. Tanaka, S. Toh, T. Uchiumi, M. Wada, *et al.*, "A canalicular multispecific organic anion transporter (cMOAT) antisense cDNA enhances drug sensitivity in human hepatic cancer cells," *Cancer Res,* vol. 57, pp. 5475-9, Dec 15 1997.

[117] S. L. Soignet, P. Maslak, Z. G. Wang, S. Jhanwar, E. Calleja, L. J. Dardashti, *et al.*, "Complete remission after treatment of acute promyelocytic leukemia with arsenic trioxide," *N Engl J Med,* vol. 339, pp. 1341-8, Nov 5 1998.

[118] Y. Kiuchi, H. Suzuki, T. Hirohashi, C. A. Tyson, and Y. Sugiyama, "cDNA cloning and inducible expression of human multidrug resistance associated protein 3 (MRP3)," *FEBS Lett,* vol. 433, pp. 149-52, Aug 14 1998.

[119] G. L. Scheffer, M. Kool, M. de Haas, J. M. de Vree, A. C. Pijnenborg, D. K. Bosman, *et al.*, "Tissue distribution and induction of human multidrug resistant protein 3," *Lab Invest,* vol. 82, pp. 193-201, Feb 2002.

[120] R. Allikmets, L. M. Schriml, A. Hutchinson, V. Romano-Spica, and M. Dean, "A human placenta-specific ATP-binding cassette gene (ABCP) on chromosome 4q22 that is involved in multidrug resistance," *Cancer Res,* vol. 58, pp. 5337-9, Dec 1 1998.

[121] Y. Honjo, C. A. Hrycyna, Q. W. Yan, W. Y. Medina-Perez, R. W. Robey, A. van de Laar, *et al.*, "Acquired mutations in the MXR/BCRP/ABCP gene alter substrate specificity in MXR/BCRP/ABCP-overexpressing cells," *Cancer Res,* vol. 61, pp. 6635-9, Sep 15 2001.

[122] H. Mitomo, R. Kato, A. Ito, S. Kasamatsu, Y. Ikegami, I. Kii, *et al.*, "A functional study on polymorphism of the ATP-binding cassette transporter ABCG2: critical role of arginine-482 in methotrexate transport," *Biochem J,* vol. 373, pp. 767-74, Aug 1 2003.

[123] K. Noguchi, K. Katayama, and Y. Sugimoto, "Human ABC transporter ABCG2/BCRP expression in chemoresistance: basic and clinical perspectives for molecular cancer therapeutics," *Pharmgenomics Pers Med,* vol. 7, pp. 53-64, 2014.

[124] F. Staud and P. Pavek, "Breast cancer resistance protein (BCRP/ABCG2)," *Int J Biochem Cell Biol,* vol. 37, pp. 720-5, Apr 2005.

[125] G. Moreno-Sanz, B. Barrera, A. Guijarro, I. d'Elia, J. A. Otero, A. I. Alvarez, *et al.*, "The ABC membrane transporter ABCG2 prevents access of FAAH inhibitor URB937 to the central nervous system," *Pharmacol Res,* vol. 64, pp. 359-63, Oct 2011.

[126] S. Balabanov, A. Gontarewicz, G. Keller, L. Raddrizzani, M. Braig, R. Bosotti, *et al.*, "Abcg2 overexpression represents a novel mechanism for acquired resistance to the multi-kinase inhibitor Danusertib in BCR-ABL-positive cells in vitro," *PLoS One,* vol. 6, p. e19164, 2011.

[127] U. Consoli, W. Priebe, Y. H. Ling, R. Mahadevia, M. Griffin, S. Zhao, *et al.*, "The novel anthracycline annamycin is not affected by P-glycoprotein-related multidrug resistance: comparison with idarubicin and doxorubicin in HL-60 leukemia cell lines," *Blood,* vol. 88, pp. 633-44, Jul 15 1996.

[128] R. Perez-Soler, N. Neamati, Y. Zou, E. Schneider, L. A. Doyle, M. Andreeff, *et al.*, "Annamycin circumvents resistance mediated by the multidrug resistance-associated protein (MRP) in breast MCF-7 and small-cell lung UMCC-1 cancer cell lines selected for resistance to etoposide," *Int J Cancer,* vol. 71, pp. 35-41, Mar 28 1997.

[129] T. Fojo and S. Bates, "Strategies for reversing drug resistance," *Oncogene,* vol. 22, pp. 7512-23, Oct 20 2003.

[130] G. Dayan, J. M. Jault, H. Baubichon-Cortay, L. G. Baggetto, J. M. Renoir, E. E. Baulieu, *et al.*, "Binding of steroid modulators to recombinant cytosolic domain from mouse P-glycoprotein in close proximity to the ATP site," *Biochemistry,* vol. 36, pp. 15208-15, Dec 9 1997.

[131] A. Breier, M. Barancik, Z. Sulova, and B. Uhrik, "P-glycoprotein--implications of metabolism of neoplastic cells and cancer therapy," *Curr Cancer Drug Targets,* vol. 5, pp. 457-68, Sep 2005.

[132] G. Cornaire, J. Woodley, P. Hermann, A. Cloarec, C. Arellano, and G. Houin, "Impact of excipients on the absorption of P-glycoprotein substrates in vitro and in vivo," *Int J Pharm,* vol. 278, pp. 119-31, Jun 18 2004.

[133] A. Boumendjel, H. Baubichon-Cortay, D. Trompier, T. Perrotton, and A. Di Pietro, "Anticancer multidrug resistance mediated by MRP1: recent advances in the discovery of reversal agents," *Med Res Rev,* vol. 25, pp. 453-72, Jul 2005.

[134] E. Bakos, R. Evers, E. Sinko, A. Varadi, P. Borst, and B. Sarkadi, "Interactions of the human multidrug resistance proteins MRP1 and MRP2 with organic anions," *Mol Pharmacol,* vol. 57, pp. 760-8, Apr 2000.

[135] N. Zelcer, T. Saeki, G. Reid, J. H. Beijnen, and P. Borst, "Characterization of drug transport by the human multidrug resistance protein 3 (ABCC3)," *J Biol Chem,* vol. 276, pp. 46400-7, Dec 7 2001.

[136] S. K. Rabindran, D. D. Ross, L. A. Doyle, W. Yang, and L. M. Greenberger, "Fumitremorgin C reverses multidrug resistance in cells transfected with the breast cancer resistance protein," *Cancer Res,* vol. 60, pp. 47-50, Jan 1 2000.

[137] H. Minderman, K. L. O'Loughlin, L. Pendyala, and M. R. Baer, "VX-710 (biricodar) increases drug retention and enhances chemosensitivity in resistant cells overexpressing P-glycoprotein, multidrug resistance protein, and breast cancer resistance protein," *Clin Cancer Res,* vol. 10, pp. 1826-34, Mar 1 2004.

[138] Y. Imai, S. Tsukahara, S. Asada, and Y. Sugimoto, "Phytoestrogens/flavonoids reverse breast cancer resistance protein/ABCG2-mediated multidrug resistance," *Cancer Res,* vol. 64, pp. 4346-52, Jun 15 2004.

[139] H. C. Cooray, T. Janvilisri, H. W. van Veen, S. B. Hladky, and M. A. Barrand, "Interaction of the breast cancer resistance protein with plant polyphenols," *Biochem Biophys Res Commun,* vol. 317, pp. 269-75, Apr 23 2004.

[140] R. Duncan, "The dawning era of polymer therapeutics," *Nat Rev Drug Discov,* vol. 2, pp. 347-60, May 2003.

[141] R. Duncan, M. J. Vicent, F. Greco, and R. I. Nicholson, "Polymer-drug conjugates: towards a novel approach for the treatment of endrocine-related cancer," *Endocr Relat Cancer,* vol. 12 Suppl 1, pp. S189-99, Jul 2005.

[142] T. Lammers and K. Ulbrich, "HPMA copolymers: 30 years of advances," *Adv Drug Deliv Rev,* vol. 62, pp. 119-21, Feb 17 2010.

[143] K. Ulbrich and V. Subr, "Structural and chemical aspects of HPMA copolymers as drug carriers," *Adv Drug Deliv Rev,* vol. 62, pp. 150-66, Feb 17 2010.

[144] B. Rihova and M. Kovar, "Immunogenicity and immunomodulatory properties of HPMA-based polymers," *Adv Drug Deliv Rev,* vol. 62, pp. 184-91, Feb 17 2010.

[145] J. Kopecek, "Reactive copolymers of N-(2-hydroxypropyl) methacrylamide with N-methacryloylated derivatives of L-leucine and L-phenylalanine. 1. Preparation, characterization, and reactions with diamines," *Makromolekulare Chemie-Macromolecular Chemistry and Physics,* vol. 178, pp. 2169-2183, 1977.

[146] B. Říhová, J. Kopeček, K. Ulbrich, and V. Chytrý, "Immunogenicity of N-(2-hydroxypropyl) methacrylamide copolymers," *Die Makromolekulare Chemie,* vol. 9, pp. 13-24, 1985.

[147] P. Flanagan, R. Duncan, B. Rihova, V. Šubr, and J. Kopeček, "Immunogenicity of protein-N-(2-hydroxypropyl) methacrylamide copolymer conjugates in A/J and B10 mice," *Journal of Bioactive and Compatible Polymers,* vol. 5, pp. 151-166, 1990.

[148] R. Duncan, "Polymer conjugates as anticancer nanomedicines," *Nat Rev Cancer,* vol. 6, pp. 688-701, Sep 2006.

[149] T. Etrych, M. Jelinkova, B. Rihova, and K. Ulbrich, "New HPMA copolymers containing doxorubicin bound via pH-sensitive linkage: synthesis and preliminary in vitro and in vivo biological properties," *J Control Release,* vol. 73, pp. 89-102, May 18 2001.

[150] K. Ulbrich, T. Etrych, P. Chytil, M. Jelinkova, and B. Rihova, "HPMA copolymers with pH-controlled release of doxorubicin: in vitro cytotoxicity and in vivo antitumor activity," *J Control Release,* vol. 87, pp. 33-47, Feb 21 2003.

[151] B. Rihova, T. Etrych, M. Pechar, M. Jelinkova, M. Stastny, O. Hovorka, *et al.*, "Doxorubicin bound to a HPMA copolymer carrier through hydrazone bond is effective also in a cancer cell line with a limited content of lysosomes," *J Control Release,* vol. 74, pp. 225-32, Jul 6 2001.

[152] Y. Matsumura and H. Maeda, "A new concept for macromolecular therapeutics in cancer chemotherapy: mechanism of tumoritropic accumulation of proteins and the antitumor agent smancs," *Cancer Res,* vol. 46, pp. 6387-92, Dec 1986.

[153] H. Hashizume, P. Baluk, S. Morikawa, J. W. McLean, G. Thurston, S. Roberge, *et al.*, "Openings between defective endothelial cells explain tumor vessel leakiness," *Am J Pathol,* vol. 156, pp. 1363-80, Apr 2000.

[154] K. Greish, "Enhanced permeability and retention of macromolecular drugs in solid tumors: a royal gate for targeted anticancer nanomedicines," *J Drug Target,* vol. 15, pp. 457-64, Aug-Sep 2007.

[155] R. Duncan, "Drug-polymer conjugates: potential for improved chemotherapy," *Anticancer Drugs,* vol. 3, pp. 175-210, Jun 1992.

[156] T. Lammers, R. Kuhnlein, M. Kissel, V. Subr, T. Etrych, R. Pola, *et al.*, "Effect of physicochemical modification on the biodistribution and tumor accumulation of HPMA copolymers," *J Control Release,* vol. 110, pp. 103-18, Dec 10 2005.

[157] T. Lammers, P. Peschke, R. Kuhnlein, V. Subr, K. Ulbrich, P. Huber, *et al.*, "Effect of intratumoral injection on the biodistribution and the therapeutic potential of HPMA copolymer-based drug delivery systems," *Neoplasia,* vol. 8, pp. 788-95, Oct 2006.

[158] M. Sirova, J. Strohalm, V. Subr, D. Plocova, P. Rossmann, T. Mrkvan, *et al.*, "Treatment with HPMA copolymer-based doxorubicin conjugate containing human immunoglobulin induces long-lasting systemic anti-tumour immunity in mice," *Cancer Immunol Immunother,* vol. 56, pp. 35-47, Jan 2007.

[159] T. Etrych, T. Mrkvan, P. Chytil, Č. Koňák, B. Říhová, and K. Ulbrich, "N-(2-hydroxypropyl) methacrylamide-based polymer conjugates with pH-controlled activation of doxorubicin. I. New synthesis, physicochemical characterization and preliminary biological evaluation," *Journal of applied polymer science,* vol. 109, pp. 3050-3061, 2008.

[160] M. Sirova, T. Mrkvan, T. Etrych, P. Chytil, P. Rossmann, M. Ibrahimova, *et al.*, "Preclinical evaluation of linear HPMA-doxorubicin conjugates with pH-sensitive drug release: efficacy, safety, and immunomodulating activity in murine model," *Pharmaceutical research,* vol. 27, pp. 200-208, 2010.

[161] L. W. Seymour, D. R. Ferry, D. Anderson, S. Hesslewood, P. J. Julyan, R. Poyner, *et al.*, "Hepatic drug targeting: phase I evaluation of polymer-bound doxorubicin," *J Clin Oncol,* vol. 20, pp. 1668-76, Mar 15 2002.

[162] T. Etrych, T. Mrkvan, B. Rihova, and K. Ulbrich, "Star-shaped immunoglobulin-containing HPMA-based conjugates with doxorubicin for cancer therapy," *J Control Release,* vol. 122, pp. 31-8, Sep 11 2007.

[163] H. Jatzkewitz, "Peptamin (glycyl-L-leucyl-mescaline) bound to blood plasma expander (polyvinylpyrrolidone) as a new depot form of a biologically active primary amine (mescaline)," *Z. Naturforsch,* vol. 10, pp. 27-31, 1955.

[164] L. W. Seymour, D. R. Ferry, D. J. Kerr, D. Rea, M. Whitlock, R. Poyner, *et al.*, "Phase II studies of polymer-doxorubicin (PK1, FCE28068) in the treatment of breast, lung and colorectal cancer," *Int J Oncol,* vol. 34, pp. 1629-36, Jun 2009.

[165] P. A. Vasey, S. B. Kaye, R. Morrison, C. Twelves, P. Wilson, R. Duncan, *et al.*, "Phase I clinical and pharmacokinetic study of PK1 [N-(2-hydroxypropyl)methacrylamide copolymer doxorubicin]: first member of a new class of chemotherapeutic agents-drug-polymer conjugates. Cancer Research Campaign Phase I/II Committee," *Clin Cancer Res,* vol. 5, pp. 83-94, Jan 1999.

[166] T. Etrych, P. Chytil, M. Jelínková, B. Říhová, and K. Ulbrich, "Synthesis of HPMA copolymers containing doxorubicin bound via a hydrazone linkage. Effect of spacer on drug release and in vitro cytotoxicity," *Macromolecular bioscience,* vol. 2, pp. 43-52, 2002.

[167] K. Ulbrich, T. Etrych, P. Chytil, M. Pechar, M. Jelinkova, and B. Rihova, "Polymeric anticancer drugs with pH-controlled activation," *Int J Pharm,* vol. 277, pp. 63-72, Jun 11 2004.

[168] B. Říhová, N. L. Krinick, and J. Kopeček, "Targetable photoactivalable drugs. 3. In vitro efficacy of polymer bound chlorin e6 toward human hepatocarcinoma cell line (PLC/PRF/5) targeted with galactosamine and to mouse splenocytes targeted with anti-Thy 1.2 antibodies," *Journal of Controlled Release,* vol. 25, pp. 71-87, 5/27/ 1993.

[169] M. Kovar, J. Strohalm, T. Etrych, K. Ulbrich, and B. Rihova, "Star structure of antibody-targeted HPMA copolymer-bound doxorubicin: a novel type of polymeric conjugate for targeted drug delivery with potent antitumor effect," *Bioconjug Chem,* vol. 13, pp. 206-15, Mar-Apr 2002.

[170] M. Jelinkova, J. Strohalm, T. Etrych, K. Ulbrich, and B. Rihova, "Starlike vs. classic macromolecular prodrugs: two different antibody-targeted HPMA copolymers of doxorubicin studied in vitro and in vivo as potential anticancer drugs," *Pharm Res,* vol. 20, pp. 1558-64, Oct 2003.

[171] S. Wroblewski, M. Berenson, P. Kopeckova, and J. Kopecek, "Biorecognition of HPMA copolymer-lectin conjugates as an indicator of differentiation of cell-surface glycoproteins in development, maturation, and diseases of human and rodent gastrointestinal tissues," *J Biomed Mater Res,* vol. 51, pp. 329-42, Sep 5 2000.

[172] B. Rihova, M. Jelinkova, J. Strohalm, M. St'astny, O. Hovorka, D. Plocova, *et al.*, "Antiproliferative effect of a lectin- and anti-Thy-1.2 antibody-targeted HPMA copolymer-bound doxorubicin on primary and metastatic human colorectal carcinoma and on human colorectal carcinoma transfected with the mouse Thy-1.2 gene," *Bioconjug Chem,* vol. 11, pp. 664-73, Sep-Oct 2000.

[173] T. Tsuruo, H. Iida, S. Tsukagoshi, and Y. Sakurai, "Overcoming of vincristine resistance in P388 leukemia in vivo and in vitro through enhanced cytotoxicity of vincristine and vinblastine by verapamil," *Cancer Res,* vol. 41, pp. 1967-72, May 1981.

[174] H. Goldberg, V. Ling, P. Y. Wong, and K. Skorecki, "Reduced cyclosporin accumulation in multidrug-resistant cells," *Biochem Biophys Res Commun,* vol. 152, pp. 552-8, Apr 29 1988.

[175] A. Ramu, D. Glaubiger, and Z. Fuks, "Reversal of acquired resistance to doxorubicin in P388 murine leukemia cells by tamoxifen and other triparanol analogues," *Cancer Res,* vol. 44, pp. 4392-5, Oct 1984.

[176] V. J. Wacher, C. Y. Wu, and L. Z. Benet, "Overlapping substrate specificities and tissue distribution of cytochrome P450 3A and P-glycoprotein: implications for drug delivery and activity in cancer chemotherapy," *Mol Carcinog,* vol. 13, pp. 129-34, Jul 1995.

[177] V. Fischer, A. Rodriguez-Gascon, F. Heitz, R. Tynes, C. Hauck, D. Cohen, *et al.*, "The multidrug resistance modulator valspodar (PSC 833) is metabolized by human cytochrome P450 3A. Implications for drug-drug interactions and pharmacological activity of the main metabolite," *Drug Metab Dispos,* vol. 26, pp. 802-11, Aug 1998.

[178] Z. Binkhathlan, D. A. Hamdy, D. R. Brocks, and A. Lavasanifar, "Development of a polymeric micellar formulation for valspodar and assessment of its pharmacokinetics in rat," *Eur J Pharm Biopharm*, vol. 75, pp. 90-5, Jun 2010.

[179] N. R. Patel, A. Rathi, D. Mongayt, and V. P. Torchilin, "Reversal of multidrug resistance by co-delivery of tariquidar (XR9576) and paclitaxel using long-circulating liposomes," *International Journal of Pharmaceutics*, vol. 416, pp. 296-299, Sep 15 2011.

[180] J. Wu, Y. Lu, A. Lee, X. Pan, X. Yang, X. Zhao, *et al.*, "Reversal of multidrug resistance by transferrin-conjugated liposomes co-encapsulating doxorubicin and verapamil," *J Pharm Pharm Sci*, vol. 10, pp. 350-7, 2007.

[181] R. Krishna and L. D. Mayer, "Liposomal doxorubicin circumvents PSC 833-free drug interactions, resulting in effective therapy of multidrug-resistant solid tumors," *Cancer Res*, vol. 57, pp. 5246-53, Dec 1 1997.

[182] T. Minko, P. Kopeckova, and J. Kopecek, "Chronic exposure to HPMA copolymer-bound adriamycin does not induce multidrug resistance in a human ovarian carcinoma cell line," *J Control Release*, vol. 59, pp. 133-48, May 20 1999.

[183] T. Minko, P. Kopeckova, V. Pozharov, and J. Kopecek, "HPMA copolymer bound adriamycin overcomes MDR1 gene encoded resistance in a human ovarian carcinoma cell line," *J Control Release*, vol. 54, pp. 223-33, Jul 31 1998.

[184] T. Minko, "HPMA copolymers for modulating cellular signaling and overcoming multidrug resistance," *Adv Drug Deliv Rev*, vol. 62, pp. 192-202, Feb 17 2010.

[185] M. St'astny, D. Plocova, T. Etrych, K. Ulbrich, and B. Rihova, "HPMA-hydrogels result in prolonged delivery of anticancer drugs and are a promising tool for the treatment of sensitive and multidrug resistant leukaemia," *Eur J Cancer*, vol. 38, pp. 602-8, Mar 2002.

[186] V. Omelyanenko, P. Kopeckova, C. Gentry, and J. Kopecek, "Targetable HPMA copolymer-adriamycin conjugates. Recognition, internalization, and subcellular fate," *J Control Release*, vol. 53, pp. 25-37, Apr 30 1998.

[187] V. Omelyanenko, C. Gentry, P. Kopeckova, and J. Kopecek, "HPMA copolymer-anticancer drug-OV-TL16 antibody conjugates. II. Processing in epithelial ovarian carcinoma cells in vitro," *Int J Cancer*, vol. 75, pp. 600-8, Feb 9 1998.

9 Appendix

Some results presented in this diploma thesis were already published:

Subr, V., L. Sivak, E. Koziolova, A. Braunova, M. Pechar, J. Strohalm, M. Kabesova, B. Rihova, K. Ulbrich and M. Kovar (2014). "Synthesis of Poly[N-(2-hydroxypropyl)methacrylamide] Conjugates of Inhibitors of the ABC Transporter That Overcome Multidrug Resistance in Doxorubicin-Resistant P388 Cells in Vitro." *Biomacromolecules* 15(8): 3030-3043.